Development of virtual reality tools for arthroscopic surgery training

Fadi Yaacoub

HAL Id: tel-00481944
https://theses.hal.science/tel-00481944

Submitted on 7 May 2010

UNIVERSITÉ
— PARIS-EST

Université PARIS-EST

École Doctorale ICMS

THÈSE

Pour obtenir le grade de

Docteur de l'Université PARIS-EST

Spécialité: Informatique

Présentée et soutenue publiquement par

Fadi YAACOUB

Développement d'Outils de Réalité Virtuelle pour L'enseignement de la Chirurgie Arthroscopique

Development of Virtual Reality Tools for Arthroscopic Surgery Training

Directeur de thèse : Yskandar HAMAM , Professeur Émérite

Date de soutenance : 12 Novembre 2008

Composition du Jury :

Président du jury:	Etienne COLLE	Professeur, Université d'Evry, IBISC CNRS
Rapporteur:	Fathi BEN-OUEZDOU	Professeur, Université de Versailles, LISV
Rapporteur:	Karim DJOUANI	Professeur, F'SATIE-TUT, Afrique du Sud
Examinateur:	Gilles BERTRAND	Professeur, Université Paris-Est, ESIEE, LIGM
Examinateur:	Alain GILBERT	Professeur, M.D., Institut de la Main
Examinateur:	Yskandar HAMAM	Professeur, Université Paris-Est, ESIEE, LIGM
Examinateur:	Antoine ABCHE	Professeur Associé, Université de Balamand

To my family

Acknowledgements

A few lines are too short to express my deep appreciation for a number of people who contributed in different ways to my thesis. It is a pleasure to convey my gratitude to them all in my humble acknowledgment.

In the first place, I would like to record my gratitude to Professor Yskandar Hamam for his supervision, and guidance from the very early stage of this research as well as giving me experiences throughout the work. Above all and the most needed, he provided me with encouragement and support in various ways.

I would like to express my profound appreciation to all the reporters and committee members who honored me by reading my thesis and assisting at my defense.

I gratefully acknowledge Dr. Antoine Abche for his advices and contributions, which made him a backbone of this research and so to this thesis. Many thanks go to Dr. Eric Tallier, orthopedist surgeon at "Centre Hospitalier de Falaise", for his valuable remarks. I also acknowledge the Lebanese CNRS for the financial support during my last year of research.

I would also like to thank the members of the A^{2}SI laboratory: Gilles Bertrand, François Rocaries, Michel Couprie, Denis Bureau, Hugues Talbot, Mohamad Akil, Laurent Najman, Thierry Grandpierre for their support. It was a great pleasure working with them. Many thanks go in particular to Tarik Al Ani for his helpful advices and his encouragement. I am not forgetting Eric Lorens and Christophe Dietrich the A^{2}SI engineers as well as Martine Elichabe and Elisabeth Bastien. They were always available for my needs.

Special thanks to Lina Bouhaya for everything she made for me. Also, thank you Benoit Kaufmann, William Kobersy, Salah Helmy, Sami Sassine and John Altrip for all your support. Without you my friends, life would not be the same.

Finally, I would not be sitting in front of my PC typing these acknowledgement lines without my family. I owe my parents, Michel and Maha Yaacoub much of what I have become. I thank my sister Olga and my brother Chadi for their prayers and their encouragement throughout my graduate work in France.

Fadi YAACOUB

November 2008

Abstract

The minimally invasive approach of arthroscopy means less pain and faster recovery time for patients compared to open surgery. However, it implies a high difficulty of performance. Therefore, surgeon should remain at a high level of technical and professional expertise to perform such operations. Surgeon's skills are being developed over years of surgical training on animals, cadavers and patients. Nowadays, cadavers and animal specimens present an ethical problem also the practice on real humans is usually risky. For surgeons to reach a high level, new and alternative ways of performing surgical training are required.

Virtual reality technology has opened new realms in the practice of medicine. Today, virtual reality simulators have become one of the most important training methods in the medical field. These simulators allow medical students to examine and study organs or any structure of the human body in ways that were not possible few years earlier. Similarly, the surgeon as well as the medical student can gain a valuable experience by performing a particular surgery with an anatomical accuracy and realism as it is actually performed in the real world. Thus, they can practice on virtual operation before they proceed and operate on real patients.

In this thesis, a virtual reality training simulator for wrist arthroscopy is introduced. Two main issues are addressed: the 3-D reconstruction process and the 3-D interaction. Based on a sequence of CT images a realistic representation of the wrist joint is obtained suitable for the computer simulation. Two main components of the computer-based system interface are illustrated: the 3-D interaction to guide the surgical instruments and the user interface for haptic feedback. In this context, algorithms that model objects using the convex hull approaches and simulate real time exact collision detection between virtual objects are presented. A force feedback device, coupled with a haptic algorithm, is used as a haptic interface with the computer simulation system. This leads in the development of a low cost system with the same benefits as professional devices. In this regard, the wrist arthroscopy can be simulated and medical students can learn the basic skills required with safety, flexibility and less cost.

Keywords : Virtual Reality, Arthroscopic Surgery, 3-D modeling and Visualization, Convex Hull, Collision Detection, Haptic Feedback, Healthcare Technology.

Résumé

La chirurgie arthroscopique présente actuellement un essor très important pour le bénéfice du plus grand nombre des patients. Cependant, cette technique possède un certain nombre d'inconvénients et il est donc nécessaire pour le médecin de s'entrainer et répéter ses gestes afin de pouvoir exécuter ce type d'opération d'une façon efficace et certaine. En effet, les méthodes traditionnelles d'enseignement de la chirurgie sont basées sur l'autopsie des cadavres et l'entrainement sur des animaux. Avec l'évolution de notre société, ces deux pratiques deviennent de plus en plus critiquées et font l'objet de réglementations très restrictives. Afin d'atteindre un niveau plus élevé, de nouveaux moyens d'apprentissage sont nécessaires pour les chirurgiens.

Récemment, la réalité virtuelle commence d'être de plus en plus utilisée dans la médecine et surtout la chirurgie. Les simulateurs chirurgicaux sont devenus une des matières les plus récentes dans la recherche de la réalité virtuelle. Ils sont également devenus une méthode de formation et un outil d'entrainement valable pour les chirurgiens aussi bien que les étudiants en médecine.

Dans ce travail, un simulateur de réalité virtuelle pour l'enseignement de la chirurgie arthroscopique, surtout la chirurgie du poignet, a été présenté. Deux questions principales sont abordées : la reconstruction et l'interaction 3-D. Une séquence d'images CT a été traitée afin de générer un modèle 3-D du poignet. Les deux principales composantes de l'interface du système sont illustrées : l'interaction 3-D pour guider les instruments chirurgicaux et l'interface de l'utilisateur pour le retour d'effort. Dans ce contexte, les algorithmes qui modélisent les objets en utilisant les approches de "Convex Hull" et qui simulent la détection de collision entre les objets virtuels en temps réel, sont présentés. En outre, un dispositif de retour d'effort est utilisé comme une interface haptique avec le système. Cela conduit au développement d'un système à faible coût, avec les mêmes avantages que les appareils professionnels. À cet égard, l'arthroscopie du poignet peut être simulée et les étudiants en médecine peuvent facilement utiliser le système et peuvent apprendre les compétences de base requises en sécurité, flexibilité et moindre coût.

Mots-clés : Réalité Virtuelle, Chirurgie Arthroscopique, Modélisation et Visualisation 3-D, Enveloppes Convexes, Détection de Collision, Retour d'effort, Technologie Médicale.

Table of contents

List of Figures

List of Algorithms

List of Tables

Chapter 1

Introduction

Virtual Environment (VE) provides a new dimension of graphical simulation [1]. It is described as an application that allows users to navigate and interact with a computer-generated three dimensional space in real time. In this context, Virtual Reality (VR) is not only a hardware system. It is also an emerging technology that changes the way individuals interact with computers. VR has revolutionized several scientific disciplines by developing novel methods to visualize complex data structures and by providing means to manipulate the data in real-time and in a natural way. Most promising fields in which VR systems are applied include: engineering, education, entertainment, military simulations and medicine.

Recently, medicine has entered a period of intense technological transition, driven by the need to provide improved care at a lower cost. Since, the outcomes of surgical procedures are closely related to the skills of the surgeon, the latter should remain at a high level of technical and professional expertise. These skills are being developed over years of surgical training on animals, cadavers and patients. Consequently, new and alternative ways of performing surgical training are required. In addition, the low availability and high cost of cadaver and animal specimens for traditional medical training and the public concern with the inhuman treatment of animals have become another impetus for surgeons and medical students to use new technology in their education and their training to gain valuable information and experience. VR technology has opened new realms in the practice of medicine. The graphics capabilities of VR tools, particularly in

modeling and displaying medical data can be of great assistance in teaching, learning, training and experimenting surgeries [2].

Today, researchers on surgical education depend heavily on VR simulators that have become one of the most important training methods in the medical field. Simulators allow medical students to examine and study organs or any structure of the human body in ways that were not possible few years earlier. They provide an important tool to acquire valuable information during their education. Similarly, the surgeon as well as the medical student can gain a valuable experience by performing a particular surgery with an anatomical accuracy and realism as it is actually performed in the real world. Thus, the surgeon can practice his operation before he proceeds and operates on real patients. Therefore, the risks to surgical patients are reduced and the ethical issues associated with animal experimentation are avoided.

One of the most advanced and important type of surgeries is the Minimally Invasive Surgery (MIS). The minimally invasive approach means less pain and faster recovery time for patients in comparison with an open surgery. On the other hand, it implies a high difficulty of performance. Arthroscopy is a form of endoscopy or minimally invasive surgery that is concerned specifically with the joints. It offers several advantages over the traditional open surgery for both: the patient and the healthcare provider. The corresponding procedures are generally less invasive, resulting in smaller wounds, increased rates of recovery, reductions in hospitalization episodes and consequently reductions in patient intervention costs. While these advantages are attractive to the healthcare provider, the arthroscopy is associated with some disadvantages. Arthroscopic equipments are expensive and surgeons require additional training to acquire the competence to operate efficiently and safely. In addition, surgeons agree that the current initial training protocols are insufficiently challenging and consequently they are entering the operating room with inadequate skills to use arthroscopic technique to its best advantage. Thus, patients could be at risk in such an environment. Therefore, computer-based surgical simulation systems, one of the most developed technologies in VR, are used to train surgeons as well as medical students to practice a particular surgery before they

enter the operating room. These simulators have become one main component that has radically changed the traditional medical training and the surgical certification scenarios. They allow the process of iterative learning through assessment, evaluation, decision making and error correction and consequently create a much stronger learning environment.

1.1   Objective and Considerations

VR surgical simulators have been developed for a wide range of medical applications. Their names reflect the performed procedures i.e. laparoscopy, endoscopy, cystoscopy, ureteroscopy colonoscopy, bronchoscopy and flexible sigmoidoscopy simulators. Most simulators that are mentioned above, are expensive to acquire and need maintenance. With respect to arthroscopy simulators, developments have been mostly for the knee and the shoulder and very little work has been done for wrist arthroscopy. Even though the wrist is a very important joint of the human body that handles many activities, the work on developing corresponding VR surgical simulators is limited. Thus, the problem of building an inexpensive and a practical simulator to train medical students and treat the issue of the wrist arthroscopy remained. In this context, our project has been proposed by a team of medical professors and surgeons at the *"Institut de la Main"*, *"Clinique JOUVENET"*, Paris XVI. It consists of developing a VR simulator to help teaching, learning and training on wrist arthroscopic surgical procedures.

This research project, directed by Prof. Yskandar Hamam, started with Charbel Fares who graduated in June 2006. Our work is a continuation of this project in order to enhance many algorithms, propose new ones and to develop all the VR tools that are necessary to complete the project in order to have the entire prototype system.

The design of the proposed computer-based arthroscopy simulator is based on a trade-off between medical professor's needs and VR limitations. During the design of the proposed training system, two major aims are addressed:

1. Apply VR and physical simulation techniques to generate 3-D models and to simulate operations with fidelity and realism.

2. Try to cover different requirements for the apprentice learning process and provide the user with tools to facilitate teaching, learning and training on several procedures.

In addition, wrist arthroscopy is selected due to several considerations:

- Wrist arthroscopy is a frequent pathology (study of essential nature of disease) that has been studied and practiced less than the knee and shoulder arthroscopies.

- Various types of involvements and specific surgeries can be covered by wrist arthroscopy simulation such as: dorsal percutaneous scaphoid fixation, volar percutaneous scaphoid fixation, capitolunate arthrodesis ...

- There are potentially large and new pathologies that will be facing the medical practitioners when it comes to wrist arthroscopy. Therefore, there is an increasing demand on training and learning new techniques.

- Wrist arthroscopy has proven to be extremely valuable in both diagnosis and therapy. It is an important skill for all hand surgeons, in exactly the same way as shoulder and knee arthroscopies.

1.2 Design Criteria

Our work is focused on developing a VR training system to simulate arthroscopic procedures, especially wrist arthroscopy, in a virtual environment. The system is developed for both: educational and pre-operative purposes.

Two main issues are addressed: the three dimensional (3-D) reconstruction process and the 3-D interaction. The proposed system provides a virtual environment with realistic representation of the region of interest. Based on a sequence of CT images, a realistic representation of the wrist joint is obtained and is suitable for the computer simulation. Two main components of the computer-based system interface are illustrated: the 3-D interaction to guide the surgical instruments and the user interface for haptic feedback. In this context, algorithms that model objects using the convex hull

approaches and simulate real time exact collision detection between virtual objects during the training on surgical operations are needed. Also, a force feedback device must be used as a haptic interface with the computer simulation system. This will lead in the development of a low cost system that is used by medical students with the same benefits as professional devices. Then, the procedure can be performed on real patients with much less risk and injury.

1.3 The VR Surgical Simulation System

A functional prototype of a computer-based training system for simulating wrist arthroscopy is presented. Figure 1.1 outlines the main components of the proposed VR simulation system.
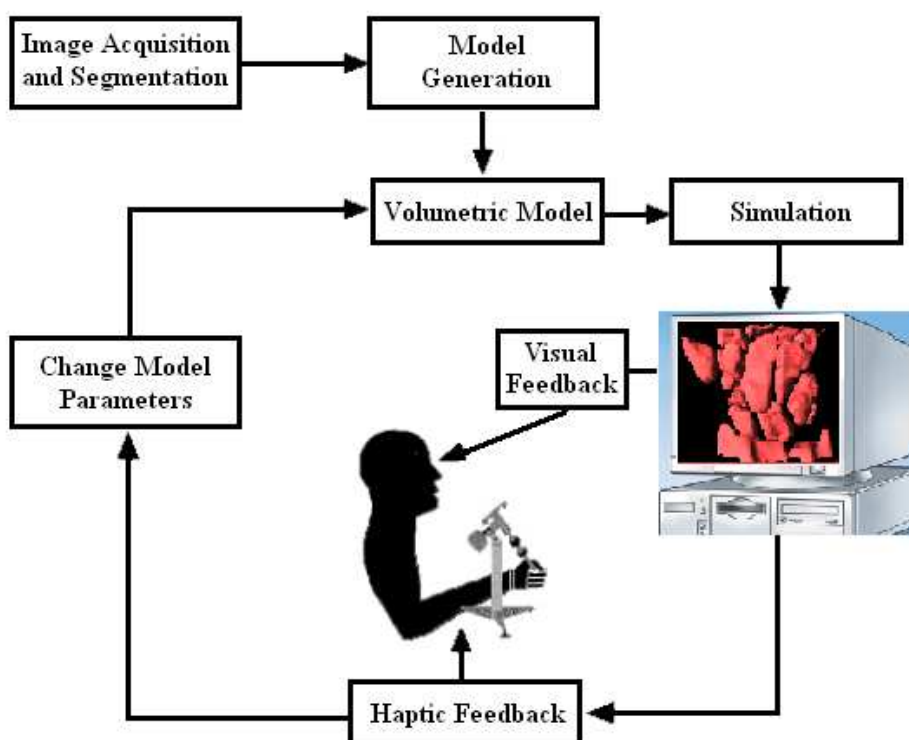
Figure 1.1: A Flowchart of the VR Simulation System

Medical images are processed to generate volumetric object models. A sequence of CT images is segmented and a 3-D virtual model of the wrist is generated. This 3-D

model is presented both visually via rendering on the computer monitor and haptically with a force feedback device. Visual parameters such as viewpoint, zooming, color and lighting effects, can be interactively controlled and object models can be manipulated with force feedback to change relative probe and object positions, and to simulate many surgical procedures. Also, simulations include an algorithm that model objects using the convex hull approach and a method that detects collisions between virtual objects during the operation. The interaction between the haptic device and the computer closes the feedback loop between the user and the simulator, offering a better understanding of the anatomical structures and the functions in the patient's model.

1.4   Motivations and Contributions

Our research is motivated by the need to develop an inexpensive and practical simulator to train medical practitioners (students, surgeons ...) and master the wrist arthroscopy techniques. In this context, several contributions are presented:

- Developing a virtual environment to visualize medical models and medical tools with high fidelity and precision.

- Developing and presenting a new hybrid approach to generate the convex hull of the 3-D models. The proposed algorithm converts each 3-D concave model to a convex representation and allows collision detection algorithms to converge quickly and report a collision, if it exists.

- Proposing and developing a new technique of collision detection for solid objects. The collision detection problem is formulated and a linear programming solution is obtained to determine whether a collision exists or not. The proposed algorithm is efficient, fast, robust and leads to a decrease of the running time that is required to detect a collision.

- Designing and implementing a 3-DOF force feedback device. This low cost system is coupled with a haptic feedback algorithm. The proposed device is used by medical practitioners with the same benefits as professional devices.

These main contributions lead to the development of the computer based medical system that is shown in figure 1.2
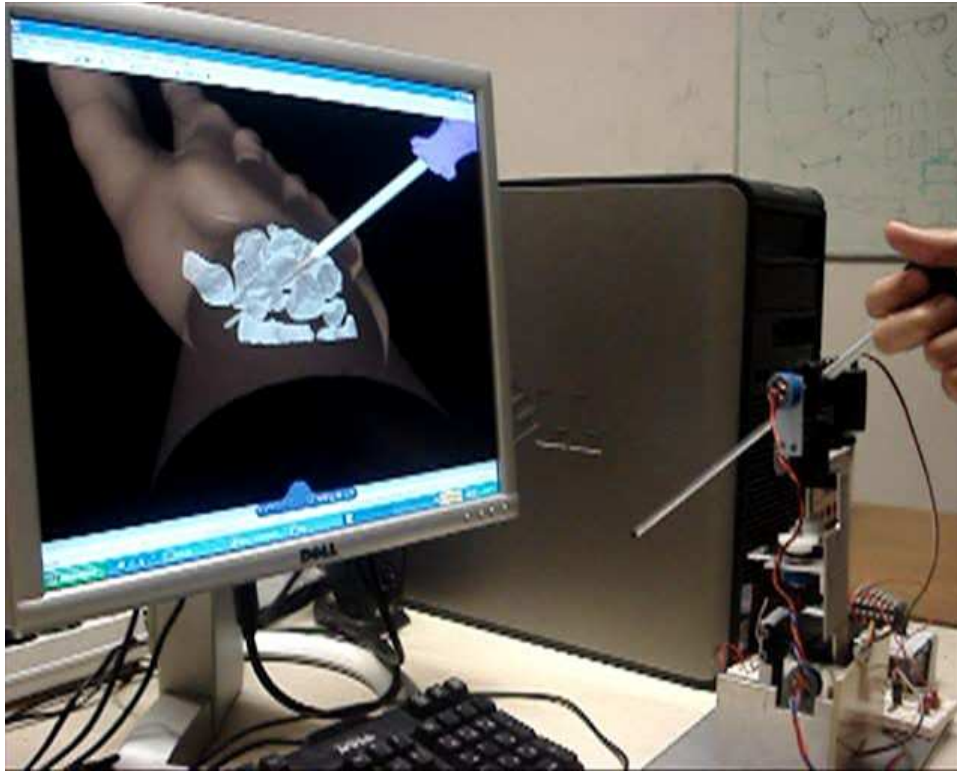
Figure 1.2: The Proposed VR Simulation System

1.5   Thesis's Structure

Chapter 1 introduces the thesis and outlines the contributions.

Chapter 2 presents different VR surgical simulators for Minimally Invasive Surgery (MIS). These simulators have been developed for a wide range of procedures. The presented VR simulators are classified based on the application and the relation with the organs or areas for which the system is developed for. A description of each type of the minimally invasive surgical simulator is presented.

Chapter 3 describes the segmentation and the generation of the medical model of the imaged object. First, the segmentation of the CT images using the watershed algorithm and the reconstruction of the 3-D wrist model are introduced. Then, the representation

of these models in the virtual environment by associating all the necessary elements (lights, materials and texture mapping) are illustrated.

In Chapter 4, a hybrid approach to generate the convex hull is developed and presented. The new algorithm is validated by performing a comparison with conventional algorithms namely, the Brute Force, the Gift Wrapping, the QuickHull and the Chan algorithms. The evaluation is achieved by generating the convex envelope of 3-D wrist bones using the five different approaches. The results show the improvement associated with the proposed approach.

Having generated the convex hulls, Chapter 5 addresses the issue of the precise Collision Detection (CD) between virtual objects and a new technique is proposed. The CD problem is formulated and a linear programming solution is obtained to determine whether a collision exists or not. The proposed CD approach is evaluated and compared with a conventional algorithm namely the Industrial Virtual Reality Institute Collision Detection (IVRI-CD) technique. It is validated using bones of the 3-D wrist model. The results show that the proposed algorithm is efficient, fast, robust and leads to a decrease of the running time required to detect a collision.

Chapter 6 proposes a force feedback device which is used as a haptic interface with the computer simulation system. The design and the implementation of this device are shown. This leads to the development of a low cost system that is used by medical students with the same benefits as professional devices. In addition, a haptic feedback algorithm is implemented and tested for the proposed force feedback device. A virtual simulation of dorsal percutaneous scaphoid fixation is shown. Also, a comparison between the real and the virtual processes of the surgery is demonstrated. Consequently, the wrist arthroscopic surgery can be simulated and students can easily acquire the system to learn the essential basic skills.

Finally, a short summary of the thesis and an outline of the contributions are presented in chapter 7.

Chapter 2

VR Simulators for Minimally Invasive Surgery

This chapter presents different VR surgical simulators for MIS. These simulators have been developed for a wide range of procedures. The VR simulators presented are classified based on their applications and their relation to the organs or areas they treat. Moreover, a description of each type of the minimally invasive surgical simulators, associated with specific involvement, is presented.

2.1 Introduction

Minimally invasive surgical procedures provide patients with many advantages such as making the surgery much easier, faster and more comfortable. Minimally invasive techniques use long slight tools that are inserted into the body through small incisions in the skin and under the membranes. An optical endoscope equipped with a video camera allows the visualization of the procedure through one of the portals, while surgical probes and other instruments are inserted through additional portals. This operation decreases soft tissue disruption which leads to less pain and less chance for infection. Also, it eliminates potential complications and it is just as effective as conventional open surgery.

There are many types of endoscope and they are named in relation to the organs or areas they explore. Endoscopes used to look directly at the ovaries, appendix, or other abdominal organs, are called laparoscopes (laparoscopy). Other endoscopes are inserted

through incisions to look at joints (arthroscopy). Moreover, others endoscopes are used to view the inside of the bladder (cystoscopy) or the lungs (bronchoscopy). While laparoscopy is usually performed under general anesthesia, most other endoscopies can be achieved while the patient is sedated. An endoscopy may be performed for a variety of signs and symptoms such as: bleeding, pain, difficulty swallowing and a change in bowel habits. Exams of the colon (colonoscopy) may also be performed to screen for colon polyps and colon cancer [3].

On the other hand, MIS is not a friendly procedure to surgeons because the hand-on tactile feedback is reduced and the visual field is limited. Thus, several minimally invasive procedures need to be learned by repetition. These procedures are complex for surgeons and require specialized training in order to reach a high level of proficiency. The VR simulators provide a new method for apprenticeship and can reduce the difficulty of the surgery by repeating the procedure as many times as needed, without the required supervision and without placing the patient at risk. In addition, new and unusual surgical procedures can be practiced, the same procedure can be carried out on different case studies which differ in terms of the pathology or anatomical structure and some complications can be simulated in a safe manner.

Several VR surgical simulators for MIS training have been developed for a wide range of procedures. However, they are associated with specific involvements. Many simulators are associated with laparoscopy, others are associated with cystoscopy and ureteroscopy procedures. Moreover, some of them are involved with colonoscopy, bronchoscopy and flexible sigmoidoscopy. Regarding arthroscopy simulators, most developments have been for knee training, the second case of arthroscopy that was treated is the shoulder arthroscopy simulations and very little work has been done for wrist arthroscopy even though the wrist is a very important joint in the human body and it handles many activities.

2.2 Laparoscopy Simulators

Laparoscopic surgeries refer to the operations within the abdomen or pelvic cavity. They allow the surgeons to look directly at the contents of a patient's abdomen or pelvis, including the fallopian tubes, ovaries, small bowel, large bowel, appendix, liver, and gallbladder. The purpose of this examination is to directly assess the presence of a problem that has not been confirmed through noninvasive tests. This approach is intended to minimize the operative blood loss, the postoperative pain, and to speed up the recovery time after the procedure.

2.2.1 LapSim

The LapSim simulator focuses on developing and implanting basic skills that would be needed by the trainee to perform bigger procedures [4]. This system is the first of a series of digital training aids. This type of training replaces the vulnerable patient by a set of digitally images (consisting of pixels or voxels) that recreates virtually the procedures and the environment of the abdominal keyhole surgery. The LapSim program utilizes an advanced 3-D technology, including an interactive live video to provide the medical practitioner with a realistic virtual working environment. Nevertheless, the interface is kept as simple as possible. Practice sessions can vary in graphic complexity as well as in the level of difficulty. Also, LapSim provides an effective learning experience and training skills. The basic training skills of LapSim can be summarized as follows: camera and instrument navigation, coordination, lifting and grasping, cutting, clip applying and suturing.

2.2.2 LapMentor

The LapMentor is a force feedback laparoscopic simulator with a realistic visualization of the intra-abdominal cavity. It allows hands-on practice for a single trainee or for a complete team [5]. It offers training opportunities to medical students as well as experienced surgeons in order to perfect basic laparoscopic skills and to perform complete laparoscopic surgical procedures. It has several important features such as: a high

performance force feedback devices, an endoscope with four degrees of freedom, a freeze picture switch and a foot switch for activation of electrosurgical coagulation. It also offers a customizable training program with realistic scenarios of patient situations.

2.2.3   MIST

MIST (Minimally Invasive Surgical Trainer) simulator is a computer-based system where the trainees are guided through a series of exercises to develop their essential skills for a good clinical practice [6]. The system allows the trainees to work through a series of essential surgical tasks with progressive complexity. Each task is based on a key surgical technique that is performed in laparoscopy. Tasks begin by using simple geometrical shapes to develop key psychomotor skills. The device is designed to teach and assess basic minimally invasive surgical skills as well as to acquire more advanced skills such as suturing. MIST has several features such as a frame that holds two standard laparoscopic instruments electronically linked to the computer and a screen that displays the VR movement of the surgical instruments in real-time 3-D graphics.

2.2.4   VIST

VIST (Vascular Intervention Simulation Trainer) is a force-feedback simulator to perform catheter based procedures. It allows a relevant and a realistic hands-on training for angiography and different levels of interventional procedures by using real devices which can be manipulated at any time during the operation [6]. The VIST provides a real technique to reproduce the physics and the physiology of the human cardiovascular system for various training procedures. The simulator consists of a simulation software, a haptic interface and two monitors: a monitor for the synthetic X-ray and another for the instructional system. Real patient's data are used to generate the simulated patient's case. Modules which replicate the hemodynamics, blood flow and contrast medium mixing are also provided. In addition, an active tactile feedback that makes the training experience more realistic is conferred. The Procedicus VIST system enables the trainee to practice several operations such as: carotid, coronary, pacemaker lead

placement, transseptal puncture and vena cava procedures.

2.2.5   LASSO

The LASSO project is an integrated development effort to construct a laparoscopic simulation platform [7]. The modeling process is divided into two stages: anatomical modeling and organ appearance modeling. The abdominal cavity was modeled using data from the Visible Human project [8]. Organ surface features were generated using a combination of texture analysis/synthesis, procedural texturing and L-systems based methods for growing vascular networks. The real-time deformation, the haptic and the rendering performance were achieved using a purpose-built 64-node parallel processor.

2.2.6   VEST

The VEST (Virtual Endoscopic Surgery Training) system was developed within the framework of the joint TT-project (Technology Transfer) and in collaboration with the Forschungszentrum Karlsruhe Institute [20]. The VEST system is a VR simulator for minimal invasive surgery. The simulator allows users to practice surgical procedures using three haptic devices as mock-up endoscopic instruments. It is used for laparoscopic cholecystectomy and gynaecology scenario.

2.2.7   Karlsruhe Endoscopic Surgery Trainer

The Karlsruhe endoscopic surgery trainer is a VR based training system for MIS [17][18]. The system is developed based on the KISMET environment for virtual surgery [19]. Trainees can interactively manipulate the modelled objects and execute surgical tasks. Several complications as well as anatomic pathologies can be implemented in a training session. Structured training steps are repeatable and are reproducible by using an expert system feedback. The simulator imitates realistically soft tissue and its physical behaviour and consequently, this leads to simulate deformable objects. Several typical surgical tasks are performed such as grasping, cutting, coagulating and setting of clips.

The calculation and the representation of realistic tissue deformations and their manipulation are done in real-time. A full stereo view with shutter glasses is offered to gain a 3-D impression. Furthermore, a special instrument guidance system is developed which provides a tactile feedback. The developed device can simulate a typical prototyping scenario of a cholecystectomy.

2.2.8   Liver Biopsy

A laparoscopic liver biopsy is done to obtain a biopsy specimen. For this purpose, small incisions are made in the abdomen and instruments are introduced through trocars. The web-based liver biopsy surgical simulator is a tool that simulates the Tru-Cut needle technique to perform the liver biopsy procedures [21]. A virtual representation of the liver is displayed so that the clinicians will be well prepared and well rehearsed. The simulator contains a "marker" tool that allows the doctor to draw on the torso and mark the edge of the liver. Force feedback can be applied by using The Wingman Force Feedback Mouse from Logitech [22].

2.2.9   ProMIS

ProMIS is another simulator to acquire the skills and the techniques of MIS [23]. It enables users to interact with virtual and physical models in the same unit and provides accurate and comprehensive feedback on performance. ProMIS can combine virtual and real worlds in the same system. Users can learn, practice and measure their proficiency either with real instruments on real models with haptics or with virtual models in the same context. The ProMIS allows the skill's development based on validated approaches and is designed to be easily integrated into existing curricula. However, the modules may vary between virtual and physical models. The simulator offers a series of tasks that replicate the critical elements of specific procedures, including: LapNissen, Ectopic pregnancy, Anastomosis, LapCholecyst-ectomy and Prostatectomy. Also, ProMIS basic skills include: laparoscope orientation, instrument handling, dissection, diathermy, suturing and intracorporeal knot-tying.

2.2.10 SEP

SEP (SurgicalSim Education Platform) is a tool for training laparoscopic procedures [24]. An important application is the laparoscopic cholecystectomy process. The SEP cholecystectomy simulator system focuses on training the removal of the gallbladder with a minimal risk of injury to the bile ducts and the surrounding structures. The basic system includes a flexible surgical interface, an administrative framework, an application framework for structured training and a basic (task) training program. The basic system can be extended with procedure modules, a robotic simulation and a 3-D stereoscopic vision. This device can perform many procedures such as: positioning the patient, surgeons and equipment; also positioning the trocars, the exploration and the exposure. Furthermore, the surgeon can practice the dissection of the calot's triangle, the clipping and the division of the cystic duct and the cystic artery, and the dissection of the gallbladder from the liver bed and the abdomen.

2.3 Cystoscopy Simulators

Cystoscopy is the procedure that enables doctors to view inside a patient's urinary bladder and urethra in great detail. Diagnostic cystoscopy is usually carried out with local anaesthesia. General anaesthesia is sometimes used for operative cystoscopic procedures. There are two types of cystoscopes: the standard rigid cystoscope and the flexible cystoscope. The method to insert the cystoscope varies. However, the test is the same. A doctor may recommend cystoscopy for several conditions. They include: frequent urinary tract infections, blood in the urine (hematuria), loss of bladder control (incontinence) or overactive bladder, urinary blockage and unusual growth, tumor or cancer.

2.3.1 UroMentor

VR simulations of cystoscopy procedures can be achieved using the UroMentor [9]. The UroMentor is a force feedback interactive computerized simulator which enables the training of basic cystoscopy and ureteroscopy skills such as the eye-hand-coordination

and the depth perception. This device has a large number of practice modules and patient's profiles in order to perform safe surgical procedures. Also, it has several features that can be summarized as follows: real-time fluoroscopy with the simulation of C-arm control, the identification of the patient's anatomy, diagnostic and therapeutic procedures, and a correct tool insertion by changing the C-arm positioning. Also, it enables to view the fluoroscopy image with the injection of a contrast agent. The offered training skills are organized into three parts. The first part includes the practice skills which consist of training the basic grasping and the cystoscope handling. The second part involves the tasks that have a specific requirement which helps the trainee to perform a full procedure. Finally, the third part consists of free training exercises such as the stone manipulation.

2.4 Colonoscopy Simulators

A colonoscopy is a procedure to view the interior's lining of the large intestine (colon) using a colonoscope (a flexible tube containing an imaging device). Colonoscopy is similar to the sigmoidoscopy. The difference between the colonoscopy and the latter is related to the part of the colon to be examined. While sigmoidoscopy allows doctors to view only the final part of the colon, colonoscopy allows a complete examination of the colon.

2.4.1 Simbionix GI Mentor II

The GI Mentor simulator is an interactive computerized force-feedback system that provides hands-on training in colonoscopic procedures with true-to-life sensations during the performance [10]. The device includes several specifications such as a specially designed mannequin that switches easily between the upper and the lower GI positions. Also, it provides a computer simulation program for both the upper and the lower endoscopic diagnostic and therapeutic procedures. In addition, the system has an authentic endoscope which is customized by Simbionix as well as other endoscopic accessories with authentic tool handles.

2.4.2 VES

Virtual Endoscope System (VES) is a simulator with a force feedback and sensation [26]. The system is developed to train medical students or practitioners on colonoscopic procedures in a virtual digestive tube. It can convey the sensation of a reactive force from a digestive tube during the insertion. The dynamical models of both, the endoscope and the digestive tube were implemented in real-time to compute the inter-actional force between them. The VES simulator consists of three main parts: a force simulation mechanism, a high-speed micro computer that calculates the reactive force between the endoscope and the digestive tube in real-time and controls the VES mechanism, and a monitor on which CT images of the colon are converted into a 3-D model and are displayed. The VES system improves the skills through the use of the simulated force and can be used as a platform to train the medical individual on the same procedure, repeatedly. It can be adapted to simulate all types of data collected from various patients of different organs or structures. As a conclusion, the system can be used to train medical students and to simulate operations that require special technical skills.

2.5 Bronchoscopy Simulators

Bronchoscopy is the visualization of the lower airways using a flexible or rigid tube equipped with a tiny camera at the end. The procedure provides a view of the airways of the lung and allows the doctors to perform several diagnosis (diagnosis of tumor, bleeding, infection, or trauma). It is also useful in the treatment of the airway's obstruction by tumors or by foreign bodies. There are two types of bronchoscope: flexible (fiberoptic) and rigid. Flexible bronchoscopy is often performed under a local anesthesia with the patient awake. Rigid bronchoscopes may be employed to remove foreign bodies or to place stents. Such procedures are achieved under a general anesthesia.

2.5.1 AccuTouch

The AccuTouch surgical simulator is a computer-based system that is developed to teach and assess motor skills and the cognitive knowledge. It enables medical students

and experienced surgeons to practice in a safe environment [27]. It consists of a PC, an interface device, a proxy bronchoscope and software modules that provide a wide range of training scenarios. AccuTouch uses real-time computer graphics that includes anatomic models, developed from actual patient data, and a robotic interface device. A force is transmitted through the flexible scope to provide tactile sensations mimicking the actual feel of procedures. In addition to bronchoscopy, the system offers the simulation of the upper and the lower gastrointestinal flexible endoscopy. It has several features such as: a mannequin that provides realistic a force feedback which allows users to experience the feel of the real procedure, a didactic content and a simulation that allows novices to learn in an integrated environment. Moreover, it offers realistic images and an audio feedback that is combined with touch to involve all the key senses. Also, the device presents digital VR patients that respond in a physiologically accurate manner and includes an extensive didactic material that can be reviewed before each practice session.

2.5.2 PREOP

Bro-Nielsen et al. described a PC-based bronchoscopy simulator: the PREOP [11]. The system integrates multimedia, 3-D graphics simulation and a force feedback technology on PC. The simulator offers realistic visual effects and a realistic force feedback during the scope's insertion. Thus, the flexible bronchoscopy can be correctly performed. Also, the system has been expanded to perform a colonoscopy and a flexible sigmoidoscopy (examination of the large intestine from the rectum through the last part of the colon).

2.6 Hysteroscopy Simulators

Hysteroscopy is the inspection of the uterine cavity by using a hysteroscope, which is a thin telescope that is inserted through the cervix into the uterus. Hysteroscopy allows the diagnosis of the intrauterine pathology and serves as a method for surgical intervention. It is useful in a number of uterine conditions such as: leiomyomata, asherman syndrome, gynecologic bleeding and uterine malformations.

2.6.1 LAHYSTOTRAIN

The LAHYSTOTRAIN training system is an advanced simulation environment to perform hysteroscopic procedures. It combines virtual reality, multimedia and intelligent tutoring techniques (ITS) [12][13]. This simulator provides a realistic training environment to rehears the various intervention procedures and gives a more intuitive 3-D interaction. It contains the various virtual anatomical structures and simulates the endoscope, the surgical instruments, and the object behaviors (collision detection, deformation and cutting). In addition, a force feedback device is integrated into the training system. Thus, the trainee is able to feel the resistance of the anatomical structures via the instruments. The whole educational process can be covered using the LAHYSTOTRAIN simulator i.e. starting with the diagnostic procedures and ending with the complex therapeutical interventions.

2.6.2 VirtaMed Hysteroscopy Simulator

As already defined, hysteroscopy is the minimally invasive inspection and treatment of the uterus through the vagina. VirtaMed has introduced a hysterscopy simulator in the market [14]. The VR-based hysteroscopy training simulator was realized in the Swiss Research Framework CO-ME (Computer-Aided and Image-Guided Medical Interventions) [15]. While the VR environment is developed at the Computer-Vision Laboratory at ETHZ, the haptic interface is provided by the "Laboratoire de Systèmes Robotiques". The purpose of the simulator is to go beyond the rehearsal of the basic manipulative skills. It permits the training of procedural skills such as decision making and problem solving.

Since the uterus is different from other human organs, it can have large variations between individuals. These variations are taken into account by developing a 4-DOF haptic device with a comparatively large workspace [16]. 2-DOF friction drive, associated with the rotation and translation of the tool, supports the insertion and the complete removal of the surgery's tool during a training session. This compact device can be completely hidden from the view of the surgeon's eye within the mannequin torso for

realistic environment.

2.7 Cholangio-pancreatography Simulators

Endoscopic Retrograde Cholangio-Pancreatography (ERCP) is a technique to analyse and treat the problems of the biliary or pancreatic ductal. This technique involves the insertion of an endoscope with a flexible tip through the oral cavity, the esophagus, the stomach and into the first portion of the small intestine, the duodenum. Subsequently, dyes are injected into the ducts of the biliary tree and the pancreas so that the corresponding organs can be seen on the collected X-rays images. ERCP is used primarily to diagnose and treat conditions of the bile ducts, including gallstones, inflammatory strictures, leaks and cancer.

2.7.1 GIT/MCG ERCP

The GIT/MCG ERCP simulator is developed by the Georgia Institute of Technology and the Medical College of Georgia (GIT/MCG). It consists of a simulation interface into which an endoscope is inserted, a computer which controls and updates the virtual environment, a dial and button box to select the simulation parameters and a video monitor to display the computer generated images [25]. A simulation session begins when a real endoscope is inserted through the "mouth" of the simulated patient. A position tracking system reports the endoscope movements to a high performance computer which controls the interactions and updates the computer generated images on the monitor. Besides, the display of the visual feedback on the monitor, a computer, which controls an arrangement of servo motors, provides a force feedback to the endoscope and to the catheter held by the trainee. The GIT/MCG prototype includes a force feedback in order to provide a realistic training session and consequently realistic skills. Interactive simulation allows the user to manipulate 3-D computer models and observe the response in real-time. An immediate and appropriate model deformation can be achieved by pushing or pulling the models that are displayed on screen.

2.8 Sinoscopy Simulators

Endoscopic sinus surgery or sinoscopy is a procedure that is used to remove blockages in the sinuses (the spaces that are filled with air in some of the bones of the skull). A thin, lighted instrument is inserted into the nose. The endoscope transmits light beams into the different parts of the nose and sinuses. Subsequently, the doctor can have an inside look through an eye-piece to see what is causing the blockages. This procedure can relieve nasal blockages, facial pain and improve the breathing of the subject under examination.

2.8.1 ESS

The (ESS) Endoscopic Sinus Surgery simulator consists of four main components: the forceps simulator, the endoscope tracking unit, the control computer and the interface card, and the host computer [28]. The forceps simulator is the heart of the ESS simulator. It includes the mounting platform, the head assembly, the calibration fixture, and a modified Impulse Engine 3GM with a 3 axis gimbal assembly and integrated forceps. The Impulse Engine 3GM is a three degree of freedom haptic interface that can track positions and apply the corresponding forces. On the other hand, the endoscope tracking unit is based on the MicroScribe 3DX. This system is equipped with a special stylus roll sensor to track the endoscope's rotation. The kinematics and the mounting configuration of the MicroScribe enable the system to accurately track the endoscope's motion throughout the entire head without interfering with the forceps simulator. In addition, the control computer communicates with a Silicon Graphics workstation. This dual processor system visualizes the 3-D models and provides a real-time control of the haptic system. The position and orientation information from the forceps simulator and the endoscope tracking unit are sent to the workstation. Then, the corresponding model is rebuilt to reflect these interactions and retransmits a revised haptic model back to the forceps control computer. This computer calculates the required forces, in real-time, from the haptic model, computes the current position and the velocity measures and transmits them to the Impulse Engine.

2.9 Interventional Radiology Simulators

Interventional Radiology (IR) is a minimally invasive therapy for endovascular treatment of vascular deseases and tumors. During an IR procedure, the interventional radiologist, under fluoroscopy guidance, inserts a catheter into a blood vessel to gain an internal access to the diseased site. Then, the catheter is used as a conduit to introduce therapeutic devices for treatment purposes.

A VR simulator that realizes IR procedures remotely is presented in [36]. This simulator contains two subsystems: the first subsystem is at the local site and the other is located at the remote site. At the local site, the interventional radiologist interacts with a 3-D vascular model extracted from the patient's data. He inserts IR devices through the motion tracking box, which converts physical motion (translation and rotation) of IR devices into a digital signal. Then, the signal is transmitted to the actuator box at the remote site that controls the IR devices in the patient. The status of the IR devices is subsequently fed back to the local site and is displayed on the vascular model. Furthermore, the simulator employs a physical angiography phantom that mimics the patient and the corresponding 3-D digital model. A magnetic tracking system provides information about the positioning of the IR devices in the phantom. In addition, the VR simulator can be potentially useful for remote education and planning purposes. The trainee is capable of manipulating the therapeutic devices with the 3-D reconstructed vascular model in real-time in order to acquire the necessary skills and to improve the hand-eye coordination capabilities.

VIRGIL is another VR system for chest tube insertion training [37]. It was developed by a team of researchers and scientists from the simulation group at CIMIT (Center for Integration of Medicine and Innovative Technology). The VIRGIL simulator combines the use of a realistic mannequin with a PC-based graphical interface that tracks the internal position of chest darts and chest tubes during the training exercises. In this context, the simulator provides 3-D anatomic models generated from the CT scans of actual human anatomy with a mannequin built that utilizes the same measurements as the computer models. Also, it provides a realistic force feedback during the skin incision,

the dissection through the intercostal muscle and the pleura, and the placement of the chest tube. Also, the VIRGIL chest trauma training system can be used in a classroom environment. The participants have responded enthusiastically to VIRGIL. They have cited a better visualization and an increase in the understanding of the procedure [38]. The system is used in a trainee/instructor configuration, with a 10 minutes per session, tracks the trainee's progress and detects the patterns of error.

2.10 Arthroscopy Simulators

Arthroscopy is a method of viewing or performing a surgery of a joint with the aid of an arthroscope, which consists of a tube, a lens, and a light source utilizing fiber optics. In an arthroscopic examination, an orthopaedic surgeon makes a small incision in the patient's skin and inserts the pencil-sized instruments that consist of a small lens and a lighting system to magnify and illuminate the structures inside the joint. The light is transmitted through fiber optics to the end of the arthroscope. By attaching the arthroscope to a miniature camera, the surgeon is able to see the interior of the joint through this very small incision. The image catured by the camera is displayed on a screen and consequently, the surgeon is capable of looking at the examined joint. Therefore, the surgeon can determine the amount or the type of the injury and repair, if it is necessary, the problem. Typically, this procedure is performed on the knee joint and is similar to the procedure performed on the shoulder, the wrist and the elbow.

Arthroscopic surgery is most commonly performed on the knee and shoulder joints. The arthroscopic surgery of the wrist, the elbow, the ankle and the hip are less common. The reason is that the knee and the shoulder are large enough to manipulate the instruments around, and they are amenable to arthroscopic surgery treatments. Due to the small incisions and reduced tissue's disruption, arthroscopy is increasingly being used in the treatment of the hand. Wrist arthroscopy, in particular, has proven to be extremely valuable in both diagnosis and therapy similar to the shoulder arthroscopy and the knee arthroscopy. It requires skills to be acquired by all hand surgeons.

2.10.1 Knee Simulators

The majority of virtual arthroscopy training systems are developed for the knee. Two important simulators are presented in [39] and [40].

In general, VR knee simulators consist of a computer platform, a video display, and usually two force-feedback interfaces that monitor the positions of the instruments in the user's hands. VR-AKS [29] is an arthroscopic simulator for knee surgeries and is developed by the American Academy of Orthopaedic Surgeons (AAOS). Besides the previous components, it contains a software that provides the mathematical representation of the physical world and replicates the visual, mechanical, and behavioral aspects of the knee. This includes the haptic interface and the execution of collision detection algorithm that prevents the instruments from moving through solid surfaces. The modeling software interacts with the algorithm to send the appropriate images to the video display. This simulator is used in an educational program. The program can be divided into two stages. The first step is to perform a proper arthroscopic examination of the knee. The second step involves the development and learning modules. In this context, the first step of the simulator is to train the users to complete a detailed and comprehensive examination of the knee joint. The simulator is programmed to provide a feedback to users during and after the training session. The measured and reported variables may include the time required to complete the examination, the user's ability to see the entire joint's space and whether the user has properly recognized all of the presented pathologies in the simulation. The second stage involves the creation of various learning modules. Furthermore, the simulator is opened for future enhancements and developments. For example, programmes can be written to reconstruct a torn anterior cruciate ligament.

Besides, a VR system that simulates arthroscopic knee surgery using volumetric object representations, real-time volume rendering and haptic feedback is presented in [30]. 3-D MRI or CT images of a specific patient are processed to generate volumetric object models. Then, they are displayed on the computer's monitor and manipulated by a force feedback device. The haptic device is used to control the relative object positions and simulate surgical procedures such as cutting, tearing, and suturing.

Another VR training system for knee arthroscopic surgery is presented in [31]. The system offers a cost-effective and an efficient alternative to the traditional knee training methods. Virtual knee models are reconstructed from the Visual Human project dataset [8]. Also, the device simulates soft tissue's deformation with a topological change in real-time using finite-element analysis. Then, a tailor-made force feedback hardware is built to offer a realistic tactile feedback.

2.10.2 Shoulder Simulators

Procedicus VA (Virtual Arthroscopy) is a VR simulator for arthroscopic surgery with interactive graphics and haptic feedback. It provides a safe and convenient way for education and training on arthroscopic procedures [34][35]. The first released module focuses on minimally invasive shoulder surgery [6]. The simulator has various modes including anatomy manipulation, pathology and subacromial decompression. Procedicus VA is virtually identical to the work with actual equipments and real patients. The primary difference is that the image observed by the surgeon is a computer generated image instead of a transmitted image from a fiber optic camera inside the shoulder. The arthroscopy trainer is geared towards surgeons who wish to adopt arthroscopic approaches to shoulder surgery as well as developers who wish to educate their customers on the same operations. Furthermore, surgeons, residents, students and physicians can practice shoulder arthroscopy and improve their skills in a fully realistic environment.

Another VR simulator for shoulder arthroscopic training is presented in [32]. The system allows the trainee to visualize the shoulder joint with a high degree of fidelity and to handle the instrumentation tools that are similar to the tools used in the procedures performed in the operating room. In addition, the simulator offers the possibility of having a panoramic view to orient the apprentice in the first learning phases of the operation. Also, the device integrates a force feedback system that enables users to feel the real touch of the anatomy during the practice and the training sessions.

The insightArthroVR arthroscopy surgical simulator is another arthroscopy training system for shoulders as well as for knees [33]. The system, manufactured by GMV,

includes: realistic anatomical models for healthy joints and a variety of pathologies, and a skill indicators subsystem that allows the evaluation of practitioner's skills. The simulator provides a training program that allows the practitioner to advance, learn and improve his skills through a series of exercises or training modules of increasing difficulty. Exercises cover a range of arthroscopic skill levels, from basic instrument handling and diagnostics to complex surgical procedures. Besides, this system contains a multipurpose tool that can be adapted to different joints and various arthroscopic techniques. Moreover, the insightArthroVR simulator comprises a base structure with interchangeable plastic models which represent the knee's anatomy and the shoulder's anatomy. The shoulder can be set up in the lateral decubitus or beachchair positions. Sensors detect the working positions of the models and recalibrate the system accordingly. A simulated arthroscopic camera and a light source can be independently rotated similar to real arthroscopic tools. As the camera is navigated through the simulated anatomy, a virtual image is displayed on the computer's monitor. Shoulder arthroscopy performed by the insightArthroVR simulator allows students to learn the correct exploration of the glenohumeral joint and the subacromial space, recognize the various pathologies, and treat them accordingly.

2.11   Advantages/Disadvantages

VR simulators allow the process of iterative learning through assessment, evaluation, decision making and error correction. Consequently, a much stronger learning environment is created. They offer a safe and a relaxed learning environment where failure does not result in an injury to a patient. Therefore, the real pressure exerted on students during training and practice sessions are avoided. Thus, medical students are trained using VR simulators and can perform different or specific surgical exercises. This allows them to develop proficiency with basic MIS skills before entering the operating room. Unlike real surgery, they are capable of performing different techniques to accomplish the same surgery and are able to view the same anatomy from different perspectives. Furthermore, VR simulators offer trainees the ability to perform exercises in real-time

with force feedback sensation which enables them to feel the resistance of the touched structure or object. Moreover, they are the solution to low availability and high cost of cadaver, and they avoid the ethical issues associated with animal experimentations. On the other hand, VR simulators are quite expensive to acquire and require certain maintenance. Also, it is necessary to purchase upgrade modules and/or new software as they are created.

2.12 Conclusion

Nowadays, the researchers on medical education depend heavily on VR simulators which have become one of the main components of changing radically the traditional medical training and the surgical certification scenarios. This chapter presented a review of most commonly MIS surgical simulators. The presented VR simulators, are classified based on their applications and their relation to the organs or areas they treat. The laparoscopic simulators are the most advanced VR systems. The commercially available laparoscopic systems can teach trainees the required skills. In addition, they are clinically validated in order to improve their performance in the operating room. Other types of simulators perform very well and they are used in several laboratories. Despite all the satisfactory results, VR surgical simulators are still research subjects.

Chapter 3

Segmentation and 3-D Object Generation

In this chapter the segmentation and the generation of the medical models of the imaged structures are described. First, the segmentation of the acquired CT images is illustrated. Subsequently, the reconstruction of the 3-D wrist model is performed. Second, the representation of the generated models in a virtual environment is presented.

3.1 Introduction

The segmentation of medical images in 2-D (slice by slice) or directly in 3-D using the volume dataset, has several useful applications in the medical field such as the visualization of the objects of interest and the estimation of the corresponding volume.

The active contour method [41][42] has been widely and successfully implemented for segmentation purposes, particularly, for medical image segmentation. This technique has been adapted and extended to achieve 3-D segmentation. However, it still suffers from initialization problems, i.e. bringing the active contour or deformable model sufficiently close to the boundary of interest to ensure convergence. On the other hand, the watershed segmentation method, a mathematical morphology based technique, has been commonly used in geological and histological images. The watershed concept was formalized by Buecher and Lantuéjoul [43] and was later turned into an "immersion-based" algorithm by Vincent and Soille [44]. The strength of the watershed segmentation approach is that it produces a unique solution for a particular image. Nevertheless, the

noise in the image results in an over-segmentation of the Region of Interest (ROI). There-fore, the over-segmentation problem can be solved by placing markers in the regions of interest.

3.2   Marker-Based Watershed Segmentation

In general, the watershed segmentation technique considers a grayscale image as a topo-graphical relief i.e. the gray level of a pixel represents the altitude of a point. In this context, the basins and the valleys of the relief represent the dark areas, whereas the mountains and the crest lines correspond to the bright areas.

The principle of the watershed algorithm can be illustrated by imagining the magni-tude of the gradient of the original image as a relief immersed in water with holes pierced at local minima. The water fills the basins starting at these local minima (bottom of the relief at grey-level 0) and dams are built at the points where waters coming from dif-ferent basins would meet. Every time the water reaches a minimum, which corresponds to a region in the original image, a catchment basin is grown. When two neighboring catchment basins eventually meet, a dam is created to avoid the water spilling from one basin into the other. When the water reaches the maximum grey-value, the edges of the union of all dams form the watershed segmentation. This approach usually leads to an over-segmentation. Therefore, the watershed algorithm is implemented based on a set of markers placed in the region of interest to avoid the over-segmentation. Thus, only catchment basins in regions with a marker are grown and consequently, a binary segmentation of the image is obtained.

3.2.1   Segmentation of CT Images

In this thesis, the objective is to detect the contour of the bones in the CT images and to generate distinct segment for each bone. The segmentation is achieved using the marker-based watershed approach [45] because it is a powerful and a fast technique for contour detection and region based segmentation [46]. Having a gradient image, the watershed approach find a thin separation between the components of the given set of points i.e.

the markers. Figures 3.1 and 3.2 shows the original image and the gradient image with markers, respectively. Consequently, the watershed algorithm is implemented by region growing from the set of markers. At the end of the process, all minima are completely separated by dams, called watershed lines. The result is shown in figure 3.3.
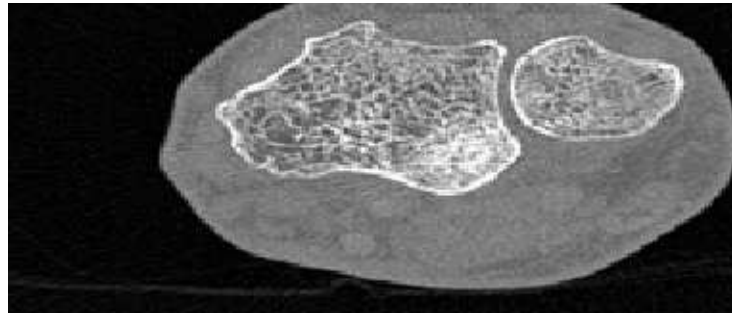
Figure 3.1: 2-D Slice of CT Image
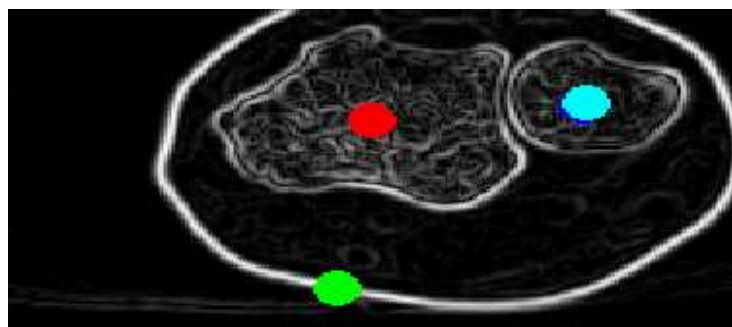
Figure 3.2: Gradient of CT Image with Markers
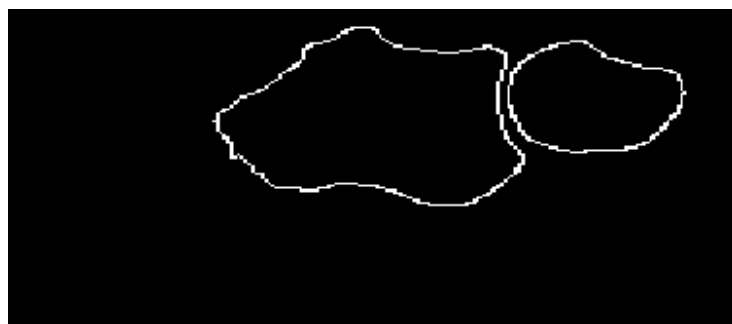
Figure 3.3: Watershed Result

The final result of segmenting the set of CT images is a volumetric image that represents the labeled bones. Figure 3.4 shows the final 3-D image of the wrist.
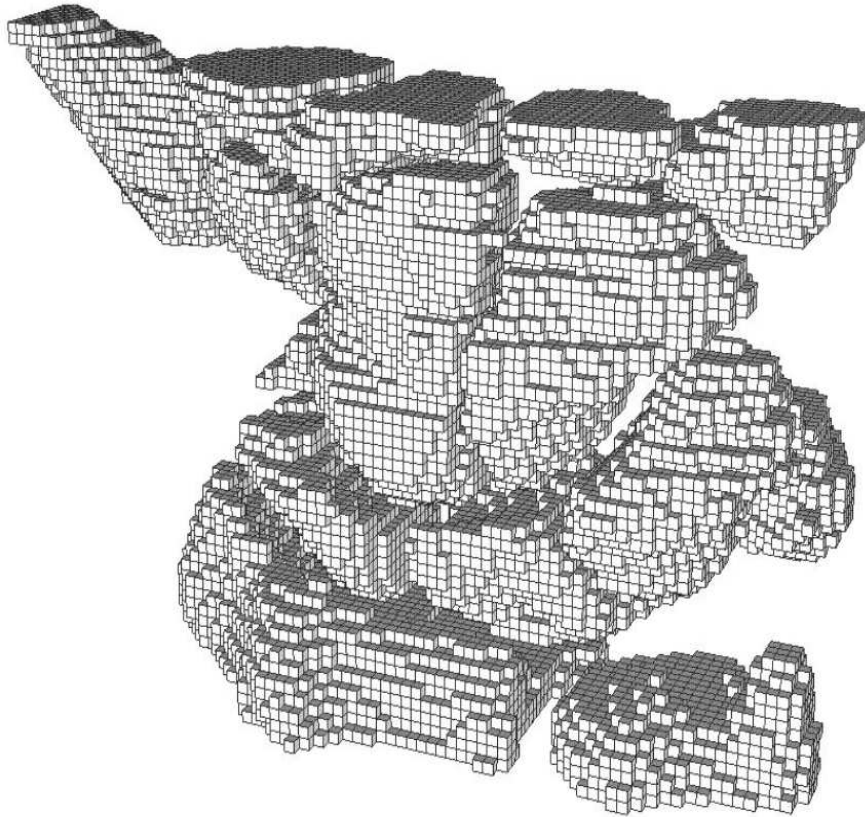
Figure 3.4: Image of the Wrist

3.3 The Marching Cube Algorithm

Having segmentated the set of the acquired CT images, the Marching Cube (computer graphics algorithm presented in [47]) is used to construct the boundaries of the objects. Each bone is considered to be one object. The algorithm finds the appropriate surface patch from a look-up table and builds the corresponding patch, interpolated according to the values of the eight corners of the unit cube. The union of all these patches constitutes the approximated iso-surface without any singularity and self-intersection. Then, a list of facets is generated. The algorithm can be summarized in three main steps:

1. Locate the surface in a cube of eight pixels

2. Calculate the normals

3. March to the next cube

The basic principle of the marching cube algorithm is to subdivide the space into a series of small cubes. Then, the algorithm instructs the user to "march" through each of the cubes by testing the corner points and by replacing the cube with the appropriate set of polygons. The sum of all generated polygons will be the surface that approximates the ones that the data set describes.

A voxel is defined by the pixel values at the eight corners of the cube. If one or more pixels of the cube have values less than the user-specified iso-value and one or more pixels have values greater than the specified value, the voxel must contribute some component of the iso-surface. Then, triangular patches are created by determining which edges of the cube are intersected by the iso-surface. The patches divide the cube into regions within the iso-surface and regions outside. The connection of the patches from all cubes on the iso-surface boundary results into a surface representation [48]. Each corner is specified as either being below or being above the iso-value and consequently there will be 256 (2 power 8) possible configurations of corner classifications. The facet configuration is looked up in a table that contains the various possible edge intersection configurations. Using the symmetric properties, the 256 configurations can be reduced to 15 basic configurations, which are shown in figure 3.5.
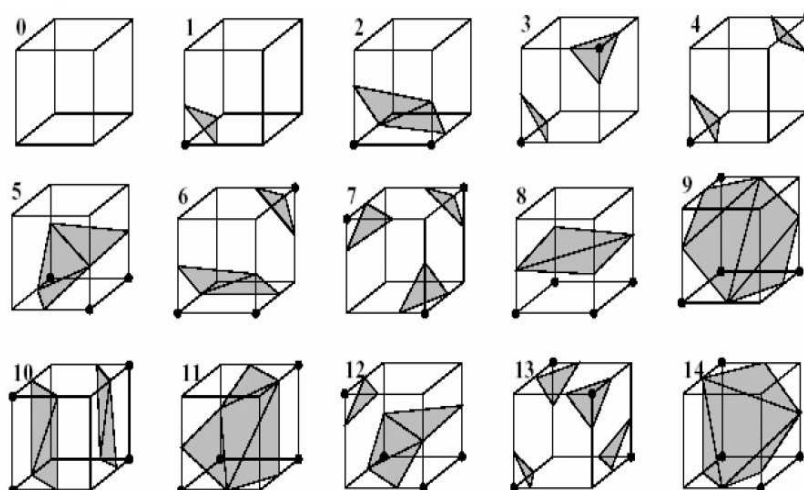
Figure 3.5: The 15 Cubes Combinations of the Marching Cube Algorithm

The output of the marching cube algorithm is a list of facet constituting the 3-D model. Figure 3.6 shows the facets of the wrist model.
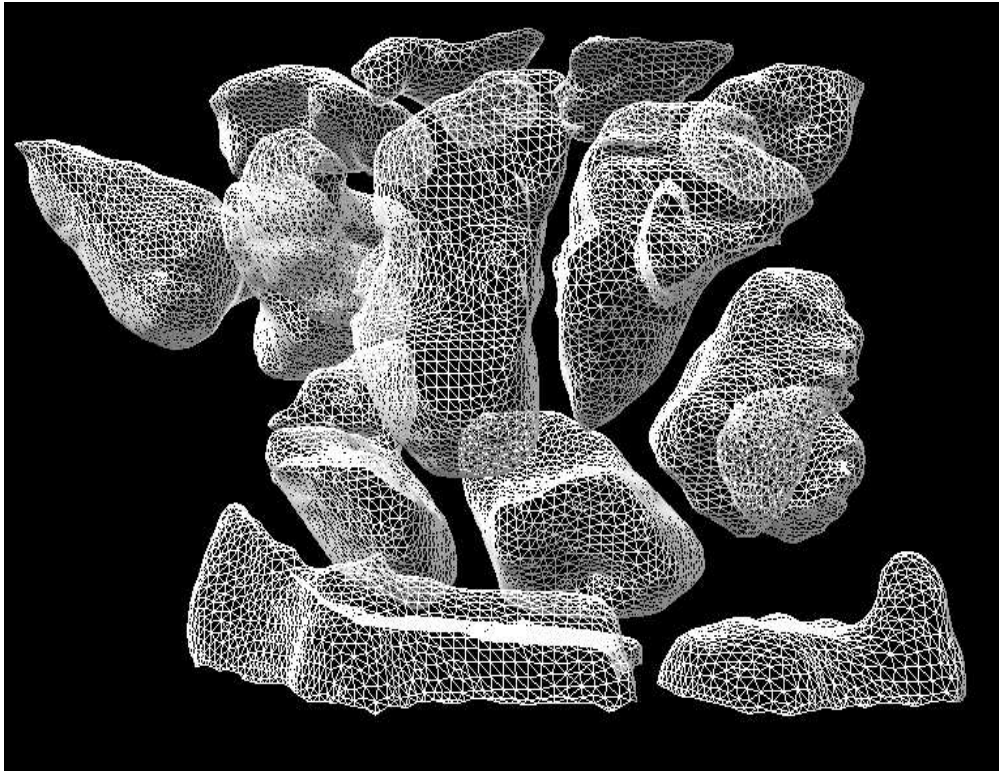
Figure 3.6: The Facets of The Wrist Model

3.4 Material and Lighting

The implementation of the Marching Cube algorithm involves the determination of the gradient of the scalar field. The latter is obtained at each grid point and is also the normal vector of a hypothetical iso-surface at that point. Therefore, the interpolation of these normals along the edges of each cube leads to the determination of the normals of the generated vertices. These normals are essential to perform a shading procedure on the resulting mesh with some illumination (lighting).

When light is added to a 3-D scene, all the objects to be lighted must have a material. The material specifies the color, the light reflection and the transparency. Usually, the material node has six fields: diffuse color, emissive color, ambient intensity, shininess,

specular color and transparency. The diffuse color field defines the color of the geometry. While, the emissive color defines the glowing objects, the specular color field reflects the color of the shiny spots of the geometry. The ambient intensity field specifies the amount of light reflected by the geometry. The shininess controls the intensity of the glow for the shiny spots i.e. small values represent soft glows and high values represent smaller and sharper highlights. Finally, the transparency field controls the transparency of the associated geometry i.e. if the value is 0, the related geometry is completely opaque and if the value is 1 the geometry is completely transparent.

Having identified the normals and defined the material, the next step is to add the light to the scene. The addition of light can make a big difference to the final appearance of the 3-D model. The reflected light from the figure is affected by the color of the material. Therefore, having selected the material, the color, the direction and the position of the light source, the virtual representation of the 3-D wrist model is generated. Figure 3.7 shows a 3-D virtual model of the wrist.
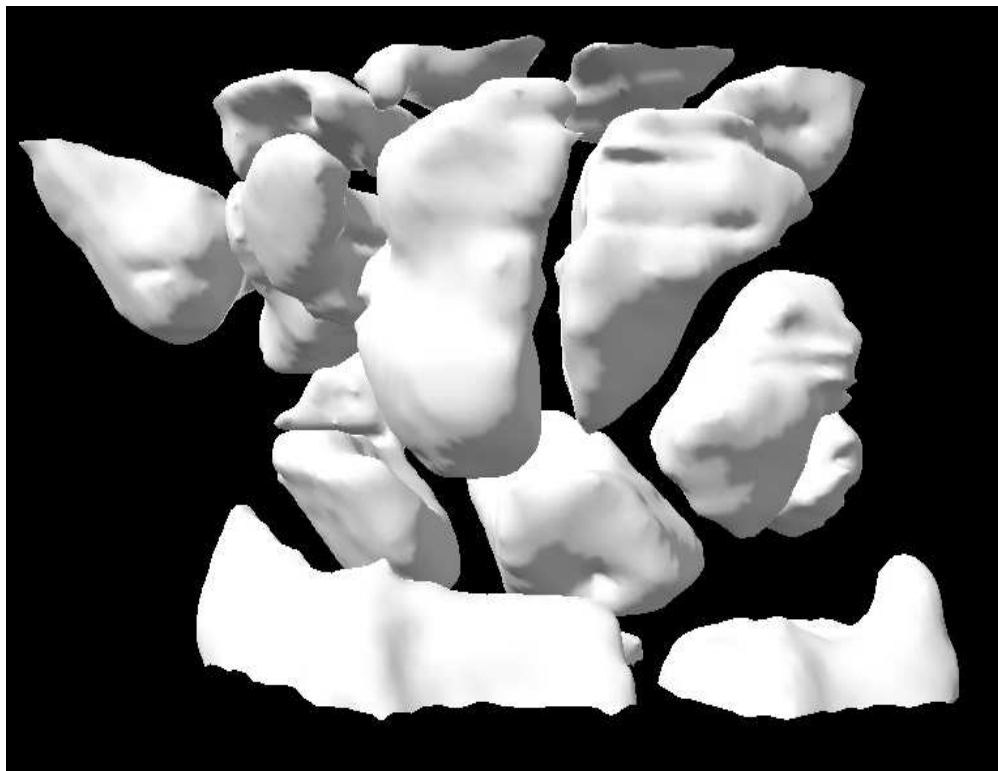
Figure 3.7: 3-D Virtual Model of the Wrist Bones

3.5   Texture Mapping

Having generated the 3-D wrist model and created the corresponding effects using the color and materials, an interesting feature called texture mapping, is introduced. This feature allows the user to attach graphic images to the created object. Therefore, the texture mapping is a method to add details and surface texture to a computer-generated graphic or 3-D model.

When a texture is mapped to a primitive shape, the same image is placed on all faces of the shape. The texture image can be stretched to fit the face if it is necessary. Figure 3.8 shows an affine texture mapper that maps a rectangular bitmap texture (120x130 pixels with 256 colors) to a triangular polygon with a full texture coordinate support.
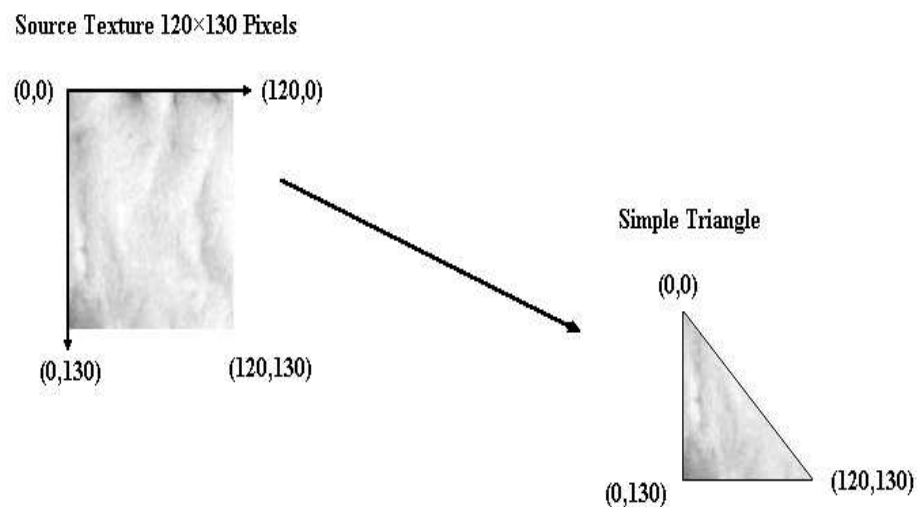
Figure 3.8: Texture Mapping: Source to Destination

The texture mapping is a multi-step process. The steps of the texture mapping process can be summarized as follows:

1. Select the texture image to be mapped

2. Use 2-D texture coordinates to describe the perimeter of the texture to be mapped

3. Bind the texture to a face on the shape

4. Bound each corner of the texture peice to a 3-D coordinate on the face

This process is applied to the generated 3-D virtual model of the wrist. Figure 3.9 shows the 3-D model after the implementation of the texture mapping process.
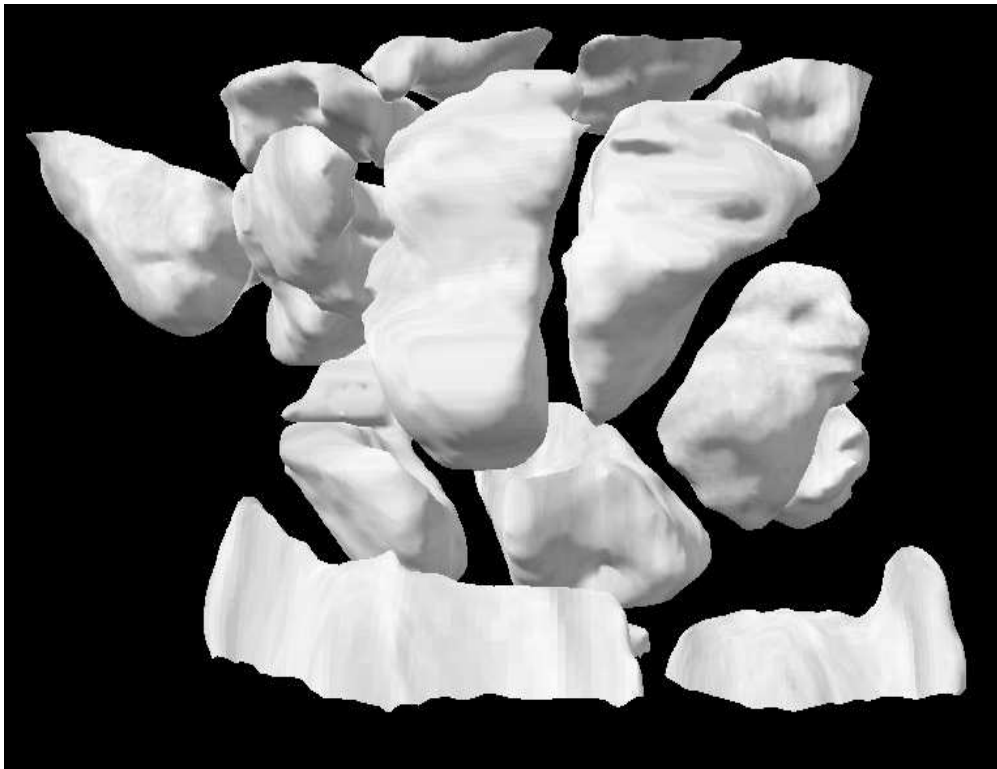
Figure 3.9: 3-D Virtual Model of the Wrist Bones After Texture Mapping

3.6   Pseudoarthrosis of the Scaphoid

3.6.1   Anatomy of the wrist

The anatomy of the wrist's joint is extremely complex. The wrist is actually a collection of many bones and joints [91]. There are fifteen bones that constitute connections from the end of the forearm to the hand. The wrist itself encloses eight small bones, called carpal bones. These bones are grouped in two rows: the proximal row and the distal row. The proximal row of carpal bones is made up of three bones: the Scaphoid, the Lunate and the Triquetrum. The second row of carpal bones, called the distal row, is made up of five bones: the Trapezium, the Trapezoid, the Capitate, the Hamate and the

Pisiform. The proximal row of carpal bones connects the two bones of the forearm, the Radius and the Ulna, to the bones of the hand. The bones of the hand are called the metacarpal bones. Five metacarpal bones exist (1st, 2nd, 3rd, 4th and 5th Metacarpal). They are the long bones that lie within the palm of the hand. The metacarpals are attached to the phalanges, which are the bones of the fingers and the thumb.

Figure 3.9 showed a 3-D virtual representation of the dorsal wrist. While, figure 3.10 illustrates a 3-D virtual representation of the volar wrist of the same patient.
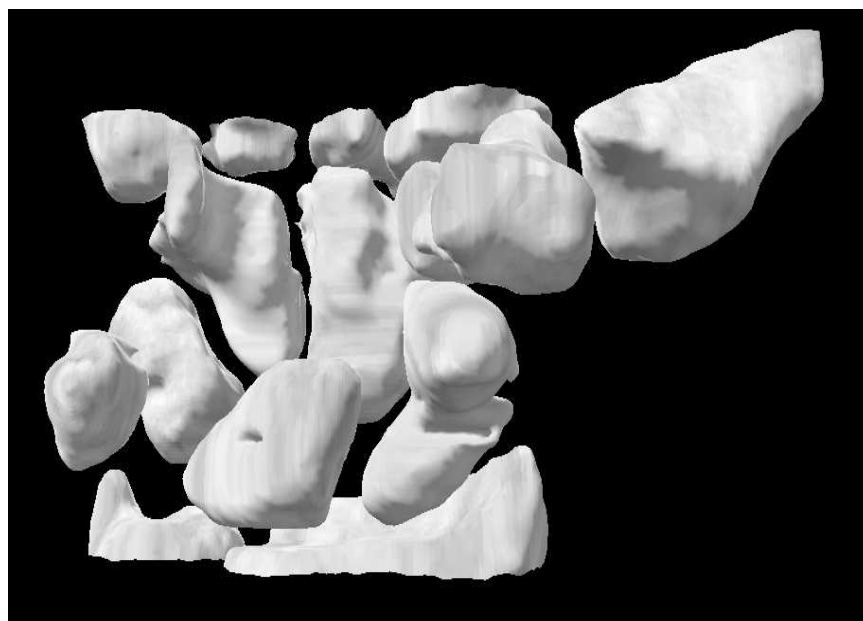
Figure 3.10: Volar Wrist Representation

3.6.2 Pseudoarthrosis

Pseudoarthrosis is the formation of a false joint caused by the failure of the bones to fuse [49]. This occurs when the bones do not heal properly after a fracture. Pseudoarthrosis usually causes pain and additional surgery is required to align the bones and fuse them together.

The 3-D wrist model generated form the scanned images of the patient has a pseudoarthrosis of the scaphoid. The arrow in figure 3.11 shows this pseudoarthrosis. Therefore, the goal of the proposed VR simulator is to operate the scaphoid in order to heal the two

fragment of the fractured bone virtually and to teach medical student on such operations.
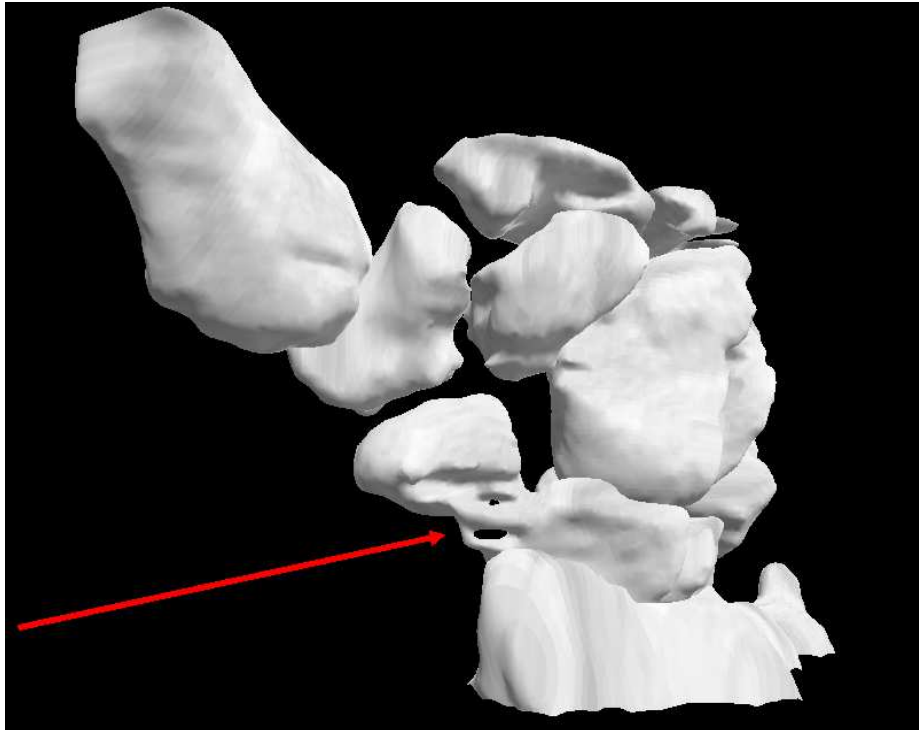
Figure 3.11: Pseudoarthrosis of the Scaphoid

3.7 Conclusion

In this chapter, the segmentation of the acquired set of CT scans of an imaged structure, namely the wrist, is presented. A 3-D representation of the corresponding medical models is also introduced. The segmentation is performed using the maker-based watershed algorithm and the construction of the boundaries of the 3-D wrist model is accomplished using the marching cube algorithm. Then, the representation of the generated models is illustrated in a virtual environment by associating all the necessary elements (light, materials and texture mapping).

Chapter 4

Convex Hull: A New Hybrid Approach

In this chapter, a new hybrid approach to generate the Convex Hull (CH) is developed and presented. The new algorithm is validated by performing a comparison with conventional algorithms namely the Brute Force, the Gift Wrapping, the QuickHull and the Chan algorithms. The evaluation is achieved by generating the convex envelope of 3-D wrist bones using the five different approaches. The results show the improvement associated with the proposed approach.

4.1 Introduction

In general, a real object does not have a deterministic shape. Therefore, it is impossible to define a geometric equation to model such an object. Thus, alternative approaches are the CH algorithms to form the convex envelopes of any object and to mimic realistic environment with exact collision detection between objects in the virtual world. Also, CHs play an important role in many applications that are based on cluster analysis, image processing and pattern recognition [50]. Other problems can be reduced to CH such as half-space intersections [51], Delaunay triangulation and Voronoi diagrams [52].

Since computers are used to simulate a physical environment, the simulation of the model is essentially based on geometry. Many of the computational problems associated with designing and building a VR system are geometric in nature. An important problem that must be addressed to make VR more realistic is the problem of real-time interactive

collision detection. Most exact collision detection systems work almost exclusively with convex objects because they have certain properties that make them highly suitable for testing the intersection. Actually, convex hulls or convex envelopes have received considerable attention to tackle geometric problems. These kinds of problems are usually not easy to deal with and they are known to be NP-hard. Also, fast algorithms that compute CH are still a challenging issue in many fields and research areas for real-time applications.

4.2 Convex Hull Definition

The convex hull or convex envelope of a finite set S of n points in the Euclidean space $\Re^d$ of dimension d, denoted as $CH(S)$, is defined by the smallest convex set containing all the points or simply the intersection of all half-spaces containing the set S. The CH in $\Re^d$ is the set of solutions to a finite system of linear inequalities in d-variables:

$$CH(S) = \{x \in \Re^d : Ax \leq b\} \tag{4.1}$$

Where $A \in \Re^{n*d}$ and $b \in \Re^n$.

A solution of the above system can be written as:

$$CH(S) = \sum_{i=1}^{n} \lambda_i p_i, \sum_{i=1}^{n} \lambda_i = 1, \lambda_i \geq 0 \tag{4.2}$$

4.3 Related Work

One of the central problems in computational geometry is the computation of CHs. It is an intensively studied subject by researchers. Early studies dealt primarily with the planer 2-D case [53]. Currently, this interest has been extended to calculate CH in 3-D space [54].

Brute Force is a simple algorithm that works in both 2-D and 3-D to construct the convex envelope of the object under analysis. It requires a running time in the

order of $O(n^3)$ and $O(n^4)$ for a 2-D and a 3-D application, respectively. A lower bound algorithm is proposed by Yao [55] to compute the CH vertices using a quadratic decision tree model and has a complexity of $O(nlogn)$. This lower bound was later generalized to the algebraic decision tree and to the algebraic computation tree models developed by Ben-Or [62].

Another 2-D approach, known as Graham's scan [56], achieves a running time in the order of $O(nlogn)$. Jarvis March algorithm constructs the convex envelope in $O(nh)$ time, where h denotes the number of vertices of the convex hull. It can be implemented for 2-D/3-D CH and it is output sensitive because it depends on h in its running time. Furthermore, a 2-D divide-and-conquer algorithm [57] is proposed following the implementation of sorting algorithms, such as MergeSort and QuickSort, and needs $O(nlogn)$ running time. Based on this algorithm, Preparata and Hong presented their first $O(nlogn)$ time algorithm in 3-D. QuickHull [58] is another fast technique that works in 2-D and can be generalized to 3-D case. The running time to compute the CH is also in the order of $O(nlogn)$. Moreover, Gift Wrapping is a 3-D algorithm that constructs the convex envelope in $O(nh)$ time [59]. This output sensitive method proposed by Chand and Kapur was a generalization of Jarvis's march and can be implemented with arbitrary dimensions.

A 3-D approach proposed by Chazelle and Matousek [60] has succeeded to accomplish running time in the order of $O(nlogh)$. Edelsbrunner and Shi [61] made up a deterministic technique that requires $O(nlog^2h)$ running time. The last two algorithms are not very practical and tend to be complicated. Thus, the problem of finding optimal and practical algorithms that construct convex envelope in 3-D remained.

4.4 3-D Convex Hull Algorithms

Four algorithms to construct the convex envelope of an imaged object in 3-D are described and discussed. They are: the Brute Force, the Chan algorithm, the Gift Wrapping and the QuickHull. Then, a hybrid technique based on the last two approaches is proposed and a comparison is performed between the individual algorithms.

4.4.1 Brute Force Algorithm

Brute Force is the simplest algorithm. However, it is the slowest. It begins by selecting a random point p_i and three other different points (p_j, p_k, p_l) as a facet on CH. Then, it checks if the point p_i is in the counterclockwise (ccw) direction with respect to the selected facet. The procedure is repeated by checking all the facets formed by all points other than p_i. If it is found that the selected point is in the counter clockwise direction with respect to all facets, then the point p_i is on the CH. In this manner, vertices on CH can be easily recovered.

It is clear that it is a time consuming algorithm. It needs $O(n^4)$ operations to construct the convex hull in 3D. This method becomes very slow if the set of input points is increased. Consequently, it is not an appropriate approach for real time applications.

4.4.2 Gift Wrapping Algorithm

The Gift Wrapping algorithm, known also as the Jarvis March approach, is developed to work with arbitrary dimensions. It consists of an initialization phase followed by a series of wrapping steps. The initialization phase begins by finding a starting edge (a, b). This is achieved by performing a 2-D algorithm on the projection of the points into the XY plane. Then, an initial plane P is pivoted around the edge (a, b) of the hull. It finds the smallest angle between the plane P containing the starting edge (a, b) and a plane T formed by point p_i and the edge (a, b). The point p_i is replaced by c and a triangular face containing (a, b, c) is formed. The plane (a, b, c) is a facet on the CH. All points now lie to the left of this plane. A set F of frontier edges is initially defined and contains the three edges (a, b), (a, c) and (b, c). Each frontier edge in F is associated with a triangle or facet on the CH of S. The wrapping steps are repeated recursively for the edges (a, c) and (b, c) to find other triangles adjacent to those edges. All steps are repeated for every explored edge until all facets have been examined. Figure 4.1 shows the steps for constructing the CH using the Gift Wrapping algorithm.

The Gift Wrapping algorithm needs $O(nh)$ time operations to construct the CH. It is clear that for every hull edge point, the algorithm requires $O(h)$ time where h is the

number of hull points. Hence for n points in the set, the total time complexity is $O(nh)$.
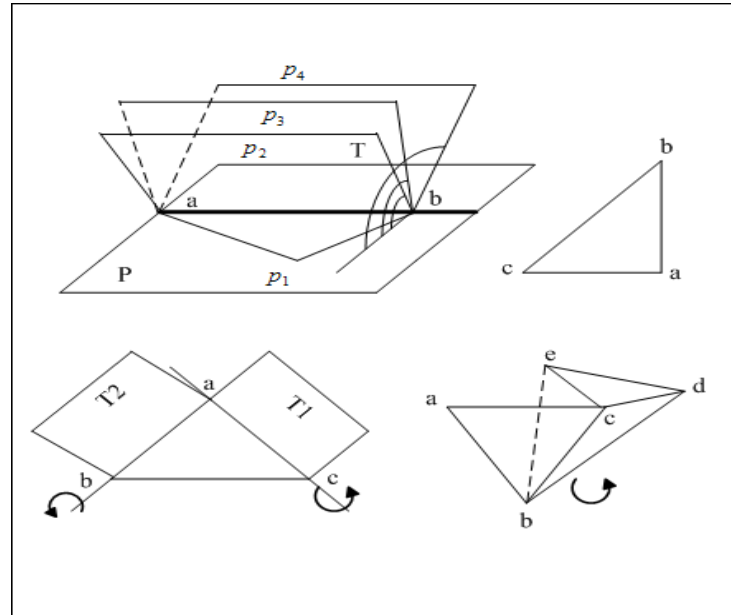
Figure 4.1: A Gift Wrapping Example

4.4.3 QuickHull Algorithm

The QuickHull algorithm finds the CH of n input points by recursively partitioning the input set. It shares similarities with sorting algorithms i.e. it is recursive and each step partitions the data set into several subsets.

QuickHull starts by dividing the set of points into two subsets with respect to a plane formed by: the vertices corresponding to the minimum (x_{min}) and maximum (x_{max}) abscises, and the vertex corresponding to the maximum distance (x_d) from the line joining (x_{min}, x_{max}). From this initial plane, QuickHull creates a polyhedra of new facets, called visible facets, by calculating the point that has the maximum distance (x_{dmax}) with respect to the plane. Therefore, QuickHull builds new sets of points from the outside set of the located visible facets. If a point is above multiple new facets, one of the new corresponding facets is selected. If it is below all the new facets, the point is inside the CH and consequently it can be discarded. Partitioning also records the furthest points of each outside set. Each point p in the outside set is processed to

locate a visible facet. Visible facet means that the point p is above the specified facet. It constructs a polyhedra from the processed point p to the horizon edges of the visible facets. Then, the visible facet is deleted and the newly created polyhedra of facets is added to the CH. The outlined steps in this paragraph are repeated recursively for every point in the new outside set. Figure 4.2 shows the steps for constructing the CH using the QuickHull algorithm.
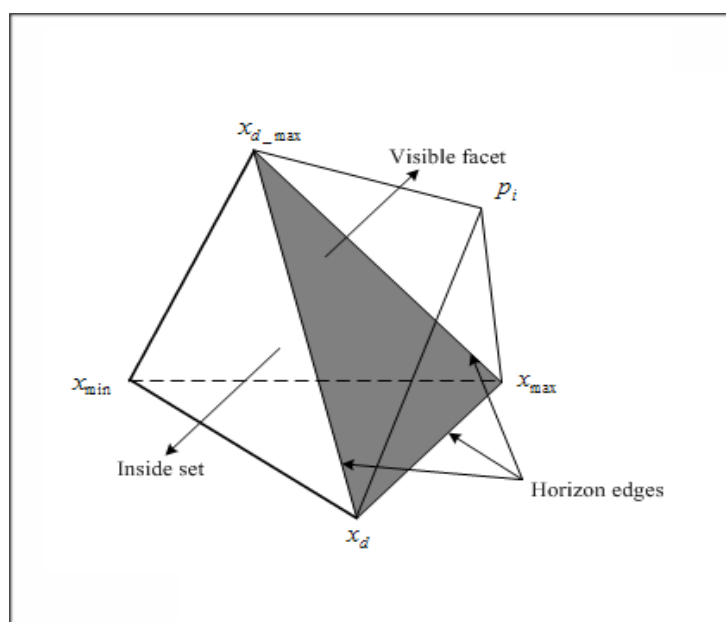
Figure 4.2: A QuickHull Example

$O(nlogn)$ time operations are required to compute the convex envelope using the QuickHull algorithm. The points will be partitioned into two equal sets and hence the depth of the recursion is $(logn)$. At each level of recursion, there are $O(n)$ operations. Therefore, the overall average time is $O(nlogn)$.

4.4.4   Chan Algorithm

This algorithm is proposed by Timothy Chan and it is an output sensitive algorithm. It constructs the CH of n points in 2-D and 3-D [64]. It starts by dividing the input points into (n/N) arbitrary disjoint and equal subsets. Each subset has a size N. In 3-D, the algorithm computes the convex envelope of each group using the Preparata and Hong's

approach and store the output in a Dobkin-Kirkpatrick hierarchy. Thus, (n/N) CHs are formed. The pre-computed convex polygons are integrated into one final convex output by executing the Gift Wrapping algorithm. The latter approach computes the hull facets one at a time as follows: for a given facet f, three adjacent facets f_j are generated by performing a wrapping step about each of the three edges e_j of f where $(j = 1, 2, 3)$. Given an initial facet f_0 obtained using two wrapping steps, a breath-first or depth-first search can generate all facets that constitute the CH.

Figure 4.3 shows the steps for constructing the convex envelope in 2-D using the Chan algorithm.
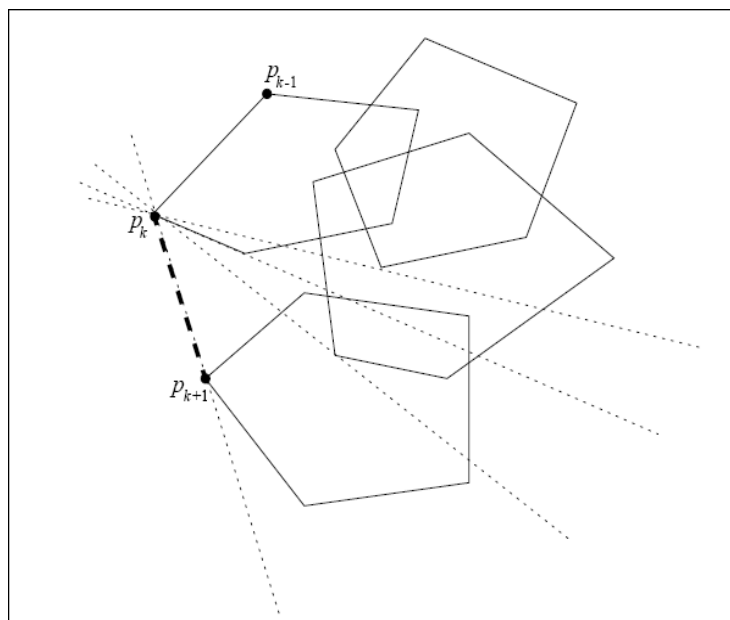
Figure 4.3: Wrapping a set of [n/m] convex polygons of size m

Assuming that N = h, Chan algorithm takes $O(nlogh)$ time operations to construct the CH. This assumption is not logical because h, the number of points on the CH, is not known. Thus, the problem is reduced to estimate the value of N. An approach can be based on guessing the value of the parameter that affects the running time. This can be achieved through trial-and-error, i.e. select N = 1,2,3..., until the value $N \geq h$ is reached. However, this could be a time consuming approach. On the other hand, if the value of N is increased quickly, there is a risk in selecting N to be much larger than h. The best

way is to choose (at the beginning) small values of N and increase it successively by squaring each time the value until the algorithm returns successful results. This process is called the doubling search. In other words, at iteration t (starting at t = 0), a value of $N = min(2^{2^t}, n)$ is selected and the steps of the Chan algorithm are repeated until $N \geq h$. Consequently, the convex envelope is formed.

4.5   The Hybrid Algorithm

Several methods are developed to speed up CH algorithms by preprocessing the input set of points. Some techniques start by dividing the input points into two arbitrary sets, right and left, followed by the computation of the final CH. Divide-and-Conquer is such an algorithm that starts recursively by computing the convex envelopes of the right and the left sets followed by merging the two hulls into a final convex output [63]. Other techniques divide the input points into many subsets such as the presented Chan algorithm. It starts by dividing the input points into (n/N) arbitrary disjoint subsets. Each subset has a size N. Then, the convex envelope of each group is computed. Thus, N partial hulls are formed and they are integrated into one final convex output. The idea underlying these techniques is always dividing a large set into several subsets in order to speed up the running time of the algorithm and reduce its complexity. In this context, a hybrid technique is proposed to construct the CH with a faster time by preprocessing the input set of points. Two important points are taken into consideration:

- The running time of the convex hull algorithms depends on the number of points n that constitutes the object.

- The wrapping step embedded in the Gift Wrapping algorithm can be achieved faster if the set of input points is preprocessed.

Therefore, a hybrid approach to generate the CH is developed. It is based on Quick-Hull and Gift Wrapping algorithms. It is decomposed into two stages. The first stage

reduces the number of the input points. The second stage underlines the reconstruction of the corresponding convex envelope. A pseudo-code of the hybrid algorithm is illustrated below (Algorithm 1).

Algorithm 1 The Hybrid Approach To Construct the CH

1: **find** an initial plane from the *min* and *max* abssice and the *max* distance with respect to (x_{min}, x_{max})
2: **construct** a polyhedron from the initial plane and the max distance to this plane
3: **for** each facet F of the polyhedra **do**
4:     **for** each unassigned point p **do**
5:         **if** p is above F **then**
6:             assign p to $F's$ outside set
7:         **end if**
8:     **end for**
9: **end for**
10: Discard all points inside the polyhedron forming a new imput set (n_{new})
11: **find** a starting edge (a, b) using the 2D Gift Wrapping algorithm on the XY projection
12: **for** i = 1 ... n_{new} **do**
13:     **find** point p_i corresponding to *min* angle bewteen plane P in XY containing (a, b) and plane $T = (a, b, p_i)$
14:     **replace** $c \leftarrow p_i$
15:     **save** (a,b,c) into Q
16:     wrap the edge (a, c)
17:     **if** facet has been explored **then**
18:         wrap the edge (b, c)
19:         **if** facet has been explored **then**
20:             **return**
21:         **end if**
22:     **end if**
23: **end for**

The hybrid method is initiated by applying the QuickHull algorithm to divide the input points into two subsets (upper and lower) with an initial plane. Then, a polyhedron of new facets is created by calculating the point having the maximum distance with respect to this plane. Consequently, the points that are inside the polyhedron are inside the convex envelope and they are discarded. The same procedure is repeated for the lower set. This leads to the reduction of the number of input points and the formation of a new data set. The new set is fed as an input to the Gift Wrapping algorithm.

Consequently, wrapping steps are performed by scanning the new data to obtain the final convex envelope. That is, the hybrid method apply the initialization phase followed by the series of the wrapping steps. It computes the facets of the hull one at a time, in the ccw direction using the sequence of the wrapping steps. The wrapping steps are repeated recursively for every explored edge until all facets have been examined.

4.6   3-D Models and Convex Hulls

The Hybrid approach to construct the CH is implemented. Different bones (3-D structures) having various dimensions (different number of vertices) and concavities are chosen. Figure 4.4 shows the Capitate bone before (upper left) and after (upper right) the implementation of proposed algorithm to construct the CH of the corresponding bone. Also, it illustrates the Ulna bone of the wrist before (lower left) and after (lower right) the CH is formed using the hybrid approach.
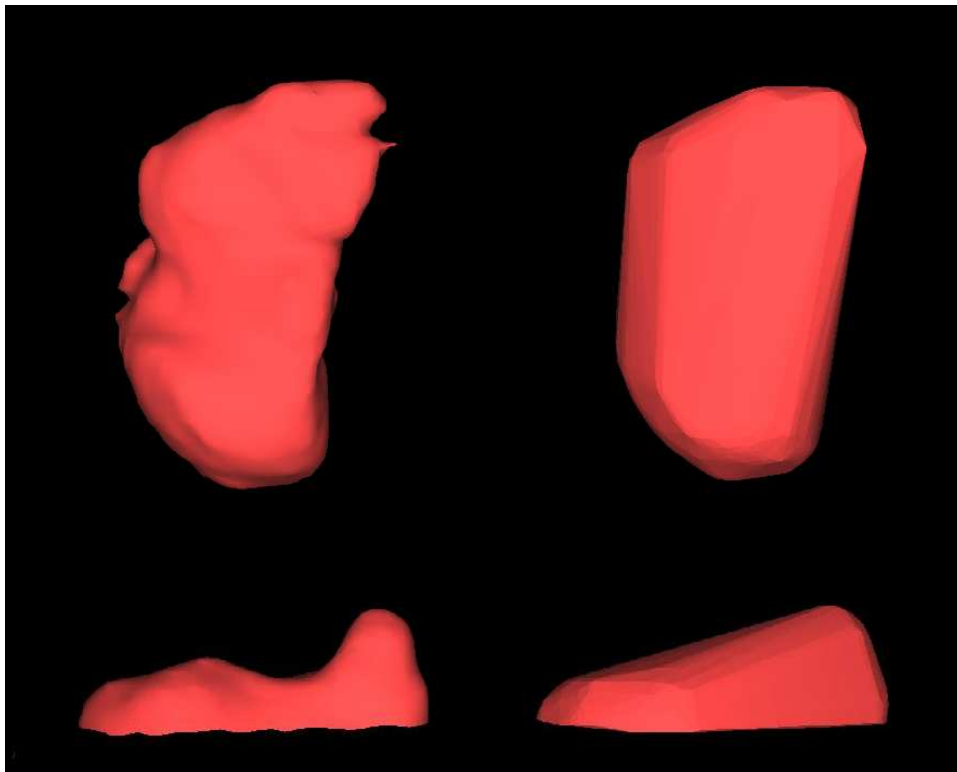
Figure 4.4: Capitate and Ulna with their Convex Hulls

Similarly, Figure 4.5 presents another two wrist bones, namely, the 3^{rd}Metacarpal (upper half) and the Scaphoid (lower half). In each half, the 3-D objects (left) and the corresponding convex hulls (right) are shown.
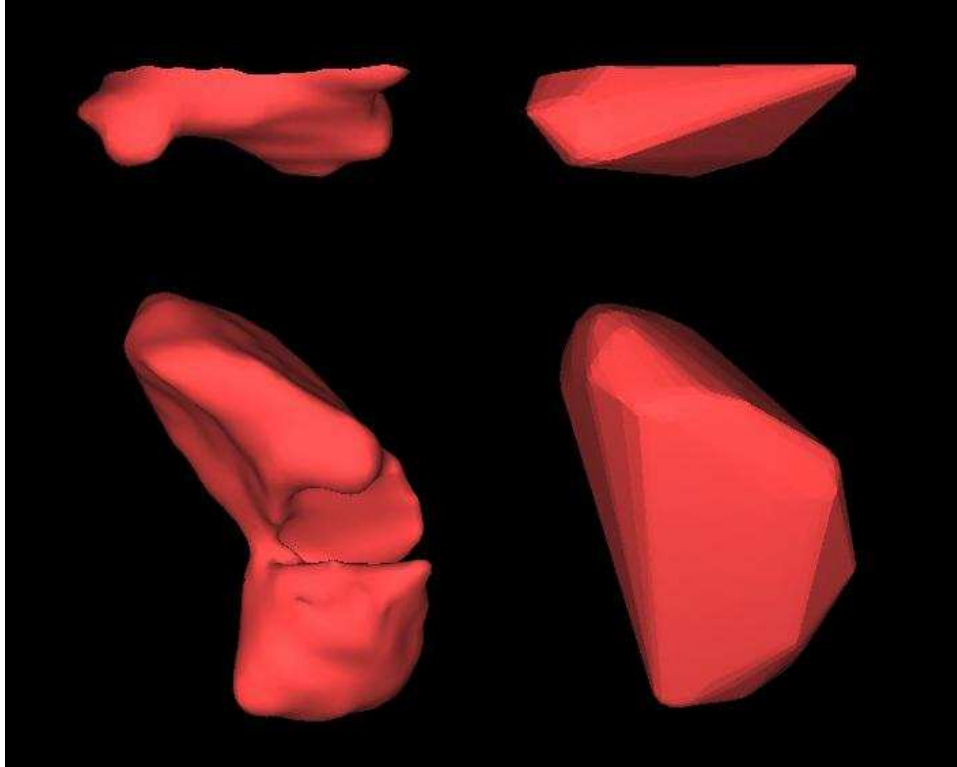
Figure 4.5: 3^{rd}Metacarpal and Scaphoid with their Convex Hulls

The conceptual basis for the collision detection is to construct a CH using the vertices of each object. Consequently, the collision is observed as the intersection of the corresponding CHs. In this regard, Figure 4.6 illustrates the collision detection problem in a realistic way. It shows different bones constituting the 3-D wrist model: 1st Metacarpal (a), 2nd Metacarpal (b), 4th Metacarpal (c), Scaphoid (d), Capitate (e), Hamate (f), Radius (g) and Ulna (h). Each bone is covered with its corresponding convex envelope.

In addition to the proposed approach (Hybrid algorithm), the conventional techniques (Brute Force, Gift Wrapping, QuickHull and Chan algorithms) are also tested and simulated using the 3-D data of a patient's wrist. A comparison is performed between these algorithms and the corresponding results are presented, analyzed and discussed.
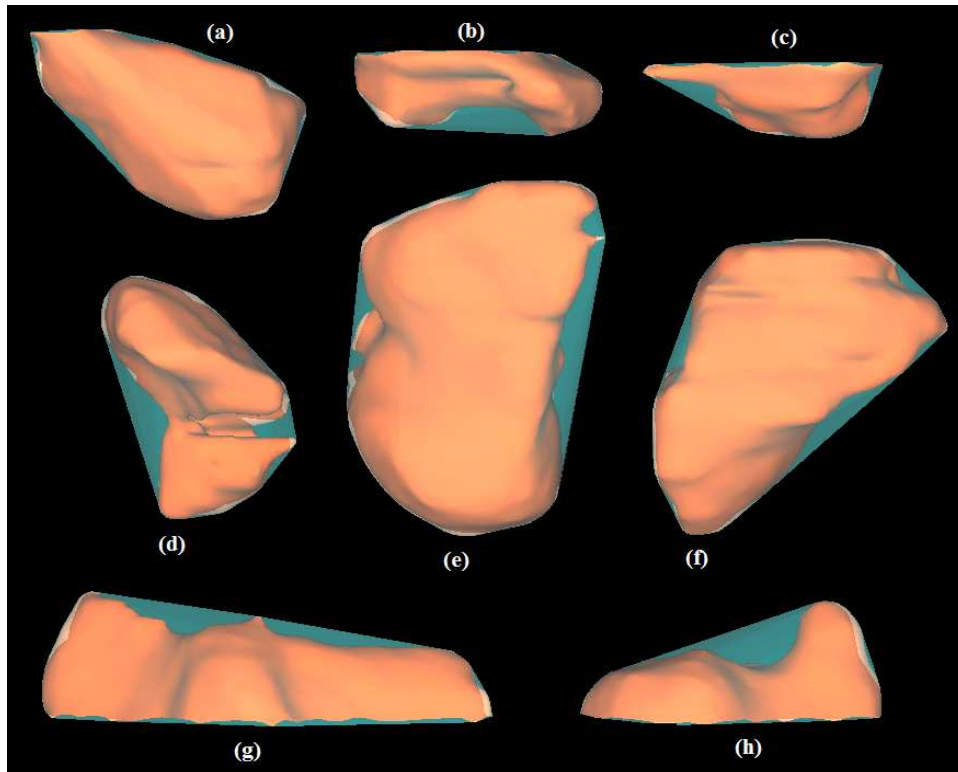
Figure 4.6: Bones of the 3-D wrist enclosed by their corresponding Convex Hulls

4.7 Simulations and Results

The Hybrid, the Brute Force, the Gift Wrapping, the QuickHull and the Chan algorithms are implemented and are evaluated quantitatively. That is, each technique is applied to reconstruct the CH of each bone and the corresponding execution times to achieve the indicated results are collected and analysed.

Table 4.1 contains the number of vertices and facets constituting the 3-D original model of the various 3-D wrist bones as well as the vertices and facets associated with the corresponding CHs. Also, it shows the execution time required by each algorithm to compute the convex envelope of a particular bone and to display the corresponding model. The results show that the Brute Force algorithm takes the longest time to construct the convex envelope compared to other techniques. Therefore, this algorithm is not practical especially in real time applications. On the other hand, the Gift Wrapping and the QuickHull algorithms are fast in computing the CH of all the wrist bones and

have approximately similar behaviour. The hybrid method and the Chan algorithm are faster than the latter approaches. The hybrid method outperforms the Gift Wrapping and the QuickHull algorithms in the reconstruction of all CHs of the various wrist bones. On the other hand, the hybrid technique surpasses the Chan algorithm in most cases especially, when the number of points that are reduced is high enough.

Table 4.1: Comparison of Execution time for Computing the 3-D Convex Hull of the Wrist Bones

3-D Model	Original Model		Convex Hull		Brute Force	Gift Wrap	QuickHull	Chan	Hybrid
	# vertices	# facets	# vertices	# facets	time (s)	time (s)	time (s)	time (s)	time (s)
1st Meta.	2179	4320	379	790	19014.22.1	0.66	0.61	0.39	0.43
2nd Meta.	1168	2258	300	596	12015.41	0.47	0.38	0.33	0.25
3rd Meta.	675	1272	150	296	2330.77	0.26	0.22	0.15	0.12
4rd Meta.	532	1002	147	290	2302.72	0.21	0.19	0.13	0.09
Hamate	2812	5620	394	784	19231.20	0.89	0.82	0.67	0.71
Ulna	977	1864	312	620	12153.03	0.41	0.37	0.32	0.22
Scaphoid	2890	5784	530	1056	22125.1	1.31	1.22	1.03	0.88
Capitate	3026	6048	635	1266	25300.35	1.46	1.38	1.31	1.25
Radius	2454	4754	288	572	11260.12	0.78	0.72	0.55	0.62

Similarly, table 4.2 shows the number of vertices and facets constituting the 3-D original model of the knee bones as well as the vertices and facets associated with the corresponding CHs. The execution time required for each algorithm to compute the convex envelope and to display the corresponding model is also presented. The table shows the results associated with the Gift Wrapping, the QuickHull, the Chan and the Hybrid algorithms. It is evident that the proposed approach surpasses the other conventional algorithms.

Table 4.2: Comparison of Execution time for Computing the 3-D Convex Hull of the Knee Bones

3D Model	Original Model		Convex Hull		Gift Wrap	QuickHull	Chan	Hybrid
	# vertices	# facets	# vertices	# facets	time (s)	time (s)	time (s)	time (s)
Fibula	3732	7460	914	1924	3.32	3.01	2.56	2.28
Patella	7058	14112	2228	4452	10.04	9.53	9.15	9.04
Tibia	27342	54680	2653	5301	46.16	44.02	33.19	30.12
Femur	34716	69428	3664	7324	83.27	81.03	69.89	63.32

4.7.1   Result Interpretation

In this subsection, the results are analyzed and a discussion is provided for both cases: the wrist and the knee.

Wrist

It is evident that the hybrid method reduces the number of vertices of the 3rd Metacarpal from 675 to 559 as a first stage. Then, the wrapping process constructs the corresponding convex envelope, i.e. translated into a reduction of the running time to 0.12 s. On the other hand, the Gift Wrapping algorithm, the QuickHull and the Chan algorithm require 0.26, 0.22 and 0.15 s, respectively. Thus, the proposed technique decreases the execution time by 53.87% in comparison with the Gift Wrapping, by 42.85% with respect to the QuickHull and by 13.33% with respect to Chan algorithm.

In the same way, the number of vertices of the Scaphoid is decreased form 2890 to 2539 using the proposed approach. Consequently, a decrease in the running time from 1.31 s (for the Gift Wrapping), 1.22 s (for the QuickHull) and 1.03 s (for Chan algorithm) to 0.88 s is achieved. That is, the running time of the proposed algorithm is decreased by 32.82, 27.86 and 14.56% in comparison with the Gift Wrapping, the QuickHull and the Chan algorithm, respectively. On the other hand, if the number of points is not reduced much, the Chan algorithm can outperform the hybrid approach in some cases and consequently, it constructs the convex envelope faster. The 1st Metacarpal and the Radius are illustrative examples of this case.

The achieved improvement using the hybrid approach is further illustrated in figure 4.7. It shows a graph representing the execution time of the 3-D CH algorithms for the various wrist bones. In this graph, each plot is associated with a different algorithm: the Hybrid, the Gift Wrapping, the QuickHull and the Chan algorithms. The execution time is plotted as a function of the number of vertices constituting each bone. The number of vertices represents nine of the 15 bones forming the 3-D wrist model presented in Table 4.1. It is evident that the hybrid method surpasses the Gift Wrapping and the QuickHull approaches for all the wrist bones and it performs better than the Chan algorithm in

constructing the CH of most of the bones. Subsequently, the hybrid method is very efficient and is practical in modelling 3-D medical data (wrist) and simulating them in the virtual environment.
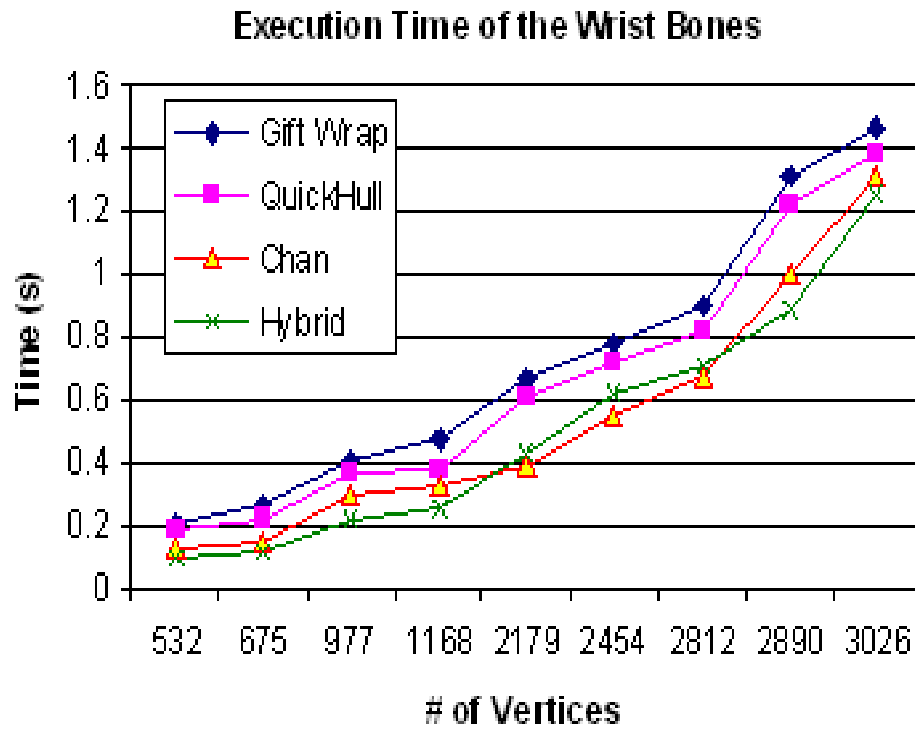
Figure 4.7: Execution Time of the 3-D CH Algorithms for Wrist Bones

Knee

The proposed method reduces the number of vertices of the Fibula from 3732 to 3662 as a first stage. Then, the wrapping process constructs the corresponding convex envelope leading to a reduction of the execution time to 2.28 s. On the other hand, the Gift Wrapping, the QuickHull and the Chan algorithm require 3.32, 3.01 and 2.56 s, respectively. Thus, the proposed technique decreases the execution time by 31.33% in comparison with the Gift Wrapping, by 24.26 % with respect to the QuickHull and by 10.93% with respect to the Chan algorithm. In a similar fashion, the number of vertices of the Femur is decreased from 34716 to 32490 using the hybrid approach. Consequently, a decrease in the running time from 83.27 s (for the Gift Wrapping), 81.03 s (for the QuickHull)

and 69.89 (for Chan algorithm) to 63.32 s is achieved. That is, the running time of the proposed algorithm is decreased by 23.96, 21.92 and 9.4 % in comparison with the Gift Wrapping, the QuickHull and the Chan algorithm, respectively. Therefore, the proposed approach reconstructs the CH of the knee faster than the other conventional algorithms.

The quantative evaluation of the hybrid approach is also illustrated in figure 4.8. It shows a graph representing the execution time of the 3-D CH algorithms for the knee bones. The execution time is plotted as a function of the number of vertices constituting each bone. The number of vertices represents the four bones forming the 3-D knee model presented in Table 4.2.
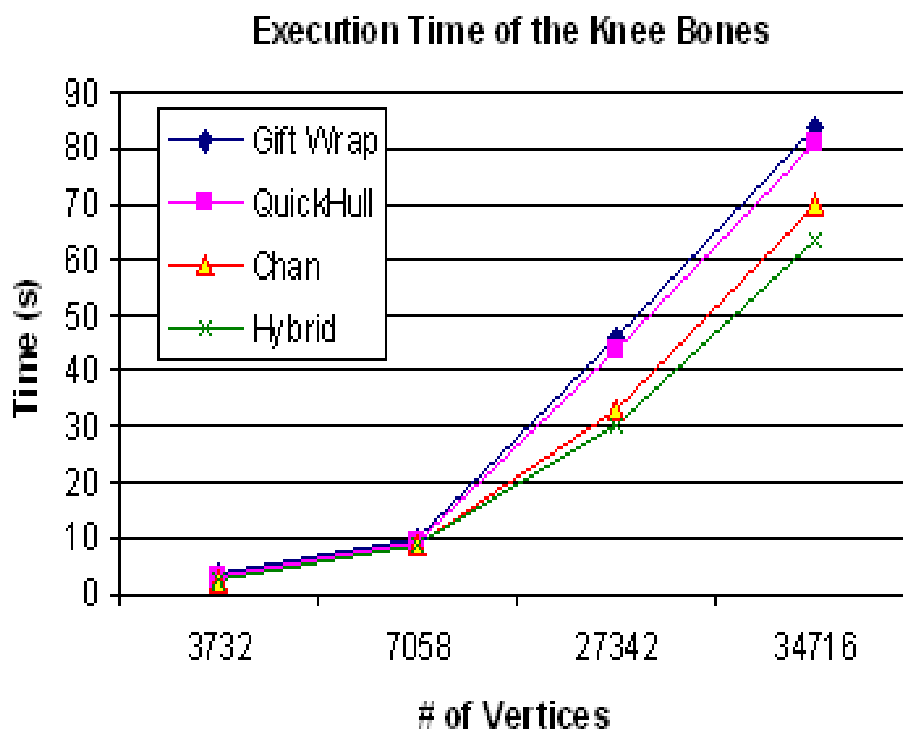
Figure 4.8: Execution Time of the 3-D CH Algorithms for Knee Bones

Similarly, it is evident that the hybrid method outperforms the three conventional approaches in the reconstruction of the CH of the bones constituting the knee model. That is translated into a reduction in the overall execution time (smaller value) and is clearly observed when the number of vertices is high.

4.8 Conclusion

Since most 3-D objects are not characterised by a shape that could be modelled using precise mathematical equations, CH algorithms are considered as a solution to model such objects. The need to CH algorithms arises with the intention of simulating realistic scenes with a real-time interactive collision detection between objects in the virtual world. Since fast collision detection systems work almost exclusively with convex objects, quick CH algorithms are implemented to fulfil real-time requirements. In this chapter, a hybrid approach to construct the CH of 3-D objects (bones of the wrist and the knee) is proposed and is compared with four published algorithms: the Gift Wrapping, the QuickHull, Chan and the Brute Force algorithms. The results show that the proposed approach performs faster than the other conventional techniques. That is, the execution time to construct the convex envelope is achieved in less time than the other approaches (i.e. a faster execution time). The proposed hybrid method is an output sensitive algorithm that works in 2-D as well as in 3-D. It is very efficient, practical and useful in modelling and simulating 3-D medical data in a virtual environment.

Chapter 5

Collision Detection: A Linear Programming Technique

In this chapter, the issue of the precise Collision Detection (CD) between virtual objects is addressed and a new technique is proposed. The CD problem is formulated and a linear programming solution is obtained to determine whether a collision exists or not. The proposed approach is compared with a conventional algorithm, namely, the Industrial Virtual Reality Institute Collision Detection (IVRI-CD) technique and is validated using bones from the 3-D wrist model. The results show that the proposed algorithm is efficient, fast, robust and leads to a decrease of the running time that is required to detect a collision.

5.1 Introduction

Collision detection or contact determination is the approach that reports a geometric contact when a collision is about to happen or has actually happened. It is of interest in several research areas such as robotics and computational geometry. CD is provided in every prototype system of computer-based surgical simulators. Most CD algorithms integrated in surgical simulators are based on solving systems of equations with dimensions proportional to the number of contact points between the objects. For example, in 3-D object models, the number of contact volume elements is proportional to the area of the contact surfaces resulting in thousands of contact elements for relatively small surfaces. In this regard, the issue of a precise CD between virtual objects is addressesed

and a new technique is proposed. First, the CH of each object is constructed. Then, the problem is formulated and a linear programming solution is obtained to determine whether a collision exists or not. The proposed CD approach is compared with a conventional algorithm namely the IVRI-CD technique and validated using bones from the 3-D wrist model. The results show that the proposed approach is efficient, accurate, fast and robust in detecting collision between virtual objects during training and experimenting surgery.

5.2   Previous CD Algorithms

One of the central problems in computational geometry and computer graphic applications is the real-time interactive collision detection. It is an intensively studied subject by researchers. It is of great importance in several applications such as robotics, interactive design, computer graphics and virtual reality [65]. CD algorithms are classified by their complexity, their overlap test and their computational time [79]. Figure 5.1 illustrates different types of bounding volumes for the same object. It shows the trade-off between the tightness of fit, the complexity and the precision in one hand and the overlap test and the computational time on the other hand.
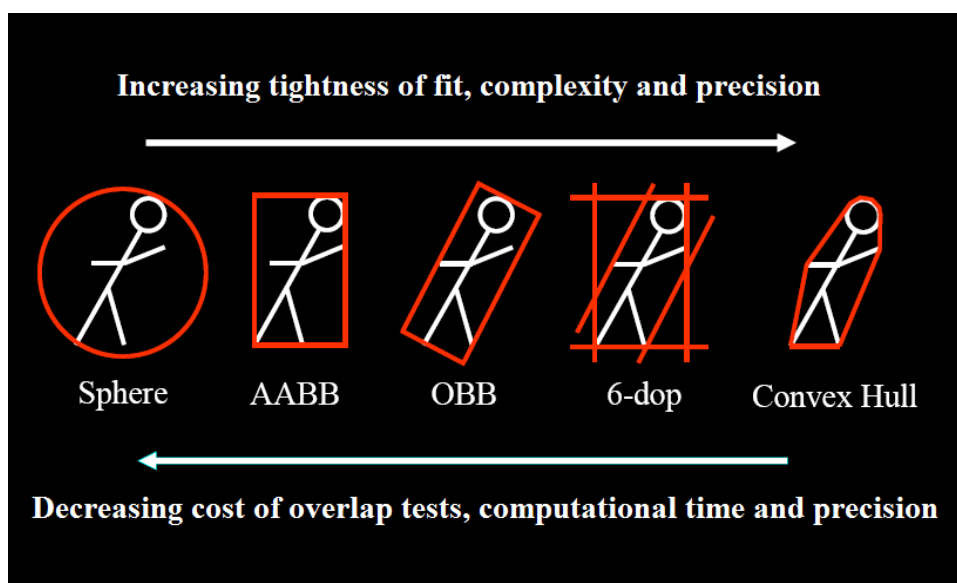
Figure 5.1: Different Types Of Bounding Volumes

5.2.1 AABB/OBB

Most collision detection algorithms are based on the bounding volumes approach. The absence of bounding volume collisions guarantees the absence of a collision between the corresponding objects. The bounding boxes techniques are used to identify the objects that may be in contact (in pairs) and to reduce the number of facets. Different kinds of static and dynamic sizes of bounding boxes are implemented. The bounding boxes are a preliminary test of collisions. The two effective methods are: Axis-Aligned Bounding Boxes (AABB) [66] and Oriented Bounding Boxes (OBB) [67].

5.2.2 Lin-Canny (LC)

An important CD approach is the Lin-Canny (LC) closest feature algorithm [68]. Lin and Canny have proposed the first algorithm that exploits the coherence [61]-[62]. This technique retains the pair of closest features i.e. vertices, edges or facets between two convex polyhedra by exploiting the fact that the current closest features are probably near the previous one. Having identified those features, the distance between the two polyhedra is found and a collision is declared. The algorithm starts from the closest pair that is computed in the last time step, and "walks" on the surface of the polyhedra until it reaches the new closest pair. The convexity guarantees that one can determine locally whether a pair of features is the closest pair, and if it is not, a neighboring pair is closer. Once those features are identified, the distance , which is below some ϵ, between the two polyhedra is found and a collision is declared. Finally, the Lin-Canny algorithm does not handle penetrating polytopes.

5.2.3 Gilbert-Johnson-Keerthi (GJK)

Another significant technique is the Gilbert-Johnson-Keerthi (GJK) algorithm [69]. The GJK approach involves an iterative procedure to determine the Minkowski difference between the convex objects among which the collision is being detected. The GJK algorithm is a Simplex-based algorithm. This approach uses the CH of a polytope and performs on the simplex defined by the subsets of these points [96]. The main strength

of this algorithm is that, in addition to detect whether two objects have collided or not, it can also return a measure of interpenetration. GJK achieves almost the same time complexity as Lin-Canny. Researchers have developed an enhanced version of the GJK algorithm, known as SOLID (Software Library for Interference Detection) [70]. It is a fast and a robust way to check for collision.

Besides, the use of bounding boxes is essential to speed up the computational time for collision checks when objects are far away. On the other hand, algorithms such as the LC and the GJK are required when the objects to be tested for collision are sufficiently close.

5.2.4 Voronoi-Clip (V-Clip)

Voronoi-Clip (V-Clip) [71] is another approach that tracks the closest pairs of features of convex objects in a similar fashion to the LC algorithm. However, it handles penetrating polyhedra and can be extended to the non convex polyhedra by representing them as groups of convex polyhedra.

5.2.5 I-Collide

The I-Collide [72] is an interactive and an exact CD library for large environments composed of convex polyhedra. It exploits the coherence and the properties of convexity to achieve a very fast and an exact collision.

5.2.6 Q-Collide

The Q-Collide [73] algorithm is developed to deal with the convex polyhedra. It works as follows: if two objects are not colliding, the algorithm finds a separating plane between them. Otherwise, a collision is reported. If a collision does not occur, the separating plane found for one time frame is cached as a witness for the next time frame.

5.2.7 Quick-CD

The Quick-CD algorithm is based on constructing hierarchies of bounding volumes (BV-trees) to approximate the input models [74]. The choice of bounding volumes is made

using Discrete Orientation Polytopes (DOP), which are convex polytopes whose facets have normals composed from a given discrete set of k vectors. In addition, Ehmann and Lin have introduced a new algorithm called SWIFT [75]. They have shown that this approach is faster and more robust than earlier techniques.

5.2.8 SWIFT

SWIFT is a C++ collision detection package. It can compute an exact and an approximate distance, and it allows the contact's determination between the 3-D polyhedral objects undergoing a rigid motion. It has been successfully applied to many applications such as virtual prototyping, dynamic simulation and path planning.

SWIFT works with geometric models that are closed, convex or composed of convex pieces and with any objects composed of a set of polygons that describe the boundary of a solid in 3-D. The SWIFT algorithm is based on the Lin-Canny approach to minimize the distance between two convex models. The intersection is tested directly without the need to construct any bounding volume hierarchy. However, the bounding volume hierarchies are implemented at a higher level. The SWIFT algorithm has many advantages over the conventional techniques. It is faster and is robust than the other packages such as the I-Collide and the V-Clip algorithms. It automatically identifies the hierarchy's bounding properties, computes the deviation and builds its own simplified hierarchy in two different ways: the modified Dobkin-Kirkpatrick and the QSlim methods. Moreover, SWIFT shares the sweep and prune algorithm with I-Collide. In other words, the bounding boxes which are chosen automatically, are placed around each object to prune the unnecessary computation using the sweep and prune sorting algorithm. Besides, SWIFT supports object geometry sharing. The objects may be added to a scene using arrays or files of different formats. Also, the objects that are declared as static (fixed or not moving) are automatically optimized and any pair may be activated or deactivated.

5.3 The Proposed CD Approach

The possibility of using mathematical programming techniques has helped researchers to correlate the Linear Programming (LP) and the CD problem. Thus, a compact formulation of the collision detection coupled with a methodology that effectively implements the LP problem is proposed. The theory of this algorithm is proposed in [76], [77]. This will be a promising step toward the computer-based applications in terms of precision, speed and robustness.

The goal of a medical simulator is to support medical students during the training and the practice on surgeries and to perform the operations with a high precision. In this regard, medical objects are modeled with a tightness fit i.e. each object is modeled by its corresponding CH as shown in the previous chapter. CHs or convex envelopes have less contact points than real objects and can be quickly computed. This leads to a decrease in the size of the system of equations needed to test for a collision. Hence, the real time performance of CD algorithms is increased and the algorithms become faster. In addition, most exact CD systems work almost exclusively with convex objects. This is due to the fact that convex objects allow CD algorithms to converge quickly and detect the collision if it exists. This will give the simulator a high degree of precision but at the same time an increase in the cost of the complexity and the computational time to check for a collision. Therefore, by taking advantages of the speed and the robustness of LP techniques, the problem of collision detection is formulated and solved. In this regard, the CH of each object is reconstructed and the CD problem is formulated as an optimization problem based on convex objects and is solved using LP (simplex method).

5.3.1 Linear Programming Solution

To formulate the problem, each facet i of the convex envelope is represented by the plane inequality in the form of:

$$a_i x + b_i y + c_i z \leq d_i \tag{5.1}$$

Any point lying on the object must satisfy the inequalities of the planes constituting

the object. These equations form the constraints of the collision problem and represent the facets that separate two regions in space. Therefore, if a point satisfies two sets of inequalities simultaneously, it belongs to the corresponding convex objects. Thus, a collision is detected at that point between these two objects.

The problem is reduced to maximize an objective function in the form of $(x + y + z)$. It is formulated as follows:

$$max \ c^T X \tag{5.2}$$

subject to

$$AX \leq b \tag{5.3}$$

where $X = [x \ y \ z]^T$,

$$A = \begin{bmatrix} a_1 & b_1 & c_1 \\ a_2 & b_2 & c_2 \\ a_3 & b_3 & c_3 \\ . & . & . \\ . & . & . \end{bmatrix} \tag{5.4}$$

$$b = [d_1 \ d_2 \ d_3 \ . . .]^T, \quad c = [1 \ 1 \ 1]^T \tag{5.5}$$

The coefficients of the matrices A and b are calculated using the facets obtained from the convex hulls reconstructed by the proposed approach presented in the previous chapter (i.e. using the hybrid approach). Using the duality property, the problem becomes:

$$min \ b^T \pi \tag{5.6}$$

subject to

$$A^T \pi \geq c \tag{5.7}$$

Having formulated the problem, the dual system is solved using a linear programming algorithm (simplex method). If the system is bounded, a feasible solution exists and consequently, a collision is detected. Otherwise there is no collision.

Axis-Aligned Bounding Boxes (AABB) approach can be used as a preliminary test for collisions. For AABB construction, the minimum and maximum points that are orthogonally projected on the x, y and z axes are determined. Then, the projections are used to determine the intervals on each axis for each object. If two objects are in collision, the corresponding AABBs are also in collision.

5.4 The IVRI-CD Technique

In this section, an exact CD algorithm, namely the IVRI-CD, is described and discussed. Then, a comparison is performed between the proposed CD approach and this conventional technique.

5.4.1 IVRI-CD

The IVRI-CD approach [80] checks if a collision occurs between a pair of objects based on their CHs. Given an object P_1 with n_1 vertices and a second object P_2 with n_2 vertices, the problem of collision is formulated using the definition of CH and by minimizing the following function:

$$u\phi = -\left(\sum_{i=1}^{n_1} v_i\alpha_i - \sum_{i=1}^{n_2} w_i\beta_i\right) \tag{5.8}$$

where

$$\sum_{i=1}^{n_1} \alpha_i = 1 \tag{5.9}$$

$$\sum_{i=1}^{n_2} \beta_i = 1 \tag{5.10}$$

v_i and w_i are the vertices constituting the first and the second object, respectively. The variable u represents the coordinates of the distance between a point that is guaranteed to belong to P_1 and another point that is guaranteed to belong to P_2. Assuming that $\mu = max\{abs(u)\}$, the problem is reduced to minimize the following objective function:

$$minμφ \tag{5.11}$$

subject to

$$Aγ = b \tag{5.12}$$

$$γ \geq 0 \tag{5.13}$$

where

$$A = \begin{bmatrix} v_1^x & ... & v_{n_1}^x & -w_1^x & ... & -w_{n_2}^x & u^x \\ v_1^y & ... & v_{n_1}^y & -w_1^y & ... & -w_{n_2}^y & u^y \\ v_1^z & ... & v_{n_1}^z & -w_1^z & ... & -w_{n_2}^z & u^z \\ 1 & ... & 1 & 0 & ... & 0 & 0 \\ 0 & ... & 0 & 1 & ... & 1 & 0 \end{bmatrix} \tag{5.14}$$

$$b^T = [0\,0\,0\,1\,1], \quad γ^T = [α_1...α_{n_1} \ β_1...β_{n_2} \ φ] \tag{5.15}$$

If the objective function $μφ \leq ε$ (where $ε$ is a very small quantity), a collision is detected. It is to be noted that the matrix "A" in this method contains all the elements constituting the objects while the matrix "A" in the proposed approach is composed of the elements constituting the convex hull of the objects to be tested. Since the convex hulls have less contact points than the real objects, the real time performance of the new algorithm will increase and the cost of updating the matrices during each iteration of the simulation process decreases.

5.5 Simulations and Results

The wrist's bones of a patient are used to evaluate quantitatively the proposed approach by performing a comparison with the IVRI-CD technique. That is, each method is applied to test the collision between the different bones and the corresponding execution time to achieve the indicated results are collected and analyzed.
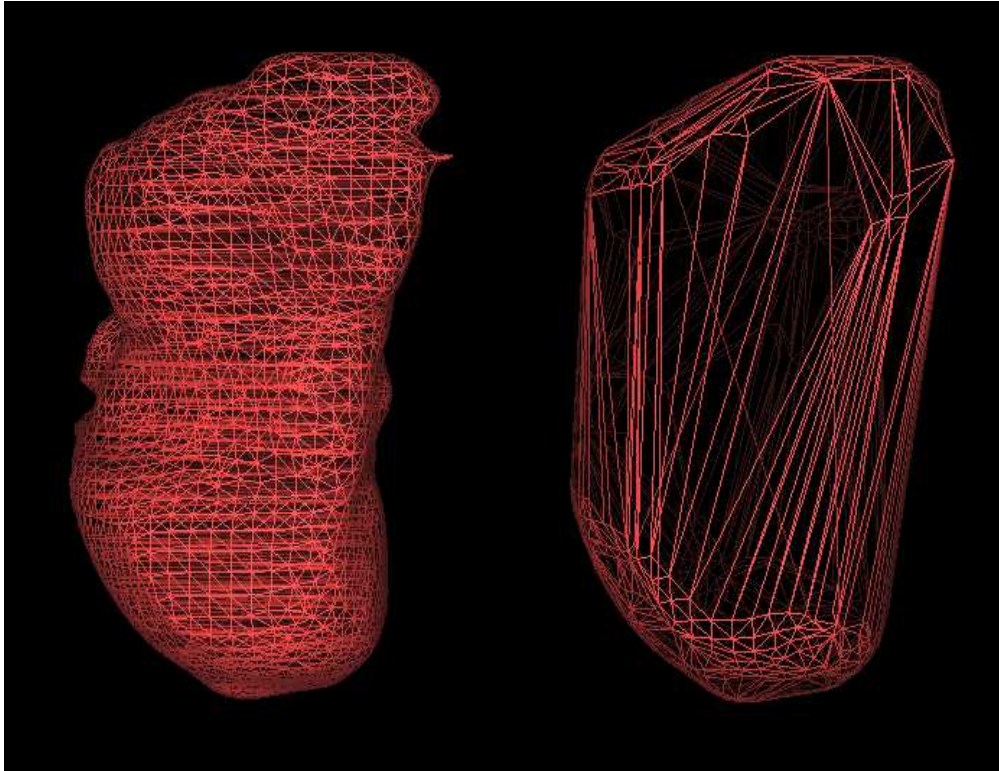
Figure 5.2: Facets of the Capitate and its Convex Hull

First, the CH of each bone is computed once during the simulation process. Figure 5.2 shows the facets of the Capitate bone of the wrist (left) and the facets of the corresponding convex hull (right). While the vertices of the object are the basis in the IVRI-CD technique, the vertices of the convex hull are used to formulate the collision problem using the new approach. It is evident that the number of facets of the convex envelope is much less than the number of facets that form the original object. Thus, the cost of updating the matrices during each iteration of the simulation process decreases and consequently the real time performance of the proposed CD algorithm is increased.

5.5.1   Results

Table 5.1 summarizes the simulated results of the two CD algorithms, namely, the proposed CD approach and the IVRI-CD approach. It shows the number of facets for different bones that are extracted from the 3-D wrist model as well the facets of the corresponding convex envelopes. Also, it shows the execution times required by the

Table 5.1: Comparison of Execution Time for Collision Detection Algorithms

3D Model	Original Model		Convex Hull		Proposed Approach	IVRI-CD Approach
	# vertices	# facets	# vertices	# facets	time (s)	time (s)
1st Meta.	2179	4320	379	790	0.0369	0.0397
2nd Meta.	1168	2258	300	596	0.0391	0.0441
3rd Meta.	675	1272	150	296	0.0411	0.0521
4rd Meta.	532	1002	147	290	0.0431	0.0661
Hamate	2812	5620	394	784	0.0523	0.0703
Ulna	977	1864	312	620	0.0563	0.0753
Scaphoid	2890	5784	530	1056	0.0583	0.0769
Capitate	3026	6048	635	1266	0.0592	0.0782
Radius	2454	4754	288	572	0.0623	0.0812

proposed algorithm as well as the IVRI-CD technique to detect a collision. It is clear that the running time of the new approach is always less than the time of the IVRI-CD method. Thus, it can be concluded that the proposed method is fast in detecting collisions and consequently is more suited for real time applications. The improvement that is achieved by the new approach is further illustrated in figure 5.3.
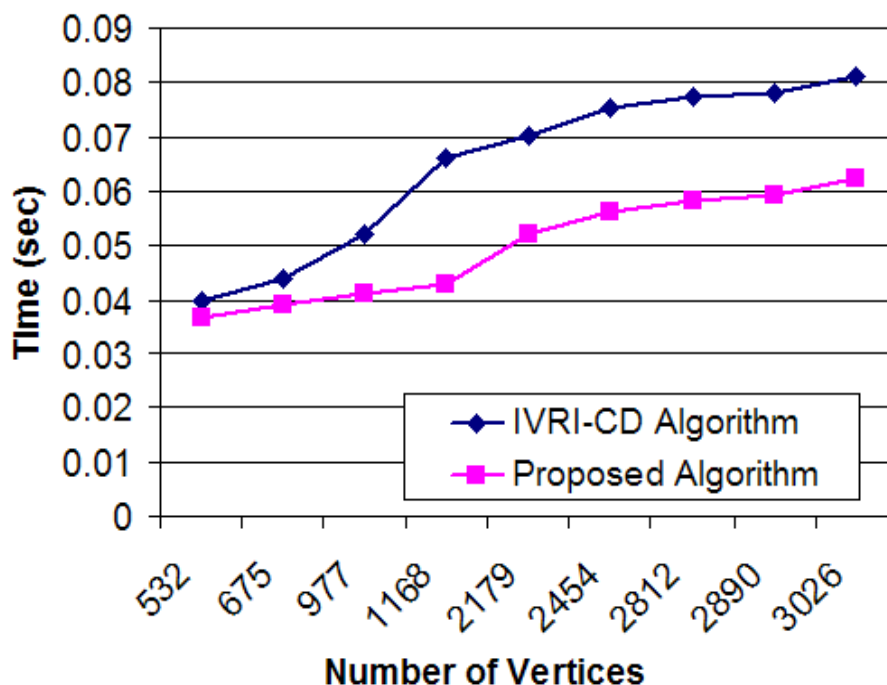
Figure 5.3: Execution time of the two CD algorithms for bones of the 3-D wrist model

It shows two plots, each plot is associated with a different algorithm: the IVRI-CD

and the proposed approach. The execution time (in second) is plotted as a function of the number of vertices that form each object (i.e. the bones of the wrist). The vertices represent nine of the fifteen bones of the 3-D wrist model (table 5.1). It is evident that the proposed method outperforms the IVRI-CD approach for every number of vertices. Furthermore, the new algorithm is more efficient as the number of vertices is increased.

5.6 Proximity Queries (PQ) and Penetration Depth (PD) Computation

The CD method can be generalized to calculate the proximity vector [78]. The proximit query problem is also formulated as an optimisation problem and is solved using LP. Each pair of convex objects in the scene is treated separately.

Similarly, each object is represented by a set of triangular facets i in the form of planes inequality:

$$a_i x + b_i y + c_i z \leq d_i \tag{5.16}$$

Since the time step is small enough, all the movements in the scene can be approximated by a local translation without any level of detail's degradation. The movement of the objects is assumed to be at a constant velocity. Thus, the problem may be reformulated by adding a variable t which represents the time to the equation of each facet i as follows:

$$a_i x + b_i y + c_i z + e_i t \leq d_i \tag{5.17}$$

Based on the above formula, if a point satisfies two sets of inequalities simultaneously, then this point belongs to the corresponding objects and a collision is detected at that point. This collision takes place at time t. Thus the obtained solution will be a vector of four elements: the direction components *(x, y, z)* and the time t. Since the velocity is considered constant, the distance D is proportionel to t and consequently, D is computed. Therefore, the proximity vector of two objects is obtained by minimizing t subject to the constraints simultaneously.

The PQ problem is written as follow:

$$min \ c^T X \tag{5.18}$$

subject to

$$AX \geq b \tag{5.19}$$

where $X = [x \ y \ z \ t]^T$,

$$A = \begin{bmatrix} a_1 & b_1 & c_1 & e_1 \\ a_2 & b_2 & c_2 & e_2 \\ a_3 & b_3 & c_3 & e_3 \\ . & . & . & . \\ . & . & . & . \end{bmatrix} \tag{5.20}$$

$$b = [d_1 \ d_2 \ d_3 \ \ldots]^T, \quad c = [0 \ 0 \ 0 \ 1]^T \tag{5.21}$$

the above *max* problem is converted to *min* using the duality property and the problem has the following form:

$$max \ b^T \lambda \tag{5.22}$$

subject to

$$A^T \lambda \leq c \tag{5.23}$$

Depending on the sign of t, the results will be the PQ vector if t is positive and the PD vector if it is negative.

5.7 Conclusion

The detection of collision is an essentiel problem that occurs in the computer-based surgical simulators. In this chapter, a new approach to detect collision with a fast execution time is presented. A compact formulation of the CD problem coupled with a methodology that effectively implements the LP problem is introduced. The new approach is compared with a conventional algorithm, namely, the IVRI-CD method.

The two CD techniques are simulated and are tested using the bones from the 3-D wrist model. The CD problem is extended to treat the PQ and PD computation. The results show that the proposed algorithm is efficient, fast, robust and leads to a decrease of the running time that is required to detect a collision with the bones of the 3-D wrist model.

Chapter 6

Design and Implementation of a 3-DOF Haptic Feedback Device

Most of the professional 3-DOF haptic feedback devices that are incorporated in VR surgical simulators are relatively expensive. In this chapter, a low cost force feedback device is proposed and is used as a haptic interface with the computer simulation system. The design and the implementation of this device are shown. The proposed device has a 3-DOF along the three different axis (X, Y, Z) and provides force feedback to them all. In addition, a haptic feedback algorithm is implemented and is tested for the proposed force feedback device. Also, a virtual simulation of dorsal percutaneous scaphoid fixation is presented and a comparison between the real and the virtual process is shown. This have lead to the development of a low cost system that can be easily used by medical students with the same benefits as professional devices. The trainees can easily acquire the system and can learn the basic skills required with a great safety and a high flexibility.

6.1 Introduction

The word "haptic" is derived from the Greek word "haptesthai" which means "to touch". Therefore, the haptic sensing is defined as the use of motor behaviors in combination with the touch to identify the objects [81]. In other words, haptics deal with the control of the human movements and the reception of a feedback through the sense of touch. A haptic interface transmits the forces to a person's hand in a way that mimics the sensation of touching the real objects. Thus, it becomes possible for the user to touch

virtual objects, corresponding to the way a sighted person can see objects or pictures on a computer screen. Haptics are considered as an important key component of the VR systems by adding the sense of touch to the visual-only models. Researchers in the VR field are concerned with the development of force feedback devices and software that permit users to feel and manipulate virtual objects. Hence, force feedback plays an important role in collaborative VR environments, mainly to the programmers of the haptic visualization tools. Whereas, a lots of work has been done for graphical displays, few work has been made for the force feedback input interface side. One of the problems that has slowed down the development in this area is the difficulty of integrating the visualization of a scene, the interaction of the user with the scene, the feeling of the user to be immersed inside the scene, and finally, the input devices [82].

Various haptic interfaces for medical simulation have proven to be very useful for training on minimally invasive procedures. During the training sessions, the users are expected to perform some surgical tasks under the supervision of a trainer while they are navigating and interacting realistically with the virtual medical model. Therefore, besides the appearance and the simulation of the virtual model, realism implies also the visual embodiment of the users and the means of interaction with the world. Consequently, the trainees that uses the force feedback devices benefit from being able to manipulate the medical models, feel the form and the contact of a collision and sense a realistic touch with these models.

6.2 Haptic Devices for VR Medical Simulators

Haptic interfaces are devices that stimulate the sense of a touch such as the sensory capabilities within our hands. The surge of the computer capability and the desire for better ways to connect to the computer-generated worlds have driven the creation and the development of practical devices for haptic interaction. The addition of the haptic systems to a VR medical training simulator will greatly increase its effectiveness in simulating the real-world situations and consequently, such system provides doctors with the "feel" of virtual patients. Various force feedback systems currently exist and provide

information to the human senses of touch. The force feedback devices are classified according to the number of DOF. For example, joysticks have two DOF and provied force feedback to both. The DOF enables the joystick to restrict its movements and to exert forces in order to simulate different conditions. The professional systems often have three DOF, sometimes six, and force feedback in at least three of them. These devices can simulate 3-D objects as well as objects in the plane (2-D). An example of professional systems is the PHANToM from SensAble Technologies. This device is used in most VR medical simulators. However, other devices such as the FEELit Mouse from Immersion and force feedback joysticks from Logitech and Microsoft are also used.

6.2.1 FEELit Mouse

The FEELit Mouse which is produced by Immersion Corporation [83] is a desk-top 2-DOF interface that enables the user to feel the simulated objects, such as hard surfaces, rough textures and smooth contours. Its workspace is 2.5×1.9 cm, and its maximum output force is equivalent to 1 N in the X and Y directions. Therefore, the FEELit Desktop software renders the windows screen haptically in two dimensions. Moreover, this device works with the web and allows the user to "snap to" hyperlinks or to feel the texture of a textile using a FeeltheWeb ActiveX control. The drawback of this device is the limited work envelope and the point/arrow interaction modality.

6.2.2 Microsoft Sidewinder Force Feedback (MSFF)

The Microsoft Sidewinder Force Feedback II joystick [84] is one of several force feedback joysticks currently in the market. It is a low cost device and has a USB port and an on-board 16-bit processor running at 25 MHz. The processor handles all the force effects. There are three force effects that can be represented by the MSFF device. First, the time-based effects such as jolts and vibrations are represented. They are not really related to the orientation of the joystick handle's. Instead, they depend on the temporal profile of the force. Second, the space-based effects such as springs, dampers and walls are incorporated. In addition, the SideWinder joystick supports a number of effects that

may be combined to generate new ones. These effects vary from simple raw forces in an arbitrary direction, to complex force-waves in spatially located walls. The co-processor of the device is the main controller: it decides if the joystick is inside or outside the object and applies the corresponding forces. The basic movements of the device are: translate sideways, raise and lower vertically, push and pull forwards and backwards, tilt forwards and backwards, rotate about vertical axis, and tilt sideways. Moreover, the strength (the magnitude) of the joystick force it varies according to a percentage value. It is measured using a scale that runs from zero (indicating no force) to 10,000. The latter value indicates the maximum force that can be applied by the device.

6.2.3 PHANToM Haptic Devices

The PHANToM is a haptic interface device developed by SensAble Technologies [85]. It is primarily planned for adding 3-D touch to 3-D graphics programs. The PHANToM family of arms are the most popular haptic feedback interfaces at present. This device adds a new dimension to the human computer interaction.

The PHANToM is a small robot with a very low back drive friction. The standard model of the PHANToM has three full degrees of freedom, i.e., three motors and three encoders. The tip of the robot is attached to a stylus via a passive gimbal that allows rotational movements. However, the normal use of the PHANToM is the opposite of a robot: the user holds on to the stylus, the end of the robot arm, and moves it. Thus, the robot provides feedback to the user by applying forces via the stylus. More advanced devices of PHANToM have six degrees of freedom and three electrical actuators, and each model has different dimensions. Depending on the model, its work envelope progresses from the wrist motion to the shoulder motion. The maximum force level is 22 N, and sustained forces of only 3 N.

With the standard PHANToM models, the user places a finger in a thimble connected to a metal arm. The user can feel virtual 3-D objects that are programmed into a computer by moving his finger around. Moreover, he can control the computer as if the PHANToM was a mouse or a joystick. When it is activated, the PHANToM works

with the computer to interpret the position of the user's hand in 3-D space and to apply the appropriate and variable resisting force. The system is equipped with sensors to track the position of the user's hand and the identified location is transmitted to the computer. The haptic device works as follows: every millisecond, the computer that controls the PHANToM reads the position of the stylus. Then, it compares the position with the boundaries of the objects in the virtual environment. If the user is not near any of the virtual objects, no current is sent to the motors therefore the calculated force is zero and the user is free to move the stylus around. However, if the system detects a collision between the stylus and one of the virtual objects, it drives the motors to exert a force on the user's hand (via the stylus) to push the user's hand back to the surface of the virtual object. In practice, the user is prevented from penetrating the virtual object just as if the stylus has collided with a real object. The high frequency and the high resolution of the encoders makes it possible to feel realistically almost any shape. The characteristics of the PHANToM make it well suited for interaction mediated by a single virtual finger, a stylus or a pencil.

6.3 The Proposed Force Feedback Device

The PHANToMS are the haptic feedback systems that are mostly used in VR surgical simulators. However, they are relatively expensive. Hence, an inexpensive force feedback device which is used as a haptic interface with the computer simulation system is proposed. This will lead to the development of a low cost system that is used by medical students with the same benefits as professional devices. The design and the construction of the force feedback device are presented in the following subsections.

6.3.1 Design of the Device

The proposed force feedback device was built with the cooperation of Mr. Jean-Louis Miramand and the LISV Laboratory (Laboratoire d'Ingénierie des Systèmes de Versailles). A mechanical design of the device with a 3-DOF is proposed. The system was developed based on a well-defined plan. First, the base of the device was built and

each sensor was synchronized with the corresponding motor. Second, the system was mounted. The imitation of the surgical gestures that have made by the doctor's hand was done based on a mechanical design (the third stage). The force feedback system is shown in figure 6.1.
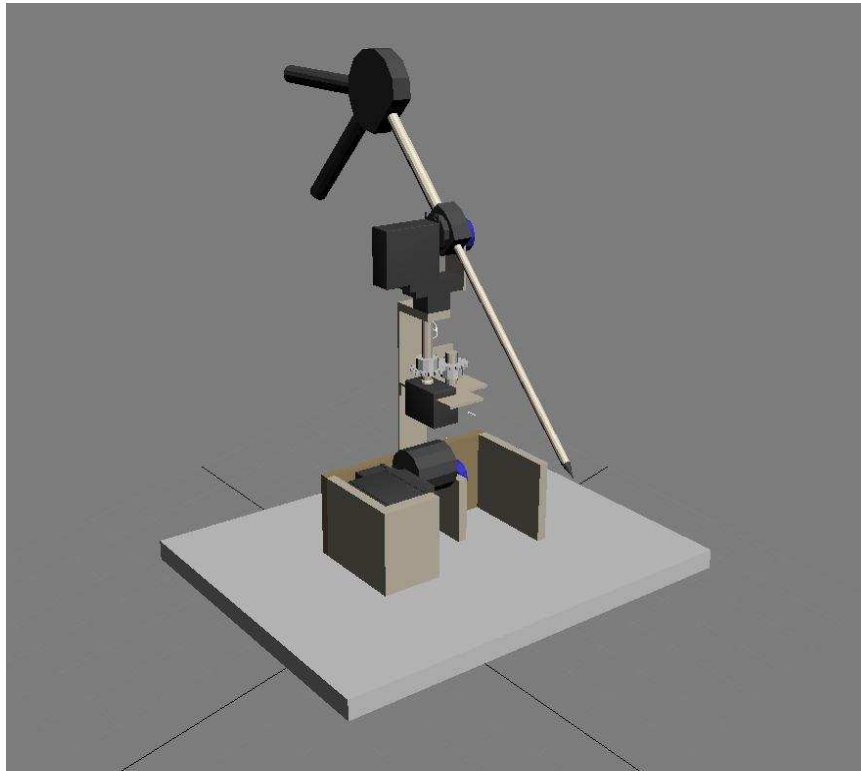
Figure 6.1: The Design of the Force Feedback System

6.3.2   Implementation of the Device

The implementation of the proposed device requires sensors that are capable to detect the positions of the surgical tool and a communication system to transmit the data to the virtual environment. Also, motors are needed to drive a force and consequently, provide the user a sense of touch when the instrument is touching the virtual object. Subsequently, a resisting force must be generated when a collision is detected.

Sensors and Motors

The trainee holds the mechanical device. The corresponding movements that are performed are recuperated by the three sensors that are placed at the three different axis (X, Y, and Z). Each sensor is a potentiometer that is manufactured by VISHAY. The potentiometers are precise and accurate in detecting the movements performed by the user with a linear tolerance of $\pm$ 0.5 and an angular tolerance of $\pm$ 2 degree. Figure 6.2 shows the potentiometer and its characteristics.
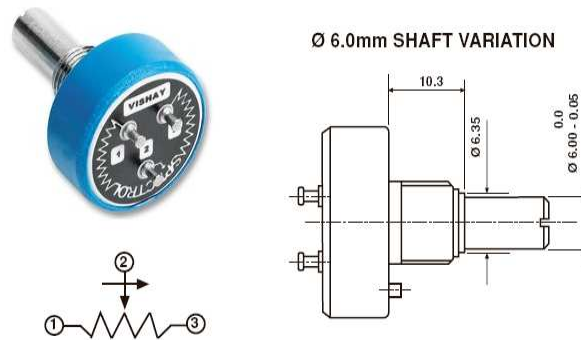
Figure 6.2: The VISHAY Potentiometer Characteristics

The force feedback is delivered to the simulator by three servo motors synchronized with the potentiometers. They are controlled using the PWM (Pulse Width Modulation). Figure 6.3 shows the type of the servo motors that are used in the design.

Figure 6.3: The Servo Motor Futaba FP-S148

The motor that is placed at the base of the simulator is bigger enough to handle a high torque and supports all the system. Figure 6.4 shows the real implementation of the force feedback system.
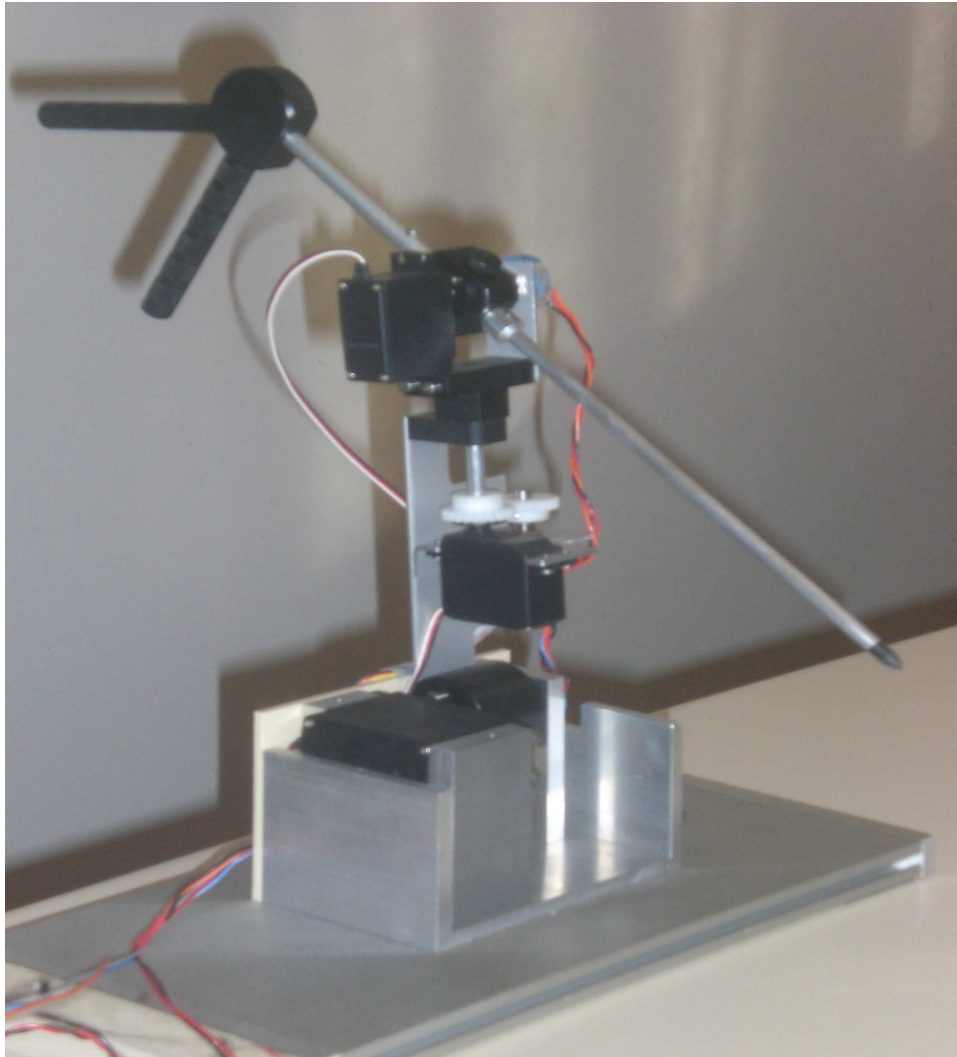
Figure 6.4: The Proposed Force Feedback System

6.4 Data Collection and Acquisition

A data acquisition board is incorporated in order to transmit the collected signals from the sensors to the main controller. Having analyzed the received data, the appropriate signals are transmitted to the motors for control purpose. The AD512 data acquisition

card form HUMUSOFT is used [86] in this work. It contains several features. The most important features for this application are:

- Eight single-ended 12-bit analog input channels and two 12-bit analog output channels

- Sampling rate up to 100 kHz

- 8 digital input channels and 8 digital output channels

- Programmable A/D ranges

- Low power consumption

The potentiometer, which is a three-terminal resistor, is connected to a voltage source to form an adjustable voltage divider. If all three terminals are connected, it can act as a variable voltage divider. Therefore, a simple linear circuit that produces an output voltage (Vout) which is a fraction of its input voltage (Vin), is created. Figure 6.5 shows the resistive strip of the potentiometer (left) that is translated into a variable voltage divider.
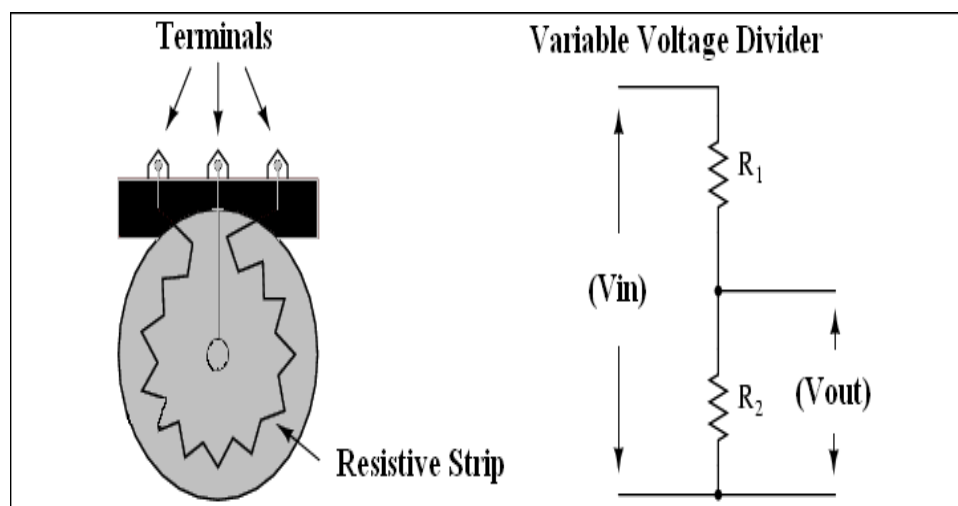
Figure 6.5: A Variable Voltage Divider

Each time the user moves the force feedback device, the voltages across the three terminals of the three potentiometers, that are placed along the different axes, are adjusted

accordingly. Then, the corresponding electric signals are generated and transmitted to the DAQ board for processing. The change of voltage is due to the rotation of the resistive strip. Subsequently, the potentiometers that indicate a change in the voltage (electric signals) also indicate a variation in the position of the virtual medical probe in the virtual environment. If there is no collision detection between the virtual medical probe and the virtual medical model, the motors are off i.e. there is no signal transmitted to control the motors. On the other hand, if a collision is detected, PWM signals are generated and transmitted via the output port of the DAQ board to the motors. Therefore, the user can feel the force feedback that is generated by these motors. Figure 6.6 shows the circuit that generates the PWM signals.
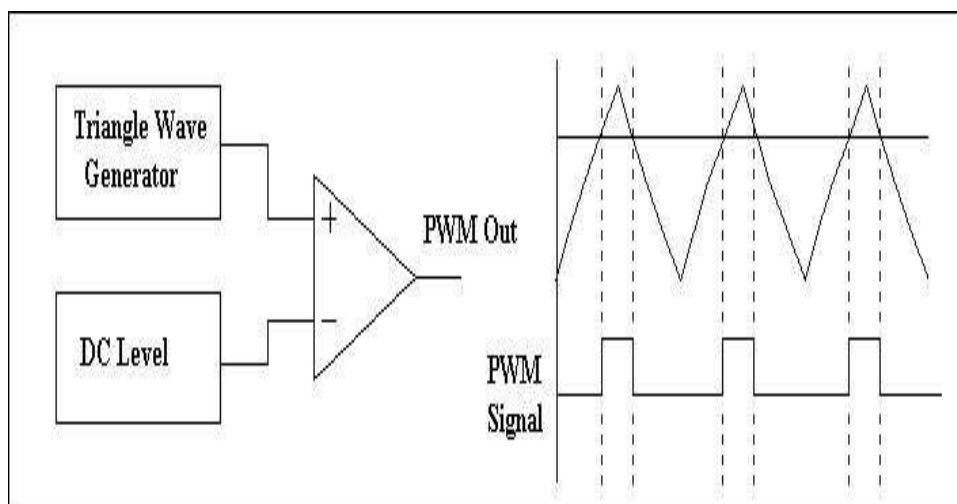
Figure 6.6: Generation of the PWM Signals

The Humusoft board is designed to deal with logic signals. It can not cope with large voltages and large currents. In addition, the output current of the board is approximately 38 mA. Therefore, this current is not sufficient to run the motors. In this regard, the IRF630 power Mosfets are used to drive the motors. That is, the generated PWM input signal is transmitted via the gate (g) of the Mosfet and the motor is attached to the output (out) of the drain (d). The drain is also connected to a source voltage (V) via a small resistance and the source node (s) of the Mosfet is grounded. Figure 6.7 shows the circuit that drives each motor.
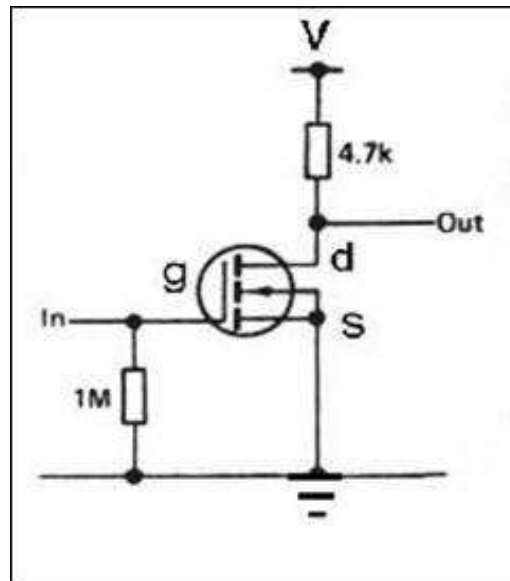
Figure 6.7: The Circuit Driving the Motors

6.5   Haptic Feedback Algorithm

Having performed the design and the implementation of the device, a haptic feedback algorithm that supervises all the corresponding activities is described. The algorithm will enhance the surgical performance by guiding the user (surgeon, student ...) and give him a sense of touch and resistance when the collision is virtually detected between the instrument and the object.

When the user moves the haptic device, sensors that are placed on different axis of rotation generate the signals. The latter are transmitted by the acquisition card, to change relatively the position of the virtual medical instrument. This change allows the dynamic interactions within the virtual environment. That is, the position of the medical tool is updated at every step and the collision detection is checked between the tool and the bones of the wrist by applying the proposed algorithm (presented in chapter 5) i.e. update the matrices that formulate the collision problem and solve the system of linear equations for every step change. If collision is detected, PWM signals are generated to control the servo motors. Consequently, these motors generate a force which is applied against the motion of the user of the haptic device. Therefore, the user can feel the resistance of the applied force against his hand's motion, i.e. against

the force applied by the trainee to move the haptic device. This force-reflecting device enables medical students during the training session to experience the real feeling of touch. Touching virtual objects rather than seeing them enhance the capability of the computer-based system and gives the user the feeling of so called "Immersion". Figure 6.8 shows the flowchart of the haptic feedback algorithm.
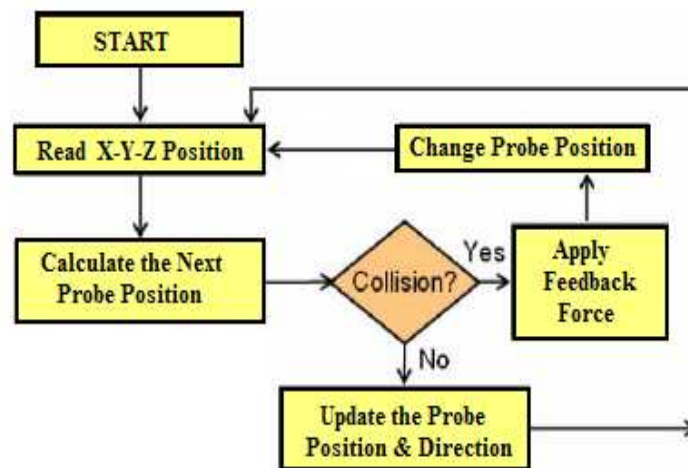
Figure 6.8: The Flowchart of the Haptic Feedback Algorithm

6.6 Virtual Simulation of Scaphoid Fixation

A virtual simulation of dorsal percutaneous scaphoid fixation is presented and a comparison between the real and the virtual process is shown.

6.6.1 Surgical Technique For Scaphoid Fracture

Techniques to perform the wrist arthroscopy have been developed to evaluate, diagnose and treat the various wrist disorders, such as scaphoid fractures. For example, the dorsal percutaneous approach is a very efficient way in the treatment of the displaced proximal pole scaphoid fractures in many clinical and operating rooms. This technique allows a faster rehabilitation without any restriction once CT scan confirms a solid union.

Scaphoid Fracture

The scaphoid is the wrist bone that is the most likely to break. It is located on the thumb side of the wrist, in the region where the wrist bends. Fractures of the scaphoid occur in people of all ages, including children, and are most common in young men due to their athletic activities. Scaphoid fractures usually cause pain in the base of the thumb, with a swelling in the same area. The pain may be severe when the thumb or wrist is moved or when the hand grips anything. When the scaphoid is broken at the waist or proximal pole, a surgery may be recommended.

Displaced fractures may need an open reduction and an internal fixation [92]. In fact, this method is very efficient and it has been associated with good results [93]. However, the drawbacks of the open reduction and the internal fixation include the need to cut the important palmar radiocarpal wrist ligaments [94] and may cause a possible injury to the limited blood supply to the scaphoid [95]. Therefore, undisplaced fractures of the scaphoid can be treated with a percutaneous screw fixation. A screw or wire may be used to stabilize the scaphoid while the bone heals.

6.6.2 Surgical Simulation

Percutaneous arthroscopically assisted internal fixation by a dorsal approach may be considered in all acute scaphoid fractures that are selected for surgical fixation [88]. The dorsal guidewire permits the dorsal and the volar implantation of a cannulated screw along the central axis of the scaphoid [89]. The surgical technique described in [87] uses the Standard Acutrak screw. This screw is a headless, cannulated, tapered screw with a graduated thread pitch to provide an interfragmentary compression without a hardware protrusion. This technique permits the percutaneous reduction and a rigid internal fixation of proximal pole fractures. First, the wrist is flexed and pronated so that the scaphoid appear's as a cylinder. The center of the cylinder is the location to guide the wire placement. Then, the guide wire is driven dorsal to volar through the center of the scaphoid. The wire exits at the base of the thumb. Figure 6.9 shows the real placement of the guide wire during the surgery. Figure 6.9 is taken from a real

operation done by Dr. Joseph F. Slade and distributed by *ACUMED* [90]. On the other hand, figure 6.10 illustrates the same process that is performed virtually using the proposed computer-based simulator.

Figure 6.9: The Placement of The Guide Wire (Real Operation)

Figure 6.10: The Placement of The Guide Wire (Virtual Operation)

Having finished this step, a hand-held cannulated reamer is placed over the guide wire and is used to prepare the scaphoid. The scaphoid is reamed to fit the length of the screw. Then, the screw is selected and is advanced with a cannulated driver to the

level of the reamed scaphoid. Figure 6.11 shows the real insertion of the screw in the scaphoid and is also taken from the real operation done by Dr. Joseph F. Slade. On the other hand, figure 6.12 shows the virtual operation of the same procedure.

Figure 6.11: The Insertion of The Screw in The Scaphoid (Real Operation)
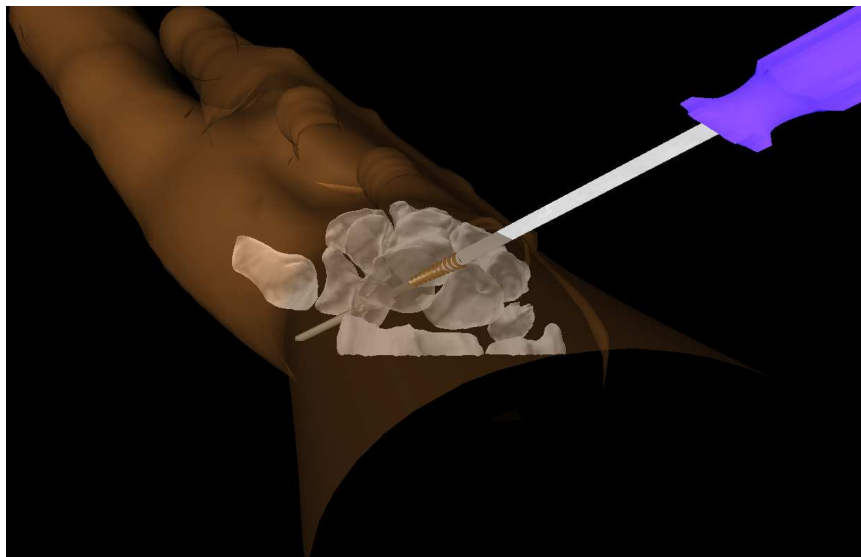
Figure 6.12: The Insertion of The Screw in The Scaphoid (Virtual Operation)

Having implanted the screw in its corresponding location, the position of the scaphoid is confirmed with a mini-fluoroscopy and the guide wire is removed. The screw is placed

at the center of the scaphoid. Figure 6.13 shows the final phase of the virtual simulation of the operation.
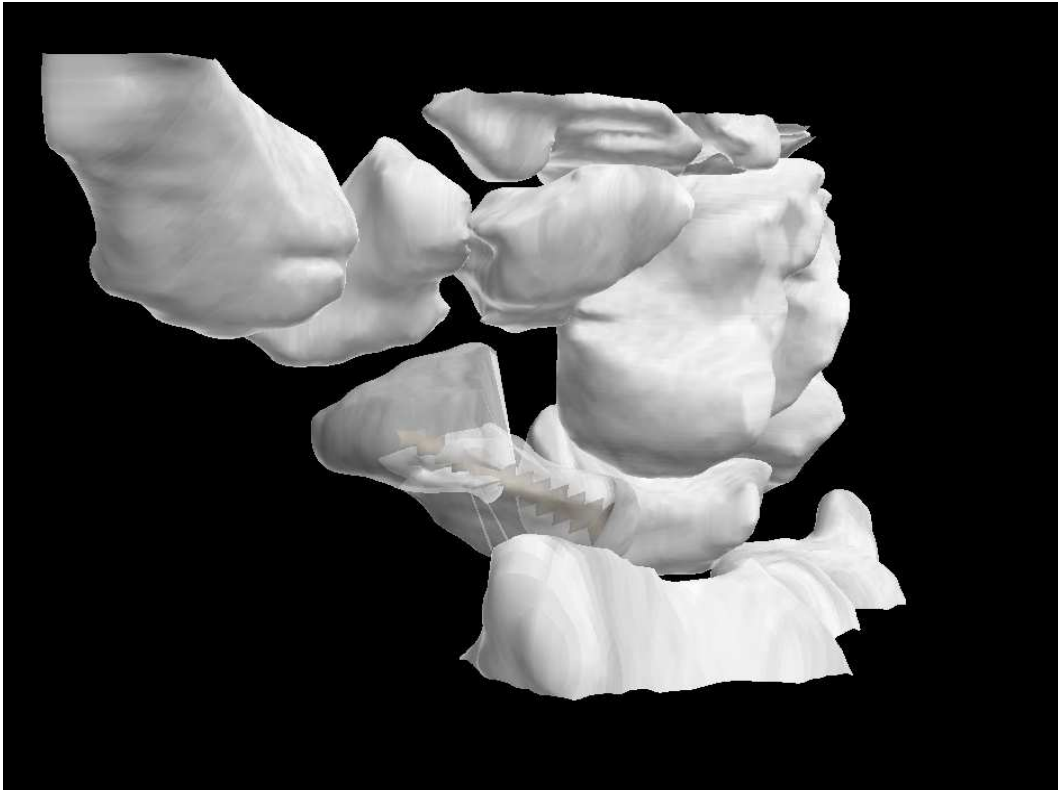
Figure 6.13: A Virtual View of The Central Placement of The Screw in The Scaphoid

6.7 Advantages

The dorsal percutaneous approach to scaphoid fixation has many advantages [87] and they can be summrized in three. This three main advantages are:

1. The proximal-to-distal placement of the guide pin and the screw allow for more precise placement along the central axis of the scaphoid, which decreases healing time and reduces risk of screw thread exposure.

2. The dorsal approach avoids injuring the vulnerable volar ligament anatomy.

3. The insertion of the screw from the proximal to distal direction allows the more rigid fixation of proximal scaphoid fractures.

6.8   Conclusion

In this chapter, the design and the implementation of a functional haptic feedback device are presented. The proposed device has a 3-DOF, each one along a particular axis (X, Y and Z). The system is capable to provide force feedback to them all. The developed prototype can be used by medical students and trainees and have the same benefits as the professional devices. The proposed force feedback device is coupled with a haptic simulation algorithm and it is incorporated in the whole computer-based system. Also, a virtual simulation of dorsal percutaneous scaphoid fixation is presented. The VR simulation is compared with the real surgery of the same procedure. The 3-D wrist model, presented in chapter 3, the model of the hand and the virtual medical tools are integrated in the simulation process. The entire system is tested and the wrist arthroscopic surgery can be simulated. The users (student, doctor, surgeon ...) can learn the required basic skills and then perform the training procedure on real patients. This low cost system is safe, flexible and can provide medical students with a precise and detailed information for training and educational purposes.

Chapter 7

Conclusions and Perspectives

The work presented in this thesis has addressed an important issue in VR and its application in the medical field: the development of a VR simulator for wrist arthroscopic surgery. In this work, two main issues are addressed: the 3-D reconstruction process and the 3-D interaction. The proposed simulator provides a virtual environment with a realistic representation of the region of interest. Based on a sequence of CT images, a realistic representation of the wrist joint suitable for the computer simulation is reconstructed. Two main components of the computer-based system interface are illustrated: the 3-D interaction to guide the surgical instruments and the user interface for haptic feedback. In this context, algorithms that model 3-D objects using the convex hull approaches and simulate real time exact collision detection between virtual objects during the training on the surgical operation are presented. Also, a force feedback device, coupled with a haptic feedback algorithm, is designed and developed as a haptic interface with the computer simulation system. A distinctive feature of this work is that the proposed computer-based system satisfies the following specifications:

1. The system treats the wrist arthroscopy problem. The wrist arthroscopy requires skills to be acquired by all hand surgeons. These skills are important as the skills needed by surgeons to perform the shoulder and the knee arthroscopy.

2. The development of an inexpensive and a practical simulator for medical students as well as for surgeons is of great value, specially if the medical practiioners can harness the same benefits as the professional devices. Then, the surgical procedure

can be performed on real patients with much less risk and injury.

7.1 Summary of the Contributions

The main contributions of this thesis are summarized as follow:

- **Survey on MIS Surgical Simulators:** In this survey, an overview of the existing MIS simulators is presented. The VR simulators are classified based on the application and the organs or structures for which the system is developed. The study may be used by the researchers to gain a general idea about the commercialized and the scientific simulators that were developed to perform different MIS approaches.

- **Virtual Environment:** A virtual environment to visualize the medical models and the medicals tools with a high fidelity and a high precision is developed.

- **Algorithms:** A new hybrid approach to generate the convex hull of the 3-D models is developed and presented. The proposed algorithm converts each 3-D concave model to a convex representation that allows the collision detection algorithms to converge quickly and report a collision, if it exists. The proposed hybrid method is an output sensitive algorithm that works in 2-D as well as in 3-D. It is very efficient, practical and useful in modelling and simulating 3-D medical data in a virtual environment. In addition, a new technique of collision detection for solid objects is proposed and introduced. The collision detection problem is formulated and a linear programming solution is obtained to determine whether a collision occurs between virtual objects or not. The proposed algorithm is efficient, fast, robust and leads to a decrease of the running time that is required to detect a collision.

- **3-DOF Force Feedback System:** A 3-DOF force feedback device is designed, developed and implemented. The low cost system is coupled with a haptic feedback algorithm. The proposed device can be used by medical students as well as surgeons to harness the same benefits as the professional devices.

- **Virtual Simulation of a Surgical Operation:** A virtual simulation of the dorsal percutaneous scaphoid fixation is presented. The virtual procedure is compared with the real surgery that is performed by doctors inside the operating room. The virtual surgery ensures that the proposed computer-based system is appropriate to train medical students as well as surgeons in order to acquire the necessary skills to perform the specific surgeries.

7.2 Future Work

The proposed computer based surgical simulator can be extended to handle other operations and medical activities.

In order to complete the system, the corresponding ligaments should be modeled and added to the 3-D wrist. In fact, the ligaments displayed in the CT images are blurred and the appearance is almost non existing in MRI images. Therefore the contour detection using the marker-based watershed algorithm can not lead to a good extraction of these ligaments from the CT and the MRI images. Thus, real images from the Visible Human dataset maybe be more suited for ligament extraction. This is achieved by addressing two main issues: the need of special information about the ligaments from an expert doctor and the implementation of preprocessing techniques for segmentation purposes such as features extraction algorithms.

Once the ligaments are modeled and extracted, new collision detection algorithms should be investigated and incorporated in the VR simulator to accomodate any variations. This is due to the fact that the ligaments have properties that are different from solid objects such as the bones.

At a later stage, the researcher may upgrade the proposed prototype so that it can handle all types of wrist surgery operations. Consequently, the surgeon will be guided through the whole process and has always the full control over the device.

Publications

- **International Journals**

1. F. Yaacoub, Y. Hamam and A. Abche, "A 3D Convex Hull Algorithm for Modeling Medical Data in a Virtual Environment", *International Journal of Intelligent Systems Technologies and Applications (IJISTA)* , Special Issue on Advances in Intelligent Systems for Applied Simulation and Prototyping, Vol. 5, Nos 1/2, PP. 3-19, ISSN: 1740-8865, Inderscience Enterprise, 2008.

2. F. Yaacoub, Y. Hamam and A. Abche, "Development of Virtual Reality Tools For Simulating Wrist Arthroscopic Surgery", Submitted to: *The International Journal of Simulation Modelling Practice and Theory* , SIMPAT, Elsevier, 2009.

- **International Conferences**

1. F. Yaacoub, Y. Hamam and A. Abche, "Computer-Based Training System for Simulating Wrist Arthroscopy", *The 21th IEEE International Symposium on Computer-Based Medical Systems*, CBMS, pp. 421-423, ISBN: 978-0-7695-3165-6, Jyväskylä, Finland, June 2008.

2. F. Yaacoub, Y. Hamam and A. Abche, "Collision Detection for Virtual Arthroscopic Surgical Simulation", *The 2007 International Conference on Computer Graphics and Virtual Reality* , CGVR'07, WORLDCOMP'07, CSREA Press, pp. 87-93, ISBN: 1-60132-028-0, Las Vegas, USA, June 2007.

3. F. Yaacoub, Y. Hamam and A. Abche, "Collision Detection in Computer Simulations for Wrist Arthroscopic Surgery Training", *The IEEE International Conference on Computer as a Tool* , EUROCON'07, pp. 2088-2095, ISBN: 978-1-4244-0813-9, Warsaw, Poland, September 2007.

4. F. Yaacoub, Y. Hamam and A. Abche, "Computer-Based Surgical Simulation System for Students Training", *The 6th EUROSIM Congress on Modelling and Simulation* , ISBN: 978-3-901608-32-2, Ljubljana, Slovenia, September 2007.

5. F. Yaacoub, Y. Hamam, A. Abche and C. Fares, "Convex Hull in Medical Simulations: A New Hybrid Approach", *The 32nd Annual International Conference of IEEE Industrial Electronics Society* , IECON'06, pp. 3308-3313, ISBN: 1-4244-0391, Paris, France, November 2006.

6. F. Yaacoub, Y. Hamam and A. Abche, "Convex Envelope in Arthroscopic Knee Surgery Simulation", *UK Society for Modelling and Simulation, European Modelling Symposium*, EMS'06, pp. 46-50, ISBN: 0-9516509-3-9, London, UK, September 2006.

7. F. Yaacoub, Y. Hamam and A. Abche, "A Virtual Reality Simulator For Training Wrist Arthroscopic Surgery", *The International Joint Conference on Biomedical Engineering Systems and Technologies* , BIOSTEC, Porto, Portugal, January 2009.

Résumé Détaillé

Introduction

L'environnement virtuel est décrit comme une application qui permet aux utilisateurs de naviguer et d'interagir dans un espace quasi-réaliste, tri-dimensionnel et en temps réel. Dans ce contexte, la réalité virtuelle repose sur l'intégration en temps réel de situations générées par ordinateur, d'information sur la position de l'individu dans l'espace et de stimuli visuels qui recréent un environnement interactif d'apparence réaliste. La réalité virtuelle permet donc d'immerger l'usager dans un environnement standardisé afin de lui permettre de s'entrainer et de simuler plusieurs expériences, ce qui lui donne certains avantages vis-à-vis des méthodes d'exposition traditionnelles.

La réalité virtuelle a révolutionné des nombreuses disciplines scientifiques en fournissant de nouvelles méthodes de visualisation des données complexes et en manipulant ces données en temps réel. Elle a été utilisée dans différentes applications : l'ingénierie, l'éducation, les simulations militaires et aérospatiales, et la médecine.

La médecine et surtout la chirurgie arthroscopique présente actuellement un essor très important pour le bénéfice du plus grand nombre des patients. Cependant, cette technique possède un certain nombre d'inconvénients et il est donc nécessaire pour le médecin de s'entrainer et répéter ses gestes afin de pouvoir exécuter ce type d'opération d'une façon efficace et certaine. En effet, les méthodes traditionnelles d'enseignement de la chirurgie sont basées sur l'autopsie des cadavres et l'entrainement sur des animaux. Avec l'évolution de notre société, ces deux pratiques deviennent de plus en plus critiquées et font l'objet de réglementations très restrictives.

Afin d'atteindre un niveau plus élevé, de nouveaux moyens d'apprentissage sont

nécessaires pour les chirurgiens. À cet égard, les simulateurs chirurgicaux sont devenus une des matières les plus récentes dans la recherche de la réalité virtuelle. Ils sont également devenus une méthode de formation et un outil d'entraînement valable pour les chirurgiens aussi bien que les étudiants en médecine.

Objectif et Considérations

Les simulateurs chirurgicaux ont été élaborés pour un large éventail de procédures médicales. Cependant, ils sont souvent associés à des engagements spécifiques. De nombreux simulateurs sont associés avec la laparoscopie, d'autres sont liés à l'endoscopie. En outre, de nombreux simulateurs sont associés à la cystoscopie et ureteroscopie. Certains d'entre eux participent à la colonoscopie, bronchoscopie et sigmoïdoscopie. Toutefois, la plupart des simulateurs mentionnés ci-dessus sont coûteux à acquérir. Concernant les simulateurs d'arthroscopie, la plupart d'entre eux ont été développés pour la formation du genou et de l'épaule alors que très peu de travail a été fait pour l'arthroscopie du poignet malgré l'importance de celui-ci. En conséquence, le problème de la construction d'un simulateur de réalité virtuelle pour l'enseignement de la chirurgie arthroscopique du poignet reste à traiter. Dans ce contexte, notre projet a été proposé par une équipe de professeurs et chirurgiens à l'Institut de la Main, "Clinique Jouvenet" Paris XVI. Il consiste à développer des outils de réalité virtuelle pour aider à l'enseignement, l'apprentissage et la formation sur la chirurgie arthroscopique du poignet. Ce projet de recherche, dirigé par le Prof. Yskandar Hamam, a commencé avec Charbel Fares. Mon travail est une continuation de ce projet afin de développer tous les outils de réalité virtuelle qui sont nécessaires à la réalisation complète du simulateur. Au cours de la conception du projet, deux objectifs principaux sont visés :

1. Développer des outils de réalité virtuelle et des techniques de simulation pour générer des modèles 3-D et pour simuler des opérations virtuelles avec fidélité et réalisme.

2. Essayer de couvrir différentes exigences pour le processus d'apprentissage et de

fournir à l'utilisateur des outils pour faciliter l'enseignement et la formation sur plusieurs expériences chirurgicales.

En outre, l'arthroscopie du poignet a été choisie en raison de plusieurs considérations:

1. L'arthroscopie du poignet est une pathologie (étude de la nature essentielle de la maladie) qui a été moins étudiée et pratiquée que celle du genou et de l'épaule.

2. Des différents types de participation et d'intervention chirurgicales peuvent être couverts par la simulation arthroscopique du poignet.

3. Les médecins confrontent de nouvelles et importantes pathologies en ce qui concerne l'arthroscopie du poignet. Par conséquent, il existe une demande croissante sur la formation et sur l'apprentissage des nouvelles techniques.

Par conséquent, un simulateur de réalité virtuelle pour l'enseignement de la chirurgie arthroscopique, surtout la chirurgie du poignet, a été présenté. Deux questions principales sont abordées: la reconstruction et l'interaction 3-D. Une séquence d'images CT a été traitée afin de générer un modèle 3-D du poignet. Les deux principales composantes de l'interface du système sont illustrées: l'interaction 3-D pour guider les instruments chirurgicaux et l'interface de l'utilisateur pour le retour d'effort. Dans ce contexte, les algorithmes qui modélisent les objets en utilisant les approches de "Convex Hull" et qui simulent la détection de collision entre les objets virtuels en temps réel sont présentés. En outre, un dispositif de retour d'effort est utilisé comme une interface haptique avec le système. Cela conduit au développement d'un système à faible coût, avec les mêmes avantages que les appareils professionnels. À cet égard, l'arthroscopie du poignet peut être simulée et les étudiants en médecine peuvent facilement utiliser le système et peuvent apprendre les compétences de base requises en sécurité, flexibilité et moindre coût.

Description du Système

Les images médicales sont traitées afin de générer des modèles volumétriques. Une séquence d'images CT est segmentée et un modèle virtuel 3-D du poignet est généré.

Ce modèle 3-D est à la fois affiché visuellement sur l'écran de l'ordinateur et manipulé avec un dispositif de retour d'effort. Aussi, les simulations comprennent un algorithme pour modéliser les objets non-convexes en objets convexes en utilisant la méthode de "Convex Hull" et une méthode permettant de détecter les collisions entre les objets virtuels au cours de l'opération. L'interaction entre l'appareil haptique et l'ordinateur ferme la boucle entre l'utilisateur et le simulateur. La figure A.1 présente les principaux éléments du projet. Ce projet a été divisé en trois étapes:
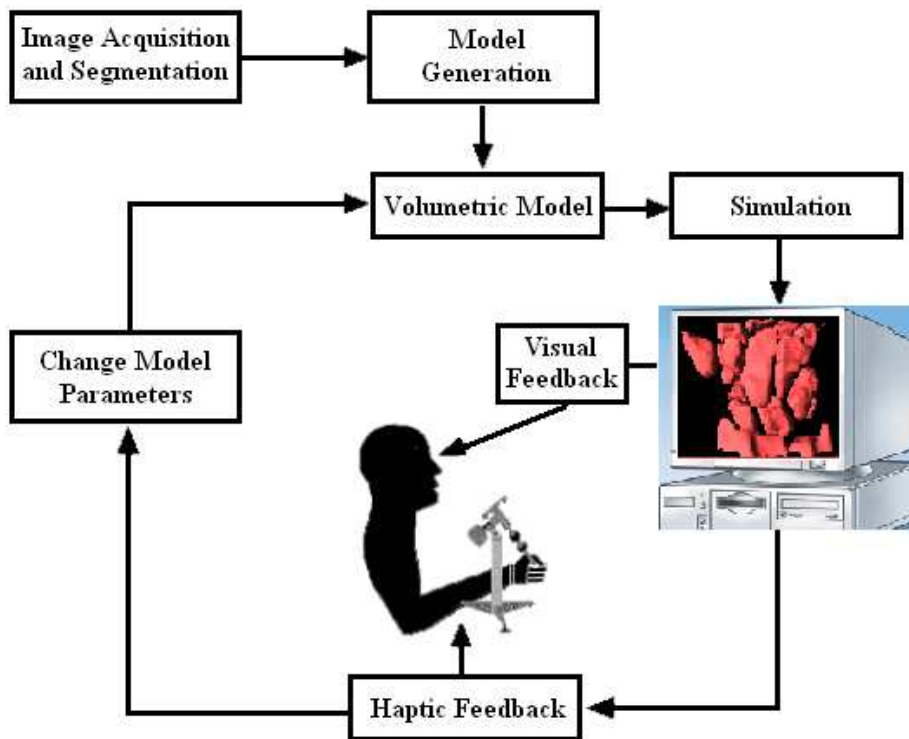

Figure A.1: Schéma du Système

Etape 1: Segmentation et génération d'objet 3-D

Dans cette étape, l'objectif est de détecter le contour des os dans les images CT pour avoir des images distinctes. Par conséquent, une séquence d'images CT a été traitée en utilisant l'algorithme de segmentation "Ligne de partage des eaux" ou "Watershed" afin

de générer un model 3-D du poignet. Après la segmentation de l'ensemble des images, l'algorithme "Marching Cube" est utilisé pour construire les frontières des objets dans la scène. Chaque os est considéré comme étant un objet et le résultat final de la segmentation el la reconstruction de l'ensemble des images est une image volumétrique constituant le poignet d'un patient. Ensuite, la représentation 3-D de ces modèles est illustrée dans un environnement virtuel en associant tous les éléments nécessaires (l'éclairage, les matériaux et les textures). La figure A.2 montre la représentation 3-D des os constituant le poignet d'un patient.
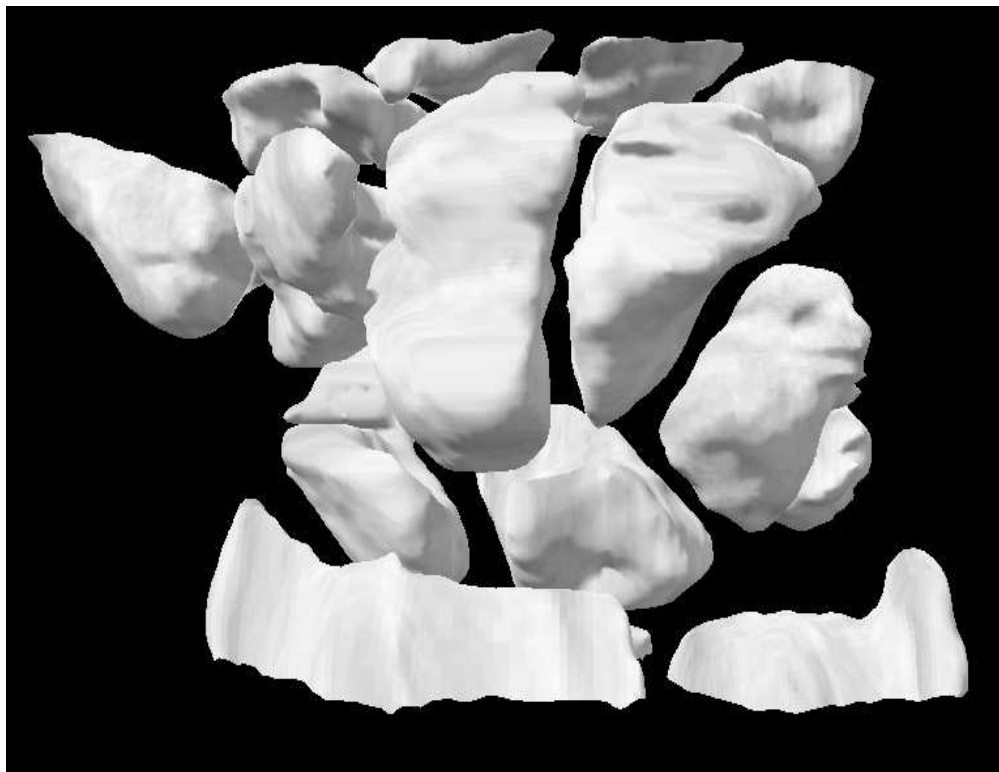

Figure A.2: Modèle 3-D du Poignet

Etape 2: Modélisation et Simulation

L'objectif d'un simulateur médical est de soutenir les étudiants en médecine au cours de leur formation sur des chirurgies avec une grande précision. À cet égard, les objets

médicaux sont modélisés suivant une méthode de "Convex Hull" proposée. Ceci donnera le simulateur plus de précision, mais en même temps une augmentation de complexité et du temps de calcul pour vérifier la collision. Par conséquent, en se basant sur les avantages des techniques de programmation linéaire (vitesse et robustesse), le problème de détection de collision est formulé et résolu. En outre, les objets convexes permettent aux algorithmes de programmation linéaire de converger rapidement et de détecter la collision, si elle existe. Ainsi, l'enveloppe convexe de chaque objet est reconstruite. Ensuite, le problème de collision est formulé comme un problème d'optimisation basé sur ces objets convexes et résolu en utilisant la programmation linéaire (méthode simplex).

Convex Hull

Etant donné que la plupart des objets 3-D ne sont pas caractérisés par une forme exacte qui pourrait être modélisée en utilisant des équations mathématiques précises, "Convex Hull" algorithmes sont considérés comme une solution pour modéliser ces objets. La nécessité des ces algorithmes se pose avec l'intention de simuler des scènes en temps réel et de détecter la collision entre les objets dans un environnent virtuel. De plus, la plupart des algorithmes de détection de collision sont basés sur les objets convexes, car ces derniers permettent aux algorithmes de collision de converger rapidement. En outre, les enveloppes convexes ont moins de points de contact que les objets réels. Cela conduit à une diminution de la taille du système d'équations nécessaires pour calculer la collision. Dans ce contexte, une approche hybride pour la construction des enveloppes convexe des objets 3-D (os du poignet) avec un temps d'exécution plus rapide a été proposée. Cette méthode a été comparée avec quatre algorithmes: Brute Force, GiftWrapping, QuickHull et Chan algorithme.

Méthode Hybride

Plusieurs méthodes sont développées afin d'accélérer les algorithmes de "Convex Hull". Certaines techniques commencent par diviser les points constituant l'objet 3-D

en deux ensembles arbitraires et fixes, droite et gauche. "Divide-and-conquer" est un algorithme qui commence par calculer récursivement l'enveloppe convexe de la partie droite puis la partie gauche suivie par la fusion des deux enveloppes dans une enveloppe convexe finale. Autres techniques divisent l'ensemble des points d'entrée en plusieurs sous-ensembles comme le Chan algorithme. Cet algorithme divise les points (n) qui constituent l'objet 3-D en différents sous-ensembles (n / N) arbitraire, disjoints et de taille N. Ensuite, l'enveloppe convexe de chaque sous-groupe est calculée. Ainsi, N enveloppes sont formées et elles sont intégrées dans une enveloppe convexe finale.

L'idée derrière ces techniques est toujours de diviser l'ensemble des points en plusieurs sous-ensembles afin d'accélérer le temps d'exécution de l'algorithme qui construit l'enveloppe convexe et de réduire sa complexité. Dans ce contexte, une méthode hybride est proposée et deux points importants sont pris en considération:

- Le temps d'exécution des algorithmes qui construit l'enveloppe convexe dépend du nombre de points (n) qui constitue l'objet.

- Les étapes d'emballage dans l'algorithme "Gift Wrapping" peuvent être acquises plus vite si l'ensemble des points d'entrée a été traité.

Par conséquent, une approche hybride pour générer les enveloppes convexes est développée. Elle est basée sur le QuickHull et le GiftWrapping algorithmes. Elle est décomposée en deux étapes: la première étape permet de réduire le nombre de points d'entrée et la deuxième étape souligne la reconstruction de l'enveloppe convexe correspondant. La méthode hybride est initiée par l'application de l'algorithme QuickHull pour diviser les points d'entrée en deux sous-ensembles (supérieur et inférieur) par un premier plan. Ensuite, un polyèdre de nouvelles facettes est créé en calculant le point ayant la distance maximale par rapport à ce plan. Par conséquent, les points qui sont dans le polyèdre sont à l'intérieur de l'enveloppe convexe et ils sont éliminés. La même procédure est répétée pour l'ensemble des points inférieurs. Cela conduit à la réduction du nombre de points d'entrée et à la formation d'un nouvel ensemble de points. Ce dernier constitue les données d'entrées pour l'algorithme GiftWrapping et les étapes

d'emballage sont effectuées sur ces nouvelles données pour obtenir l'enveloppe convexe finale. En d'autres termes, la méthode hybride applique une phase d'initialisation suivie par une série d'étapes d'emballage. Elle calcule les facettes de l'enveloppe convexe dans le sens opposé de l'aiguille d'une montre. Le conditionnement des étapes répétées est récursive pour explorer tous les bords jusqu'à ce que tous les aspects aient été examinés. Un pseudo-code de l'algorithme proposé est montré ci-dessous:

```
 1: find an initial plane from the min and max abssice and the max distance with
    respect to (x_min, x_max)
 2: construct a polyhedron from the initial plane and the max distance to this plane
 3: for each facet F of the polyhedra do
 4:     for each unassigned point p do
 5:         if p is above F then
 6:             assign p to F's outside set
 7:         end if
 8:     end for
 9: end for
10: Discard all points inside the polyhedron forming a new imput set (n_new)
11: find a starting edge (a, b) using the 2D Gift Wrapping algorithm on the XY projec-
    tion
12: for i = 1 ... n_new do
13:     find point p_i corresponding to min angle bewteen plane P in XY containing (a, b)
        and plane T = (a, b, p_i)
14:     replace c ← p_i
15:     save (a,b,c) into Q
16:     wrap the edge (a, c)
17:     if facet has been explored  then
18:         wrap the edge (b, c)
19:         if facet has been explored then
20:             return
21:         end if
22:     end if
23: end for
```

L'algorithme hybride proposé est appliqué à différents os du poignet. La figure A.3 montre le résultat sur les différents os testés : 1st Metacarpal (a), 2nd Metacarpal (b), 4th Metacarpal (c), Scaphoid (d), Capitate (e), Hamate (f), Radius (g) and Ulna (h). Chaque os est recouvert par son enveloppe convexe correspondant. Les résultats

montrent que l'approche proposée s'effectue plus rapidement que les autres techniques classiques.
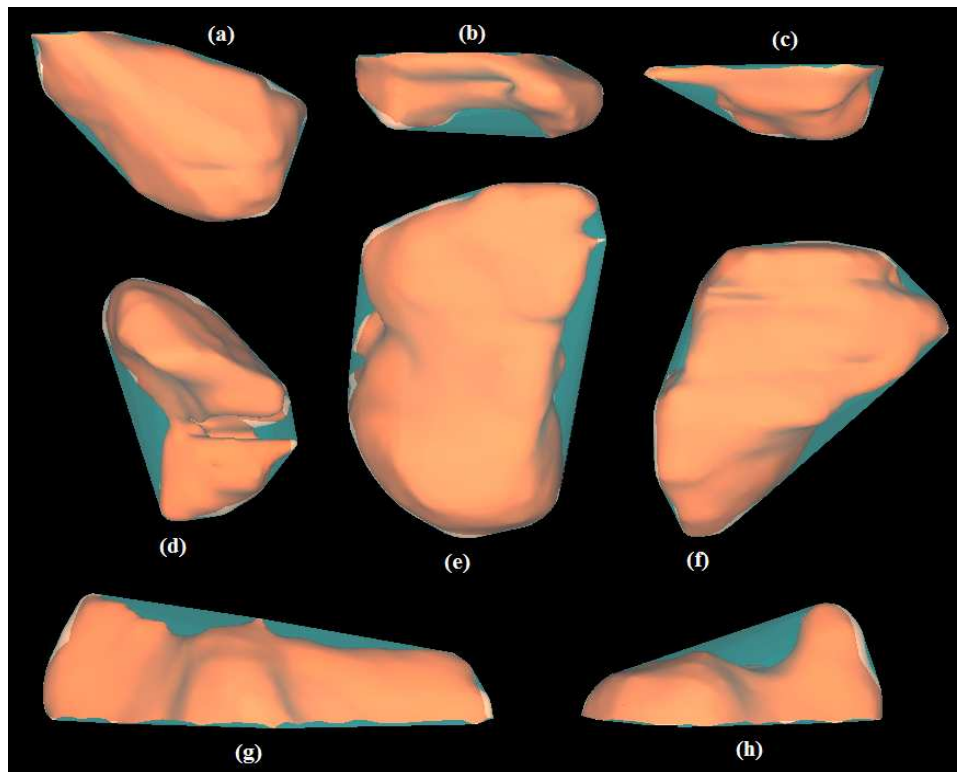

Figure A.3: Os du Poignet Recouvert par son Enveloppe Convexe Correspondant

La méthode hybride proposée est une méthode qui fonctionne en 2-D ainsi qu'en 3-D. Elle est très efficace, pratique et utile dans la modélisation et la simulation 3-D des données médicales dans un environnement virtuel.

Détection de Collision

Etant donné que les enveloppes convexes reconstruites ont moins de points de contact que les objets réels et peuvent être rapidement calculées, cela conduit à une diminution de la taille du système d'équations nécessaires pour détecter une collision. Par conséquent, les performances en temps réel des algorithmes de détection de collision sont augmentées et les algorithmes deviennent plus rapides. En outre, la plupart des systèmes exacts de CD sont basés exclusivement sur les objets convexes. Cela est dû au fait que les objets

convexes permettent aux algorithmes de CD de converger rapidement et de détecter la collision, si elle existe. Cela donnera le simulateur un degré élevé de précision, mais en même temps une augmentation du coût de la complexité et du temps de calcul pour vérifier la collision. Par conséquent, en prenant les avantages des techniques de programmation linéaire (la vitesse et la robustesse), le problème de détection de collision est formulé et résolu. Ainsi, le CH de chaque objet est reconstruit ensuite le CD problème est formulé comme un problème d'optimisation basé sur les objets convexes et résolu en utilisant la programmation linéaire (la méthode simplex).

Pour formuler le problème de collision, chaque facette i de l'enveloppe convexe est représentée par l'équation du plan dans l'espace sous la forme:

$$a_i x + b_i y + c_i z \leq d_i \tag{A.1}$$

Tout point situé sur l'objet convexe doit satisfaire les inégalités des plans constituant cet objet. Ces équations forment les contraintes du problème de collision et représentent les facettes qui séparent les deux régions dans l'espace. Par conséquent, si un point appartient à deux séries d'inégalité en même temps, une collision est détectée à ce moment entre ces deux objets. Le problème est réduit à maximiser une fonction sous la forme de (x + y + z). Il peut être formulé par l'équation suivante:

$$max \ c^T X \tag{A.2}$$

subject to

$$AX \leq b \tag{A.3}$$

where $X = [x \ y \ z]^T$,

$$A = \begin{bmatrix} a_1 & b_1 & c_1 \\ a_2 & b_2 & c_2 \\ a_3 & b_3 & c_3 \\ . & . & . \\ . & . & . \end{bmatrix} \tag{A.4}$$

$$b = [d_1 \ d_2 \ d_3 \ldots]^T, \quad c = [1 \ 1 \ 1]^T \tag{A.5}$$

Les coefficients des matrices A et b sont calculés en se basant sur les facettes de l'enveloppe convexe reconstruit par l'approche proposée. Le système linéaire présenté est résolu en utilisant un algorithme de programmation linéaire (Simplex). Cette méthode a été comparée avec un algorithme classique nommé IVRI-CD.

Etape 3: Interface Homme-Machine

Un dispositif mécanique de retour d'effort avec trois degrés de liberté est proposé et conçu. Le système a été développé suivant un plan bien défini. Tout d'abord, la base de l'appareil a été construite et chaque capteur a été synchronisé avec le moteur correspondant. Deuxièmement, le système a été monté. L'imitation des gestes chirurgicaux faites par le médecin au niveau de la main a été réalisée suite à une conception mécanique dans la troisième étape.

La mise en oeuvre du dispositif nécessite des capteurs qui sont capables de détecter les positions de l'outil chirurgical et un système de communication pour transmettre les données à l'environnement virtuel. Aussi, les moteurs sont également nécessaires pour le retour d'effort. Par conséquent, une résistance doit être générée lors d'une détection de collision entre les objets virtuels. Le système est illustré dans la figure A.4.

Collection et Acquisition des Données

Les mouvements qui sont effectués par l'utilisateur sont récupérés par les trois capteurs (potentiomètres) placés sur les trois différents axes (X, Y et Z). Chaque fois que l'utilisateur déplace le dispositif de retour de force, les tensions entre les trois terminaux des trois potentiomètres sont ajustées en conséquence. Ensuite, les signaux électriques sont générés et transmis à la carte d'acquisition pour le traitement. Le changement de tension est du à la rotation de la bande résistive. Les potentiomètres qui indiquent un changement de la tension (signaux électriques) indiquent aussi une variation de la position de l'outil médicale dans l'environnement virtuel. S'il n'y a pas de détection de collision entre cet outil et le modèle 3-D du poignet, les moteurs sont éteints c'est-à-dire
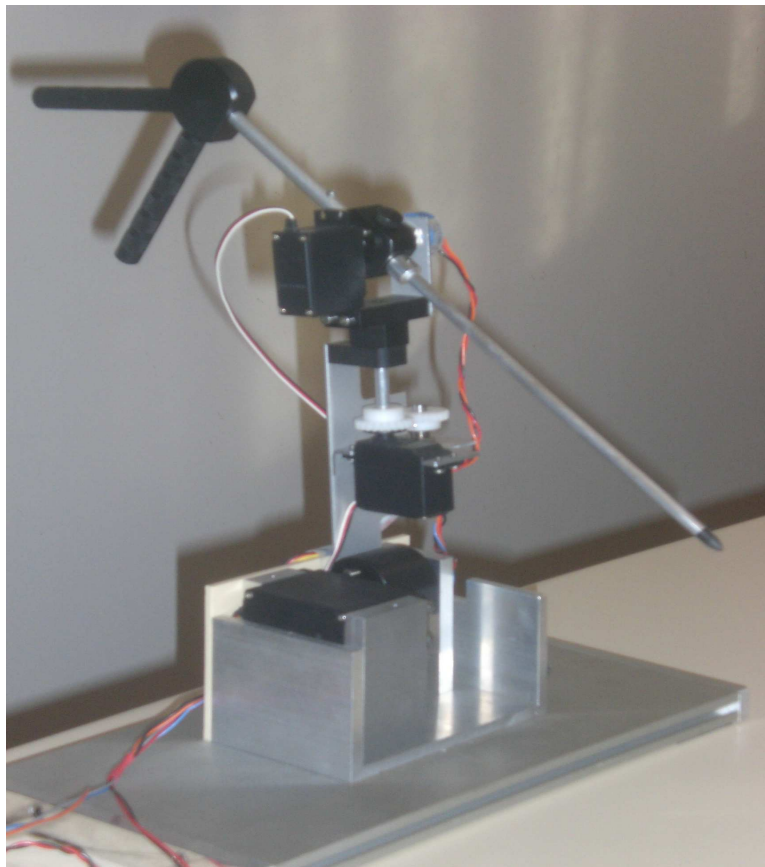
Figure A.4: Le Système de Retour D'effort

il n'y a pas de signal transmis pour contrôler les moteurs. D'autre part, si une collision est détectée, les signaux PWM sont produits et transmis via le port de sortie de la carte d'acquisition vers les moteurs. Par conséquent, l'utilisateur peut sentir le retour de force qui est généré par ces moteurs.

Résultat

La figure A.5 montre le système chirurgical proposé et construit au cours de la thèse. Afin de tester notre simulateur proposé, une comparaison entre une chirurgie réelle et une opération virtuelle est faite.

La figure A.6 montre deux étapes d'une opération chirurgicale de la main. La partie réelle est faite dans un hôpital alors que la partie virtuelle est faite par notre simulateur.

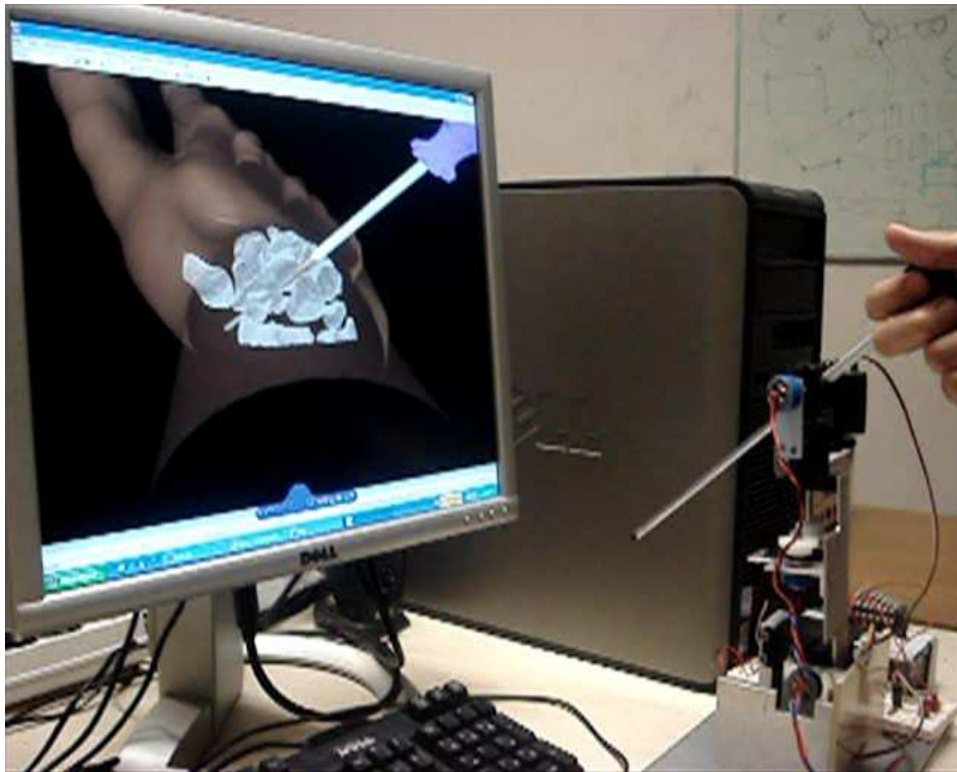Figure A.5: Le Simulateur Chirurgical Proposé

Conclusion

La force du simulateur proposé repose sur l'intégration entre le monde des ingénieurs et le monde médical. Le monde des ingénieurs qui est plutôt un monde "non-vivant" tandis que le monde médical est un "monde vivant". Cette intégration simplifie la compréhension mutuelle des deux domaines qui sont parmi les plus importants dans la vie humaine. Ce qui est aussi important dans ce projet, c'est qu'il rassemble plusieurs domaines de recherche. Il contient de l'imagerie, de la réalité virtuelle, de la détection de collision, de la robotique, du retour d'effort et de la méthodologie pédagogique. Les principaux résultats obtenus dans cette thèse sont:

- **Etat de l'Art:** Dans cette thèse, un état de l'art sur les simulateurs chirurgicaux existants est présenté. Les simulateurs sont classés selon l'application, les organes ou les structures pour lesquels ils sont développés. Cette étude peut être utilisée
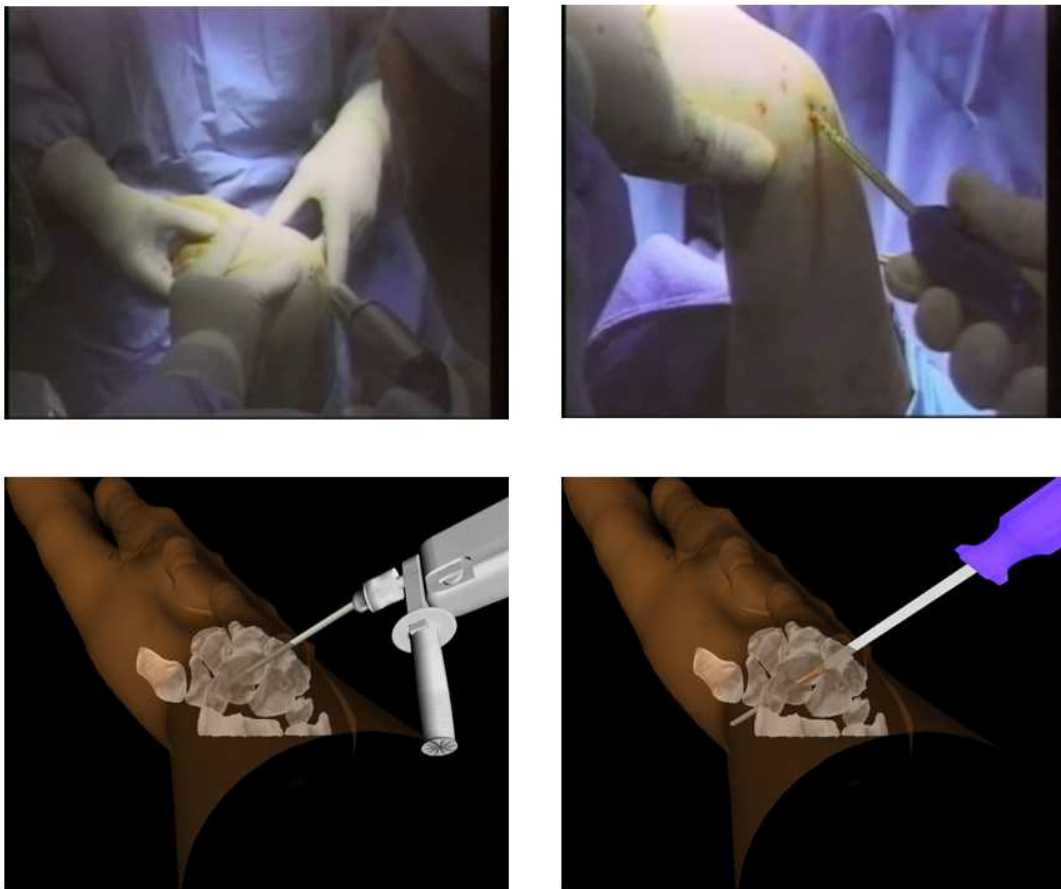
Figure A.6: Comparaison Entre une Opération Réelle et une Opération Virtuelle

par les chercheurs pour avoir une idée générale sur les simulateurs commerciaux et scientifiques qui ont été développés pour effectuer différentes approches de la chirurgie minimalement invasive.

- **Environnement Virtuel:** Un environnement virtuel pour visualiser les modèles médicaux et les instruments chirurgicaux avec une haute fidélité et une grande précision est développé.

- **Algorithmes:** Une nouvelle approche hybride pour générer les enveloppes convexes des modèles 3-D est élaborée et présentée. L'algorithme proposé convertit chaque modèle 3-D concave en un modèle convexe, ceci permet aux algorithmes de détection de collision de converger rapidement et de signaler une collision, si elle

existe. Cette méthode est très efficace, pratique et utile dans la modélisation et la simulation des données médicales dans un environnement virtuel. En outre, une nouvelle technique de détection de collision pour les objets solides est proposée et mise en place. Le problème de détection de collision est formulé et une solution de programmation linéaire est obtenue pour déterminer si une collision existe entre des objets virtuels ou non. L'algorithme proposé est efficace, rapide, robuste et conduit à une diminution de temps de calcul nécessaire pour détecter une collision.

- **Un dispositif de Retour d'Effort:** Un dispositif de retour d'effort avec trois degrés de liberté est conçu, développé et mis en oeuvre. Ce système est couplé avec un algorithme de retour haptique. Ce dispositif peut être utilisé par les étudiants en médecine ainsi que les chirurgiens avec les mêmes avantages que les appareils professionnels.

- **Simulation Virtuelle d'une Opération Chirurgicale:** Une simulation virtuelle de "dorsal percutaneous scaphoid fixation" est présentée. Une comparaison entre une chirurgie réelle effectuée par des médecins à l'intérieur de la salle d'opération et une chirurgie virtuelle réalisée par notre simulateur est montrée. La chirurgie virtuelle assure que le système proposé aide à la formation des étudiants en médecine ainsi que les chirurgiens dans le but d'acquérir les compétences nécessaires pour effectuer leurs opérations.

Bibliography

[1] M. Goebel, (Ed.): "Virtual Reality, Computers and Graphics", Special Issue. vol.17, 6, November 1993.

[2] R. Ziegler, W. Mueller, G. Fischer, M. Goebel, "A Virtual Reality Medical Training System", *Computer Vision, Virtual Reality and Robotics in Medicine*, vol. 905, pp. 282-286, April 2006.

[3] D. Watts, J. Higgins, F. Seddiqui, A. Niel, R. Desai, "Catheter With Multiple Visual Elements", *AVANTIS MEDICAL SYSTEMS, INC.*, Santa Ana Ct., Sunnyvale, CA, USA, June 2006.

[4] LapSim, Surgical Science Products, [online]. http://www.surgical-science.com

[5] LapMentor, Simbionix Products, [online]. http://www.simbionix.com/LAPMentor

[6] Procedicus VIST, MIST, VA, Mentice Products, [online]. http://www.mentice.com

[7] G. Szekely, C. Brechbuhler, J. Dual, R. Enzler, J. Hug, R. Hutter, N. Ironmonger, M. Kauer, V. Meier, P. Niederer, A. Rhomberg, P. Schmid, G. Schweitzer, M. Thaler, V. Vuskovic, G. Troster, U. Haller, and M. Bajka, "Virtual reality-based simulation of endoscopic surgery", *Teleoperators and Virtual Environments*, 9(3), pp. 310-333, 2000.

[8] The Visible Human Project, [online]. http://www.nlm.nih.gov/research/visible/

[9] UroMentor, Simbionix Products, [online]. http://www.simbionix.com/UROMentor

[10] GI Mentor II, Simbionix Products [online]. http://www.simbionix.com/GIMentor

[11] M. Bro-Nielsen, J. Tasto, R. Cunningham, and G. Merril, "PreOp endoscopic simulator: A PC-based immersive training system for bronchoscopy", *Medicine meets virtual reality, MMVR*, vol. 7, pp. 76-82, 1999.

[12] G. Voss, U. Bockholt, J. Los Arcos, W. Muller, P. Oppelt, J. Stahler, "Lahystotrain - Intelligent Training System for Laparoscopy and Hysteroscopy", *Proceedings Of Medicine Meets Virtual Reality*, pp. 359-364, 2000.

[13] W.M. Wittig, M. Becker, U. Bockholt, T. Elias, G. Voss, "Virtual Reality Hysteroscopy Training Simulator", *Proceedings of the SimTecT Conference*, 2002.

[14] VirtaMed, [online]. Available: http://www.virtamed.com/cms/

[15] M. Harders, M. Bajka, U. Spaelter, S. Tuchschmid, H. Bleuler and G. Székely, "Highly-Realistic, Immersive Training Environment for Hysteroscopy", *Medicine Meets Virtual Reality*, vol. 14, pp. 176-181, January 2006.

[16] M. Harders, U. Spaelter, P. Leskovsky, G. Székely, and H. Bleuler, "Haptic Interface Module for Hysteroscopy Simulator System", *Medicine Meets Virtual Reality*, 2007.

[17] Ch. Kuhn, U. Kuhnapfel, H.G. Krumm, B. Neisius, "Karlushe Endoscopic Surgery Trainer A Virtual Reality based Training System for Minimally Invasive Surgery", *SMIT 96*, 1996.

[18] U. Kuhnapfel, Ch. Kuhn, M. Hubner, H.G. Krumm, H. Maa, B. Neisius, "The Karlsruhe Endoscopic Surgery Trainer as an example for Virtual Reality in Medical Education", *Minimally Invasive Therapy and Allied Technologies (MITAT)* pp. 122-125, 1997.

[19] U. Kuhnapfel, Ch. Kuhn, M. Hubner, H. Krumm, "VR Technology Based Minimally Invasive Surgery Training using the KISMET Software", *Proceedings of IMAG-INA 96*, Monte Carlo, February 1996.

[20] Virtual Endoscopic Surgery Training (VEST), [online]. http://www-kismet.iai.fzk.de/KISMET/VestSystem

[21] Liver Biopsy, [online]. http://www.hpv.cs.bangor.ac.uk/Sim

[22] Wingman Force Feedback Mouse, [online]. http://www.hpv.cs.bangor.ac.uk/Sim/force

[23] ProMIS, Haptica, [online]. http://www.haptica.com/promis

[24] SEP (SurgicalSim Education Platform), SimSurgery Products, [online]. http://www.simsurgery.com/products.htm

[25] J. Peifer, W. Curtis, and M. Sinclair, "Applied virtual reality for simulation of endoscopic retrograde cholangio-pancreatography (ERCP)", *Medicine Meets Virtual Reality*, No. 4, pp. 36-42, Amsterdam. 1996.

[26] K. Ikuta, M. Takeichi, T. Namiki, "Virtual endoscope system with force sensation",*Proceedings of the IEEE International Conference on Robotics and Automation*, vol. 3, pp.1715 - 1721, Detroit, Michigan, May 1999.

[27] AccuTouch, Immersion , [online]. http://www.immersion.com/medical/products

[28] G. Wiet, R. Yagel, D. Stredney, P. Schmalbrock, D. Sessanna, Y. Kurzion, L. Rosenberg, M. Levin, K. Martin, "A Volumetric Approach to Virtual Simulation of Functional Endoscopic Sinus Surgery", *Medicine Meets Virtual Reality* San Diego, CA, January, 1997.

[29] J. D. Mabrey, S. D. Gilogly, J. R. Kasser, H. J. Sweeney, B. Zarins, H. Mevis, W. E. Garrett, R. Poss, and W. D. Cannon, "Virtual Reality Simulation of Arthroscopy of the Knee", *The Journal of Arthroscopic and Related Surgery*, vol. 18, July-August 2002.

[30] S. Gibson, J. Samosky, A. Mor, C. Fyock, E. Grimson, T. Kanade, R. Kikinis, H. Lauer, N. McKenzie, S. Nakajima, H. Ohkami, R. Osborne and A. Sawada, "Simulating Arthroscopic Knee Surgery using Volumetric Object Representations,

Real-Time Volume Rendering and Haptic Feedback", *Proceedings of First Joint Conference CVRMed-MRCAS'97* , pp. 369-378, 1997.

[31] P. Heng, Ch. Cheng, T. Wong, Y. Xu, Y. Chui, K. Chan and S. Tso, "A Virtual Reality Training System for Knee Arthroscopic Surgery", *IEEE Transactions on Information Technology in Biomedicine*, vol. 8, no. 2, pp. 217-227, June 2004.

[32] S. Bayonat, M. Garcia, C. Mendoza and J.M. Fernandez, "Shoulder Arthroscopy Training System with Force Feedback", *IEEE conference on Medical Information Visualization, MedVis* , pp. 71-76, July 2006.

[33] Arthroscopy Surgical Simulation: insightArthroVR System. Immersion , [online]. Available: http://www.immersion.com/medical/products/arthroscopy/

[34] S. Smith, A. Wan, N. Taffinder, S. Read, R. Emery, and A. Darzi, "Early experience and validation work with Procedicus VA - the Prosolvia virtual reality shoulder arthroscopy trainer", *Medicine Meets Virtual Reality* , pp. 337-343, Amsterdam, 1999.

[35] Prosolvia AB, [online]. Available: http://www.prosolvia.com

[36] M. Xin, Z. Lei, I. Volkau, Z. Weili, A. Aziz, M. Ang, and W. Nowinski, "A Virtual Reality Simulator for Remote Interventional Radiology: Concept and Prototype Design", *IEEE Transactions on Biomedical Engineering* , vol. 53, no. 8, pp. 1696-1700, August 2006.

[37] S. Dawson, "Simulators for training: Assessment, validation and acceptance strategies, Executive Summary", *Medicine Meets Virtual Reality MMVR*, January 2003.

[38] VIRGIL , [online]. Available: http://www.medicalsim.org/virgil.htm

[39] A. McCarthy, P. Harley, R. and Smallwood, "Virtual arthroscopy training: do the "virtual skills" developed match the real skills required ? ", *Medicine Meets Virtual Reality* , pp. 221-227, Amsterdam 1999.

[40] W. Muller, and U. Bockholt, "The Virtual Reality Arthroscopy Training Simulator", *Medicine Meets Virtual Reality* pp. 13-19, Amsterdam, 1998.

[41] M. Kass, A. Witkin and D. Terzopoulos, "Snakes: active contour models", *International Journal of Computer Vision* vol 1, no. 4 pp. 321-331, January, 1988.

[42] C. Xu, D. Pham and J. Prince, "Chapter 3: Image Segmentation Using Deformable Models", *Handbook of Medical Imaging. Vol.2 Medical Image Processing and Analysis*, pp. 175-272. SPIE, London, June, 2000.

[43] S. Buecher and C. Lantuéjoul, "Use of Watershed in Contour Detection", *Proceedings of International Workshop of Image Processing, Real-Time Edge and Motion Detection/Estimation*, pp. 17-21, Rennes, France, September 1979.

[44] L. Vincent and P. Soille, "Watersheds in Digital Spaces: An Efficient Algorithm Based on Immersion simulations", *IEEE Transactions on Pattern Analysis and Machine Intelligence* , vol. 13, no. 6, pp. 583-598, June 1991.

[45] M. Couprie, L. Najman, G. Bertrand, "Quasi-linear Algorithms for the Topological Watershed", *Journal of Mathematical Imaging and Vision*, vol. 22, pp. 231-249, 2005.

[46] L. Najman, M. Couprie, G. Bertrand, "Watersheds, Mosaics and the Emergence Paradigm", *Discrete Applied Mathematics*, pp. 301-324, 2005.

[47] W. E. Lorensen and H. E. Cline, "Marching cubes: A high resolution 3D surface construction algorithm", *Proceedings ACM SIGGRAPH Computer Graphics*, vol. 21, Issue 4, pp. 163-169, 1987.

[48] X. Daragon, M. Couprie, G. Bertrand, "Discrete Frontiers", *Discrete Geometry for Computer Imagery*, LNCS, Springer Verlag, vol. 2886, pp. 236-245, 2003.

[49] http://www.medicineword.com/pseudoarthrosis.shtml

[50] S. Akl, "Efficient Convex Hull Algorithms for Pattern Recognition Applications", *4th International Conference on Pattern Recognition*, Japan, 1978.

[51] M. Breg, O. Schwarzkopf, M. Kreveld, M. Overmars, *Computational Geometry: Algorithms and Applications 2nd edition*, published by Springer-Verlag, 2000.

[52] S. Fortune, "Voronoi diagrams and Delaunay triangulations", In Euclidean Geometry and Computers, *World Scientific Publishing Co.*, 1992.

[53] V. Bayer, "Survey of Algorithms for the Convex Hull Problem", Department of Computer Science, Oregon State University, 1999.

[54] A. Day, "The implementation of an algorithm to find the convex hull of a set of three-dimensional points", *ACM Transaction on Graphics*, 1990.

[55] A. C. Yao, "A lower bound to finding convex hulls", *Journal of the ACM (JACM)*, 1981.

[56] R. Graham, "An efficient algorithm for determining the convex hull of a finite planar set", *Information Processing Letters*, 1972.

[57] F. Preparata and S. Hong, "Convex hulls of finite sets of points in two and three dimensions", *ACM Transactions on Mathematical Softwares*, 1977.

[58] C. Barber, D. Dobkin, H. Huhdanpaa, "The QuickHull Algorithm for Convex Hulls", *ACM Transactions on Mathematical Softwares*, 1996.

[59] J. O'Rourke, *Computational Geometry in C*, Cambridge University Press, New York, 1994.

[60] B. Chazelle and J. Matousek, "Derandomizing an output-sensitive convex hull algorithm in three dimensions", *Computational Geometry Theory and Applications*, 1995.

[61] H. Edelsbrunner and W. Shi, "An $O(nlog^2h)$ time algorithm for the three-dimensional convex hull problem", *SIAM Journal on Computing*, 1991.

[62] M. Ben-Or, "Lower Bounds For Algebraic Computation Trees", *in Procceding of the 15th Annual ACM Symposiom Theory Comput* pp. 80-86, 1983.

[63] J. Bentley and M. Shamos, "Divide and conquer for linear expected time", *Information Processing Letters*, 1978.

[64] T. M. Chan, "Optimal output-sensitive convex hull algorithms in two and three dimensions", *Discrete and Computational Geometry*, 1996.

[65] C. M. Lin, D. Manocha, J. Cohen and S. Gottschalk. "Collision Detection: Algorithms and Applications", *Algorithms for Robot Motion and Manipulation*, pp. 129-142, 1996.

[66] S. Quinlan. "Efficient Distance Computation Between Non-Convex Objects", *Proceedings in IEEE Conference on Robotics and Automation*, pp. 3324-3329, 1994.

[67] S. Gottschalk, C. Lin, and D. Manocha. "OBB-Tree: A Hierarchical Structure for Rapid Interference Detection", *in Proceedings of ACM SIGGRAPH*, 1996.

[68] C. M. Lin, and J. F. Canny. "A Fast Algorithm for Incremental Distance Calculation", *Proceedings in IEEE Conference on Robotics and Automation*, Vol. 2, pp. 1008-1014, 1991.

[69] E. G. Gilbert, D. W. Johnson and S. S. Keerthi. "A Fast Procedure for Computing the Distance Between Complex Objects in Three-Dimensional Space", *IEEE Transaction on Robtics and Automation*, pp. 193-203, 1988.

[70] G. Van Den Bergen. "A Fast and Robust GJK Implementation for Collision Detection of Convex Objects", *Journal of Graphics Tools*, pp. 7-25. 1999.

[71] B. Mirtich. "V-clip: Fast and robust polyhedra collision detection", *ACM Transaction Graphics 17*, po 177-208, 1998.

[72] J. D. Cohen, M. C. Lin, D. Manocha, and M. Ponamgi. "I-COLLIDE: An Interactive and Exact Collision Detection System for Large Scale Environments", *ACM Int. 3D Graphics Conference* pp. 189-196, 1995.

[73] K. Chung and W. Wang. "Discrete Moving Frames for Sweep Surface Modeling", *Pacific Graphics'96, Hsinchu, Taiwan*, 1996.

[74] J. Klosowski, M. Held, J. Mitchell, H. Sowizral, and K. Zikan. "Efficient Collision Detection Using Bounding Volume Hierarchies of K-Dops", *IEEE Transactions on Visualization and Computer Graphics*, 1998.

[75] S. A. Ehmann and M.C Lin. "Accelerated Proximity Queries Between Convex Polyhedra By Multi-Level Voronoi Marching", *Proc. International Conf. on Intelligent Robots and Systems* , 2000.

[76] C. Fares, Y. Hamam, "Collision Detection Between Virtual Objects Using Optimization Techniques", *IFIP2003*, Sophia Antipolis, France, 2003.

[77] C. Fares, Y. Hamam, "A Hybrid Algorithm for Collision Detection", *EUROSIM 2004*, ESIEE-Paris, France, 2004.

[78] C. Fares, Y. Hamam, "Proximity Queries Computation Using Optimisation", *ECCO XVII, American University of Beyrouth*, Lebanon, 2004.

[79] C. Fares, Y. Hamam, "Collision Detection for Rigid Bodies: A State of the Art Review", *STAR Report in GraphiCon*, Russia, 2005.

[80] A. Akgunduz, P. Banerjee, S. Mehrotra. "A Linear Programming Solution for Exact Collision Detection", *Journal of Computing and Information Science in Engineering* , Vol. 5, Issue 1, pp. 48-55, March 2005.

[81] S. Appelle. "Haptic perception of form: Activity and stimulus attributes", *In The Psychology of Touch*, M. Heller and W. Schiff, Eds. Lawrence Erlbaum Associates Inc., Hillsdale, NJ, pp. 169-188, 1991.

[82] M. Rodrigues, R. Chaves, W. Silva. "Collaborative Virtual Training Using Force Feedback Devices", *: Proceedings in Brazilian Symposium on Computer Graphics and Image Processing*, pp. 332-3392, October 2004.

[83] Immersion Corporation, "FEELit Mouse", Technical Document, San Jose, CA, 12 pp., October 1997. Electronic version: http://www.immerse.com.

[84] The Microsoft SideWinder Force Feedback II joystick. [online]. Available: http://www.microsoft.com/ hardware/sidewinder/Joysticks.asp.

[85] PHANToM Haptic Devices, SensAble Technologies. [online]. Available: http://www.sensable.com/

[86] Humusoft DAQ Boards, [online]. Available: http://www.humusoft.cz/datacq/ad512.htm

[87] J. Slade, D. Jaskwhich, "Percutaneous Fixation of Scaphoid Fractures", *Hand clinics*, vol. 17(4), pp. 553-574, November 2001.

[88] M. Rettig, K. Raskin, "Retrograde Compression Screw Fixation of Acute Proximal Pole Scaphoid Fractures", *Journal of Hand Surgery*, vol. 24 pp. 1206-1210, 1999.

[89] G. Wozasek, K. Moser, "Percutaneous Screw Fixation of Fractures of The Scaphoid", *Journal of Bone Joint Surgery*, vol. 73, pp. 138-142, 1991.

[90] ACUMED, Innovative Orthopedic Implants and Accessories, [online]. Available: http://www.acumed.net/

[91] The Orthogate Website (Internet Society of Orthopaedic Surgery and Trauma). [Online]. Available: http://www.orthogate.org/

[92] M. Bhat, M. McCarthy, TR. Davis, JA. Oni and S. Dawson, "MRI and Plain Radiography in the Assessment of Displaced Fractures of the Waist of the Carpal Scaphoid", *Journal of Bone and Joint Surgery*, 86B: pp. 705-713, 2004.

[93] ME. Rettig, SH. Kozin, WP. Cooney, "Open Reduction and Internal Fixation of Acute Displaced Scaphoid Waist Fractures", *Journal of Hand Surgery*, 26A: pp. 271-276, 2001.

[94] M. Garcia-Elias, A. Vall, JM. Salo, AL. Lluch, "Carpal Alignment after Different Surgical Approaches to the Scaphoid: a Comparative Study", *Journal of Hand Surgery*, 13A: pp. 604-612, 1988.

[95] MJ. Botte, WW. Mortensen, RH. Gelberman, CE. Rhoades, H. Gellman, "Internal Vascularity of the Scaphoid in Cadavers After Insertion of the Herbert Screw", *Journal of Hand Surgery*, 13A: pp. 216-220, 1988.

Appendix

Appendix B

Electronic Components

B.1 AD512 Entry-Level Data Acquisition Card HU-MUSOFT

The AD512 data acquisition card by HUMUSOFT, shown in figure B.1, has many features and specifications some of them are:

Figure B.1: AD512 Data acquisition card

B.1.1 General

- Power consumption: 100 mA @ +5 V, 50 mA @ +12 V, 50 mA @ -12 V

- Operating temperature: 0 to 50 °C

- Connector: DB-37

- I/O ports: 16 consecutive addresses

B.1.2 Features

- Eight single-ended 12-bit analog input channels

- Two 12-bit analog output channels

- Sampling rate up to 100 kHz

- 8 digital input channels, 8 digital output channels

- Programmable A/D ranges

- Jumper selectable D/A ranges

- Low power consumption

- Driver for Real Time Toolbox for MATLAB included

B.1.3 Specifications

Analog I/O

- Channels: 8 single-ended

- Channels: 2 double-buffered 12-bit output channels

- A/D converter: 12-bit, 10 microsec. conversion time

- Input ranges: ± 10 V, ± 5 V, 0-10 V, 0-5 V

- Trigger mode: software

- Overvoltage: ± 16 V max

- Output Ranges: ± 10 V, ± 5 V, 0-10 V, 0-5 V

- Output current: 10 mA max.

Digital I/O

- Input lines: 8, TTL compatible

- Output lines: 8, TTL compatible

Figure B.2 shows the corresponding data sheet for analog input/output, digital input/output, voltage sources and ground of the DAQ board.

Reference

AD0	1			
AD1	2	20	DA0	
AD2	3	21	DA1	
AD3	4	22	AGND	
AD4	5	23	+5V REFOUT	
AD5	6	24	+4.096V REFOUT	
AD6	7	25	AGND	
AD7	8	26	-12V	
AGND	9	27	+12V	
AGND	10	28	+5V	
GND	11	29	GND	
DIN0	12	30	DOUT0	
DIN1	13	31	DOUT1	
DIN2	14	32	DOUT2	
DIN3	15	33	DOUT3	
DIN4	16	34	DOUT4	
DIN5	17	35	DOUT5	
DIN6	18	36	DOUT6	
DIN7	19	37	DOUT7	

Table 10. X1 Connector Pin Assignement

Figure B.2: AD512 Data Sheet

B.2   Vishay Spectrol Potentiometer Model 357

VISHAY precision potentiometers, shown in figure B.3, has many electrical and mechanical specifications. The most important are:

- Resistance standard range, 1K to 50K

- Tolerance STANDARD: ± 20% ; SPECIAL: ± 10%

- Linearity (Independent) STANDARD $\pm$ 2.0%

- Power Rating 1.0 watt at 70 degree Derate to 0 watt at 125 degree

- Electrical Travel 340 $\pm$ 3

- End Voltage 0.5% maximum

- Dielectric Withstanding Voltage 1,000VRMS, 60Hz

- Insulation Resistance 1000M, 500VDC

- Rotation 360 continuous (optional mechanical stops 340 degree $\pm$ 3)

- Operating Torque Maximum Starting and running 3.68 mNm (0.5 oz - in)

- Weight 17.5gms (0.62 oz)

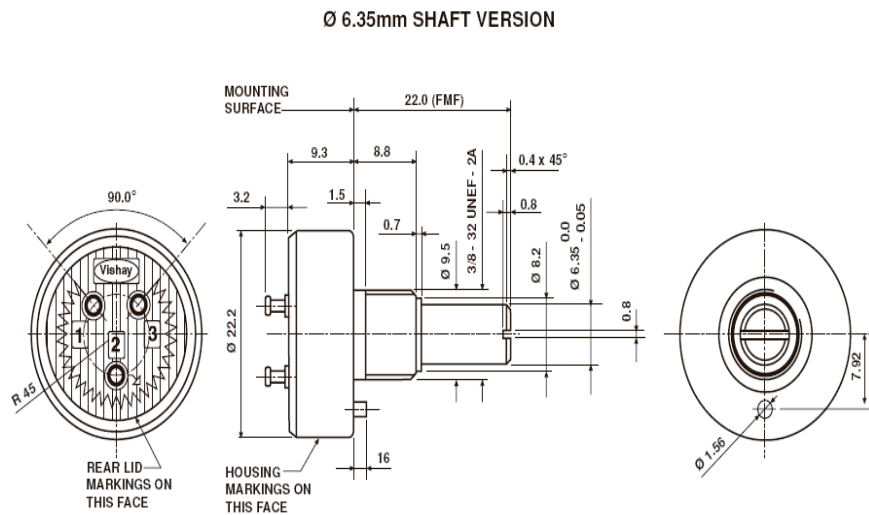

Figure B.3: Vishay Spectrol Potentiometer Model 357

B.3 Servo Motors

A servo motor is a small device that has an output shaft. This shaft can be positioned to a specific angular positions by sending to the servo a specific signal. As long as the signal exists on the input line, the servo will maintain the angular position of the shaft.

B.3.1 Servo Wiring

All servo motors have three wires, the ones chosen in our applications are the Futaba servos. Therefore, the colors of the wirings are the following: Black for ground, Red for power and white for the input signal. Servos can operate under a range of voltages. Typical operation is from 4.8V to 6V. Figure B.4 shows the wiring of the FUTABA servo motors.
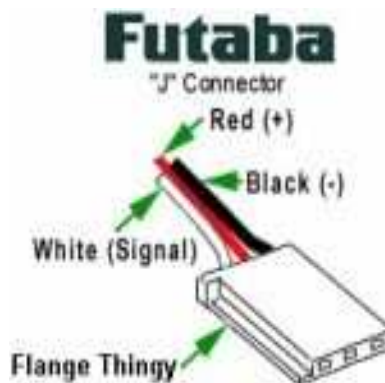

Figure B.4: Servo Motor: FUTABA Wiring

B.3.2 PWM Signals

While the black and red wires provide power to the motor, the signal wire is used to command the servo. The general concept is to simply send a logic square wave signal to the servo motor at a specific wave length. This signal is called PWM signal.

The servo expects to see a pulse every 20 milliseconds (0.02 seconds). The length of the pulse will determine how far the motor turns. A 1.5 millisecond pulse, for example, will make the motor turn to the 90 degree position (often called the neutral position). If the pulse is shorter than 1.5 ms, then the motor will turn the shaft to closer to 0

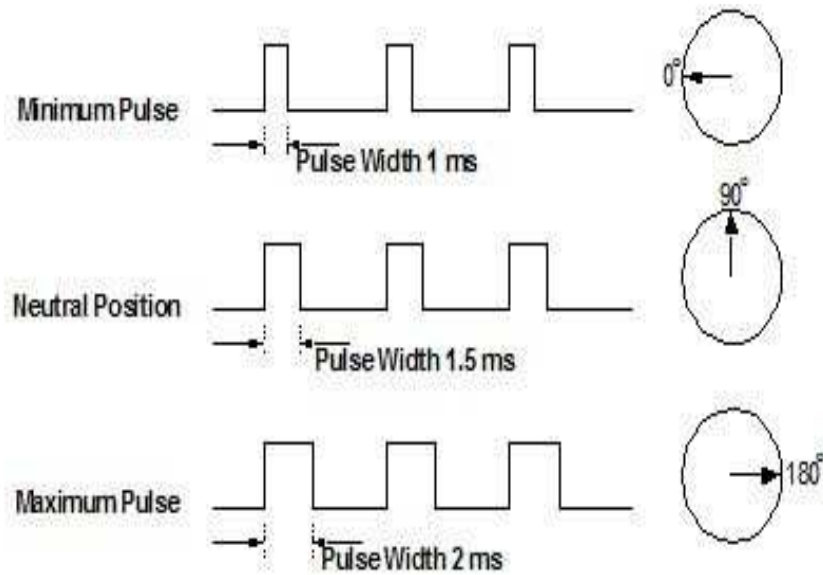degress. If the pulse is longer than 1.5 ms, the shaft turns closer to 180 degress. Figure B.5 shows the PWM signals for servo motor control.

Figure B.5: PWM Signals for Servo Control